University of Nottingham
UK | CHINA | MALAYSIA

Axonal MicroRNAs in Cortical Neuronal Development and Network Connectivity

Raquel Mesquita-Ribeiro, MRes

School of Life Sciences

University of Nottingham

Thesis submitted for the degree of
Doctor of Philosophy

Table of Contents

Acknowledgements 5

Abstract 8

1. Introduction 10

1.1 The neuron and the development of neuronal connectivity 10

1.1.1. Neuronal polarization and axon specification 10

1.1.2 Local protein synthesis in the axon 12

1.2 MicroRNAs: tiny regulators with great impact 14

1.2.1 Biogenesis 14

1.2.2 Mechanisms of microRNA-mRNA interaction and function 15

1.3 MicroRNAs in nervous system development 17

1.3.1 MicroRNAs in neuronal differentiation 17

1.3.2 MicroRNAs in the Axon 19

1.3.3 MicroRNAs at the Synapse 22

1.4 Axon-enriched microRNAs in developing cortical axons 23

1.5 Exploring brain networks: How to investigate neuronal connectivity 28

1.5.1 Network activity 28

1.5.2 Microelectrode arrays 28

1.5.3 Calcium imaging 30

1.6 Scope and Aims 31

2. Methods 33

2.1. Animals and primary cortical cultures 33

2.1.1 Dissociated cortical cultures 33

2.1.2. Microfluidic cortical cultures 34

2.2. Mammalian cell lines 35

2.3. RNA extraction 35
2.3.1. Dissociated cortical cultures 35
2.2.2. Axonal RNA from microfluidic cultures 36
2.4. Quantification by real time qPCR 37
2.4.1. Real-Time qPCR of mature microRNAs 37
2.4.2. Real-Time qPCR of mRNA targets 38
2.4.3. Real-Time qPCR analysis 39
2.5. microRNA functional analysis tools 41
2.6. Functional assays on axonal growth 43
2.6.1. Measurement of axon length in dissociated cortical cultures 44
2.6.2. Measurement of axon length in microfluidic cortical cultures 45
2.6.3. HS3ST2 mRNA levels after RNAi transfections 45
2.7 Cloning 46
2.7.1. Luciferase reporter constructs 46
2.7.2. HS3ST2 expression construct 47
2.8. In vitro target validation: luciferase reporter assay 48
2.9 Immunofluorescence 49
2.9.1. Quantitation of immunofluorescence signal 49
2.10. Primary cortical cultures on microelectrode arrays 50
2.11. Calcium imaging of cortical cultures 50
2.11.1. Loading of Fluo-5 and measurement of calcium transients 50
2.11.2. Image analysis 51
2.12. Synaptosomes (Appendix I.1) 52
2.13. microRNA expression in human samples of frontal cortex (Appendix I.2) 53
2.14. Statistical analysis 54

3. Axonal microRNAs derived from repetitive elements 56

3.1 Introduction 56

3.1.1 Evolution of microRNAs 56

3.1.2 Transposable elements: the Good, the Bad and the Evolutionary 57

3.1.3 Retrotransposons 58

3.1.4 Relevance of SINEs as motors of novelty in the evolution and function of the nervous system 60

3.1.5 The birth of microRNAs from transposable elements 61

3.1.6 Aims 63

3.2. Results and Discussion 65

3.2.1 Genomic context of axonal miRs 65

3.2.2 Species-specific miR-3470b 67

3.2.3 Role of miR-3470b in axonal development 74

3.2.3.1 Function of miR-3470b in axonal outgrowth 74

3.2.3.2 Regulation of miR-3470b over development 76

3.2.4 Pathways potentially targeted by miR-3470b 77

3.2.5 Development of network activity in cortical neurons cultured on microelectrode arrays 83

3.2.5.1 Microelectrode array model 83

3.2.5.2 Effect of miR-3470b in spontaneous network activity of neuronal cultures 84

3.6 Concluding remarks 87

4. Role of axon-enriched miR-99a in axon development and network connectivity 91

4.1 Introduction 91

4.1.1 miR-99a, an old friend of metazoan genomes 91

4.1.2 miR-99a in neuronal development and function 92

4.1.3 Aims 93

4.2. Results and Discussion 94

4.2.1 Expression and regulation of miR-99a in developing cortical neurons 94

4.2.2 Effect of miR-99a in axonal outgrowth 96

4.2.3 In search of miR-99a regulatory pathway 99

4.2.4 Expression profile of HS3ST2 in cortical cultures over development 107

4.2.5 Role of HS3ST2 in axon development 109

4.2.6 miR-99a modulates HS3ST2 in cortical neurons 114

4.2.7 miR-99a modulates axonal outgrowth through HS3ST2 regulation 117

4.2.8 miR-99a regulates cortical axonal outgrowth locally in a microfluidic compartmentalised culture model 122

4.2.9 miR-99a modulates the development of network connectivity 128

4.3 Concluding remarks and future implications 135

4.3.1 Axon-enriched miR-99a regulates axonal development 135

4.3.2 HS3ST2: a potential modulator of axon-ECM interactions over development 135

4.3.3 Impact in the development of spontaneous network activity 138

5. General discussion 141

5.1 microRNA function in neuronal wiring 141

5.2 microRNAs in axonal terminals and beyond: implications to cell-to-cell communication 145

5.3 Implications to disease 148

6. Appendix I 150

I.1. miR-99a is highly expressed in synaptic fractions of the developing mouse brain 150

I.2. miR-99a is not altered in the forebrain of Alzheimer's Disease patients 151

7. Abbreviations 151

8. References 152

Acknowledgements

The conception, execution and writing of this PhD work and dissertation would not have been possible without the support, expertise, mentorship, friendship and the shoulders to cry on of a wealth of extraordinary people.

Firstly, I'd like to express my deep gratitude to my PhD supervisor, Dr. Federico Dajas-Bailador, for seeding my passion for the makings of the brain. I cannot thank him enough for the scientific mentoring, (very) patient guidance and unshakable optimism in the course of my PhD. Your core belief in the good that comes from Science most definitely shaped the scientist I am today and paved the way to the one I'd want to become.

I wish to acknowledge the lab of Dr. Noah Russel, my second PhD supervisor, whose fascinating discussions sparked my interest in neuronal networks. I would like to offer my special thanks to Nitzan Herzog for his expertise and determination to develop the mouse microelectrode array model together, and without whom it could not have been done.

I am particularly grateful to Dr. Tom Bellamy and his lab for the valuable and constructive suggestions and critiques in the joint lab meetings and, specially, for all the assistance given with calcium imaging experiments, kindly opening the doors to his lab.

I'd also like to express my great appreciation to the Layfield lab. I'd like to thank Prof. Rob Layfield for always being kind to me and frequently acknowledging the greatness of the Portuguese national dish, Nando's peri peri chicken. Thank you to Dan, Barry, Lizzie, Jess, Charlie, Alice and James for the numerous flasks of HEK-293Ts and Neuro2As, for your companionship, the fun chats over a few pints at JA after work and the limitless supply of TBS 10x.

A big heartfelt thank you to all my lab mates. I've not only met new colleagues, but true friends who made this moving-abroad-to-do-a-PhD experience that much better! To Andrea, my Italian brother from another mother, for his persistent encouragement throughout the years and for the constant reminder of why I should be a scientist. To Alex, my cloning and qPCR buddy and mentor, thank you for introducing me to the wonders of Britishness. To Cristiano, for so many neuron preps, stainings on weekends, imaging stints together and instrumental help with the development of the trigene-immersion RNA purification protocol. To Emma for warning me of the horrors of flies and putting up with me in her house for an

indefinite amount of time. To Matt for showing me it's possible to have an actual life and a dog and still be a scientist. To Teresa for always keeping a slice of Portugal around. To Catherine for the lab's very own Pet Sematary. To Clare for her support as we started this PhD journey together. To the newer members of the lab, Asta, Alice and Sophie, thank you for showing there still are crazy folks who willingly pursuit a PhD.

A very special thanks goes to Clara, who was with me in the lab through many evenings of calcium recordings, sharing sciency thoughts and ideas sprinkled with Monty Python laughs and childhood anecdotes.

I wish to thank Kika and Catarina for the daily support and assistance in all matters of science and life, no matter how small, silly or straight out stupid. Our long-distance, close-to-heart friendship kept me sane through the PhD years.

Um abraço apertado de agradecimento pelo apoio incondicional dos meus queridos amigos da minha terra, que sempre me recebem com um sorriso nos olhos e fazem tudo, mesmo tudo ao seu alcance para que volte com o coração quentinho.

Mamã e papá, não foram ainda inventadas palavras que descrevam a gratidão que vos tenho. Obrigada por todos os sacrifícios que fizeram para que eu tivesse o poder de escolher o meu caminho, mesmo quando discordaram dele. Magui, obrigada por não teres dito aos pais que sou maluquinha for ter feito doutoramento. Adoro-vos.

Finally, a huge thank you to Chris, a minha pessoa, who saw the very worst of me and (foolishly) chose to stay and patiently wait to see the best. Σ'αγαπάω.

For Clara,

who would have enjoyed her PhD so much.

Merecias tão mais tudo isto.

"eu acabara de aprender que a vida tem de ser mais à deriva, mais ao acaso, porque quem se guarda de tudo foge de tudo."

— valter hugo mãe, a máquina de fazer espanhóis

Abstract

Cognitive brain function requires the establishment of neuronal networks, which rely on the formation and elongation and branching of axonal projections and the differentiation of presynaptic terminals during development. The cellular events involved in these processes are dependent on protein translation locally in the axon compartment, which enables rapid changes of the axonal proteome in response to neurotrophic cues to regulate axon growth and patterning. How these dynamic changes of the axonal proteome are regulated locally in the axon has been a topic of intensive investigation in the past decade. MicroRNAs are small RNAs known to regulate protein expression by controlling mRNA translation repression/degradation. Recently, these regulatory RNAs have emerged as key players in the modulation of several molecular pathways underlying neuronal differentiation in early stages of development, making this class of non-coding RNAs interesting candidate regulators of local protein translation in the axon during development. However, the role of microRNAs in the axon, in particular axonal outgrowth and presynaptic differentiation, is only beginning to be unravelled.

The work described here used next generation sequencing to identify a set of microRNAs enriched in the axonal fraction of primary cortical neurons cultured in compartmentalised microfluidic devices. Following the characterization of axonal microRNA expression levels, two microRNAs, miR-3470b and miR-99a, were selected for subsequent functional studies.

The miR-3470 family are mouse-specific repeat-derived microRNAs originating from the B1-element Mus1. Repetitive elements have a major role in shaping the structure and function of the genome, but evidence on the functional relevance of lineage-specific repeat-derived microRNAs is still limited. Inhibition of miR-3470b during early development of primary cortical neurons produced a significant decrease in axonal growth. Moreover, we discovered a significant association between miR-3470b targets and proteins involved in cell-to-cell contact/synaptic pathways. To investigate the role of miR-3470b in the formation of neuronal networks we used a microelectrode array cortical culture model, in which spontaneous electrical activity shows a progressive increase from day 9 in vitro, reflecting the establishment of functional synaptic

connections. Inhibition of miR-3470b from the beginning of the third week in culture, when its endogenous levels are high, produced a marked decrease in network activity, suggesting its role in neuron connectivity during cortical neuron development.

Functional studies in cortical cultures showed that inhibition of miR-99a in primary cortical neurons produced a significant decrease in axonal growth, with overexpression of a miR-99a mimic increasing axonal length. By using bioinformatics, luciferase reporter assays and functional rescue experiments we could identify a new target for miR-99a in axonal development, heparan sulphate 3-O-sulphotransferase 2 (Hs3st2), an enzyme part of the biosynthesis of heparan sulphate proteoglycans, key players in axon-extracellular matrix interactions. To investigate the effect of axonal miR-99a in the emergence of neuron connectivity and the functioning of neuronal networks we used imaging of calcium transients to assess the spontaneous rhythmic activity of developing neuronal cultures, demonstrating how inhibition of miR-99a alters the patterns of calcium oscillation frequency and synchronicity, suggesting its relevance for network development and maturation.

Overall, this work identified two microRNAs capable of regulating axonal outgrowth in the development of mouse cortical neurons *in vitro*. Both microRNAs were found to exert growth promoting actions in developing axons. Furthermore, this work demonstrated the ability of mR-99a and miR-3470b to act as regulators of neuronal network formation *in vitro*, raising potential implications to the development of neuronal connectivity *in vivo.*

1. Introduction

1.1 The neuron and the development of neuronal connectivity

1.1.1. Neuronal polarization and axon specification

Neurons are highly polarised cells comprising of two main morphological and functional domains, the axon and the somatodendritic compartments, which maintain their structural characteristics at the molecular level. Neuronal polarisation involves the disruption of asymmetry in post-mitotic progenitors leading to axon specification and, ultimately, the formation of these two distinct compartments.

In mouse brain development, new-born neurons undergo extensive migration from the ventricular zone to their final locations in the cortical plates shortly after neurogenesis, and it is while migrating that neurons acquire their axon-dendrite polarized structure (Lewis, Courchet, and Polleux 2013). Post mitotic neurons first develop multiple small neurites and then undergo polarisation by the formation of a leading and a trailing process, exhibiting a bipolar morphology. During migration, the trailing process becomes the axon and the leading process becomes a dendrite which undergoes arborisation in post-natal development (Polleux and Snider 2010).

In culture, neuronal polarisation of rodent primary hippocampal and cortical neurons shows remarkable similarities to the process *in vivo* (Banker 2018; Tabata and Nakajima 2003). Over three decades ago, Dotti et al. documented the development of primary hippocampal neurons in culture using very low density cultures to allow for the visualisation of single neuron morphology, and proposed that neurons acquire their characteristic polarised morphology in five well defined stages of development, detailed in figure 1.1 (Dotti et al, 1988). Upon attachment of dissociated post-mitotic neurons to the substrate, neurites continuously grow and retract until one neurite eventually enters a growth phase that persists, thus becoming the axon, and the remaining neurites become dendrites. Since the pivotal work of Dotti et al., primary hippocampal and, later, cortical neurons in culture became an important

model system for the study of cellular and molecular mechanisms underlying neuronal development and function (Banker 2018; Lewis et al. 2013).

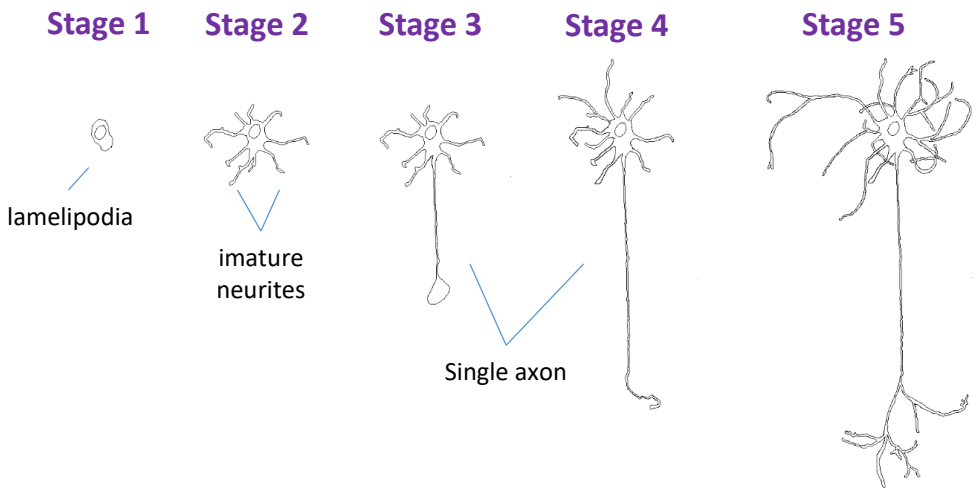


Figure 1.1 Stages of neuronal polarisation of cultured cortical neurons. In dissociated cultures, postmitotic cortical neurons display specific morphological transitions as classically described for hippocampal neurons by Dotti et al 1988. At stage 1, short after attachment to the substrate, neurons extend lamelipodia, which lead to the formation of multiple immature neurites (stage 2). At this stage the neuron still appears non polarised as immature neurites display alternate growth and retraction phases. Neuronal polarisation occurs from stage 2 to stage 3, when asymmetry breaks and one of the neurites rapidly grows into a long neurite, becoming the axon (stage 3). Stage 4 is characterized by rapid axonal outgrowth, while the remaining neurites slowly extend to become dendrites. Finally, at stage 5, axon and dendrites undergo further maturation and subsequently establish synaptic contacts.

One of the major intracellular pathways required for polarisation and axon formation involves the phosphorylation of liver kinase B1 (LKB1), a protein part of the partitioning-defective protein family (PAR), as a trigger of axon specification in developing cortical neurons *in vivo* (Dorfman and Macara 2008). The protein kinase AKT (protein kinase B) was also shown to be critical for neuronal polarity and appears to differentially localise to the developing axon, as a result of selective proteasome degradation in the dendrites (Yan, Guo, and Wang 2006). AKT is stabilised by JNK MAP kinase scaffold protein JIP1 in the growth cone of the developing axon and both proteins collaborate to promote axon growth. The loss of either protein promotes proteasomal degradation of the other and a cessation of axon growth (Dajas-Bailador et al. 2014). Moreover, AKT function seems to be mediated by GSK-3β (glycogen synthase kinase 3), an essential modulator of neuronal polarisation and development (Polleux and Snider 2010). GSK-3β targets several downstream

effectors of neuronal polarisation, many of them being regulators of cytoskeleton dynamics (Hur and Zhou 2010). In particular, collapsing response mediator protein 2 (CRMP-2), a microtubule binding protein enriched in the tip of the growing axon, displays decreased binding to tubulin upon phosphorylation by GSK-3β (Yoshimura et al. 2005). Many other signalling pathways have been described to play a role in polarisation and axon formation and elongation including PI3-kinase signalling, Ras and Rho small GTPases and the Par3/6 complex (Polleux and Snider 2010).

Interestingly, intracellular pathways leading to neuronal polarity seem to be modulated by extracellular cues that take part in defining the axon and dendritic domains. *In vitro*, brain-derived neurotrophic factor (BDNF) instructed axon specification through modulation of LKB1 pathway (Shelly et al. 2007). Further studies by the same authors found that Semaphorin 3a (Sema3a), a repellent guiding cue known to direct axon initiation toward the ventricle during cortical neuronal migration, supresses axon formation through downregulation of LKB1 phosphorylation (Shelly et al. 2011). Furthermore, transforming growth factor beta (TGF-β) was shown to initiate axon development, both *in vivo* and *in vitro*, via site-specific phosphorylation of Par6 (Yi et al. 2010). These effects suggest that the specification of a unique axon and the establishment of neuronal polarisation is somewhat regulated by extracellular factors present along the migration path (Lewis et al. 2013)

1.1.2 Local protein synthesis in the axon

The signalling pathways underlying neuronal polarisation and axon development rely on regulatory mechanisms that modulate the formation of the axon, its elongation, and its guidance towards the synaptic targets. These processes require dynamic changes of the local proteome in order to rapidly respond to extracellular cues, thus providing the rationale for local protein synthesis in the developing axon (Giuditta et al, 2002; Alvarez 2001).

Although it was previously assumed that axonal proteins were exclusively synthesised in the soma and taken through axonal transport to the axon distal/terminal regions, several lines of evidence have now contributed to the concept that messenger RNA (mRNA) translation can be localized to the axon.

Although this idea was proposed several decades ago (Giuditta, Dettbarn, and Brzin 1968; Koenig 1967; Sotelo-Silveira et al. 2006), it took time for it to be fully confirmed with modern detection techniques such as the isolation of active polysomal fractions from axoplasm preparations of the giant squid axon (Giuditta et al, 1991) and, importantly, electron spectroscopic imaging, a high sensitivity microscopy technique, that demonstrated polysomes in proximal and distal axoplasmic regions (Martin et al, 1989; Campbell and Holt 2001; Giuditta et al. 2002). More recently, components of the mRNA translation machinery such as ribosomes were identified by electron microscopy in vertebrates, specifically in embryonic cortical and sympathetic axons *in vitro* and in embryonic peripheral sensory axons *in vivo* (Jung, Yoon, and Holt 2012). Additionally, metabolic labelling experiments - reliant on the incorporation of radioactively labelled aminoacids into nascent proteins in the axonal compartment - showed that unmyelinated axons without somas are still capable of mRNA translation-dependent protein synthesis (Giuditta et al 1991; Eng et al, 1999; Jung et al. 2012).

In the last decade or so, several axonal mRNAs have been identified by candidate-based *in situ* hybridization, small axonal cDNA libraries and microarrays (Taylor et al. 2009; Yoon, Zivraj, and Holt 2009) revealing a complex mRNA population which includes transcripts encoding for cytoskeleton proteins such as β-tubulin, β-actin, microtubule associated protein b (MAP1b), tau; cell signalling molecules like RhoA and transmembrane receptors such as EphB2 and the κ-opioid receptor (Yoon et al. 2009). Overall, these findings provide further confirmation for localized protein synthesis in the axon.

Axonal mRNA translation enables the growing axon and its growth cone to locally respond to chemotropic growth and guidance cues from their environment with functional autonomy from the cell soma, in such a way that after cell soma ablation axons are still able to pathfind *in vivo* (Yoon et al. 2009). One of the most intensively studied roles of axonal mRNA translation has been the growth cone dynamic response to attractant and repellent cues (Iyer et al., 2014). In this process, the direction of growth cone turning is determined by the local synthesis of proteins that promote either assembly or disassembly of the cytoskeleton, mediating attraction or repulsion,

respectively. Stimulation by attractive cues, such as netrin 1 and BDNF, leads to asymmetric synthesis of β-actin on the side near to the source of the gradient, which in turn may lead to actin polymerization and attractive turning of the growth cone. On the contrary, repulsive cues, such as Sema3a and SLIT2, activate the axonal translation of the actin-depolymerizing proteins RhoA and cofilin, causing a repulsive turn of the growth cone (Jung et al. 2012).

Axonal mRNAs and local protein translation have also shown a role in axon outgrowth during development (Gracias, Shirkey-Son, and Hengst 2014) and in the assembly of axon presynaptic terminals upon arrival to its target. Remarkably, mRNAs encoding for proteins involved in branching and synaptic vesicle release were found to be enriched in mature growth cones when compared to younger pathfinding growth cones (Zivraj et al. 2010) of cultured *X. laevis* neurons.

The complexity of the dynamic mRNA subpopulations in the axon raises the question of what type of mechanisms regulate local axonal protein translation. To date, multiple regulation mechanisms have been reported (for review see Cioni, Koppers and Holt, 2018), including cytoskeleton dynamics, post-transcriptional modifications of the mRNA, extracellular cues and a few classes of non-coding RNAs. This thesis will focus on the role of microRNAs in the regulation of local translation in developing axons.

1.2 MicroRNAs: tiny regulators with great impact

1.2.1 Biogenesis

Cellular protein expression and function are regulated by a plethora of mechanisms that act at various levels, from gene transcription to mRNA translation and post-translation modifications. In the last decade, microRNAs emerged as major players in post-transcriptional gene expression regulation. They are a class of small non-coding RNAs (18-23 nucleotides) that mediate gene expression repression by targeting the 3' untranslated region (3'UTR) of mRNA transcripts. First discovered in C. elegans (Wightman et al. 1993),

microRNAs are highly evolutionary conserved across organisms, including vertebrates.

Scientific research in this field has seen a dramatic increase in recent years, illustrated by the latest miRBase release, which contains 24521 microRNA loci from 206 species, able to be processed to produce 30424 mature microRNA products (Kozomara & Griffiths-Jones 2014). It is now evident that microRNAs are fundamental regulatory players in most biological processes.

The biogenesis pathway of microRNAs is well established and comprises an initial transcription step mediated by RNA polymerase II, yielding a long stem-loop transcript – primary transcript (Kim 2005). In the nucleus, the complex Drosha/DGCR8 (microprocessor complex) undertakes further processing of the transcript to a ~ 70 nucleotides precursor-microRNA (pre-miRNA; Han et al. 2009), which is exported to the cytoplasm via exportin-5. Cytoplasmic Dicer, an endonuclease of the RNAase III family, cleaves the loop at the end of the hairpin and produces a mature double-stranded miR-3p/miR-5p duplex (Kim 2005). These duplexes have a short half-life in the cytoplasm and in general one strand is degraded, while the other remains a mature microRNA that is incorporated into a RNA-induced silencing complex (miRISC complex). The functional importance of each strand might vary depending on the developmental stage and/or tissue studied (Gong et al. 2014; Griffiths-Jones et al. 2011). The miRISC protein complex is composed by Argonaut 2 and a variety of other regulatory proteins (Fabian & Sonenberg 2012), and it allows the targeting of specific sequences in the 3'UTR of targeted mRNAs.

1.2.2 Mechanisms of microRNA-mRNA interaction and function

The binding of a microRNA to its targets mRNA results in repression of protein synthesis by degradation of the transcript or inhibition of protein translation (Kim 2005). The specificity of interaction is mostly determined by the complementarity between a core sequence of ~6-8 nucleotides in the microRNA and their specific seed sequence in the target 3'UTR, thus allowing the recognition of multiple mRNAs 3' UTRs by a single microRNA, while also enabling specific downregulation of each mRNA by multiple microRNAs (David P. Bartel 2009). Hence, this feature sustains the versatility and potential of

the microRNAs machinery in the regulation of cellular mechanisms in most physiological processes.

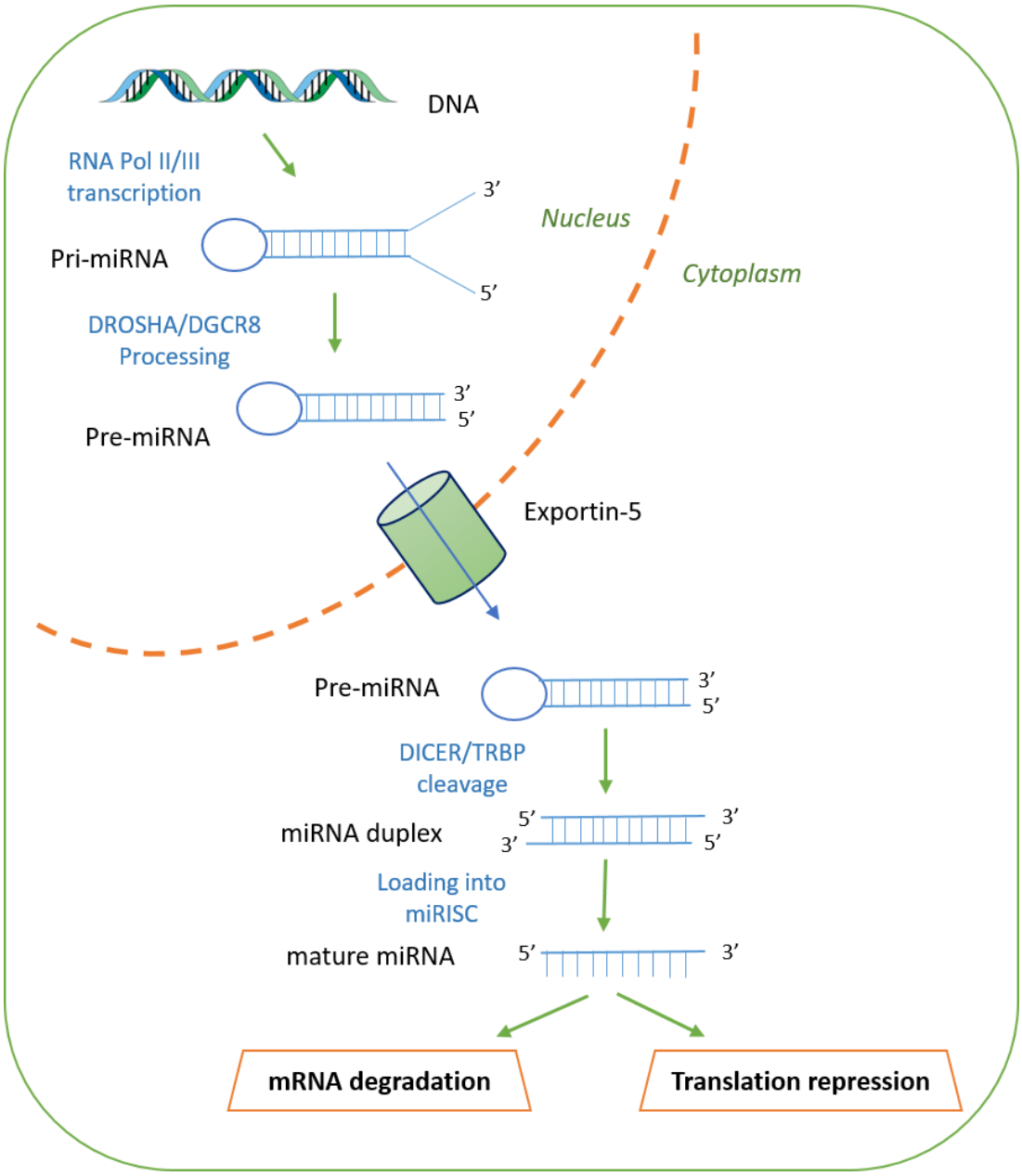


Figure 1.2. General mechanism of microRNA biogenesis and action. MicroRNAs are transcribed from intronic regions embedded in a host gene (via RNA polymerase II) or microRNA genes (via RNA polymerase III). The primary microRNA transcript (pri-miRNA) is then cleaved by the microprocessor complex (DROSHA/DGCR8) to obtain a precursor microRNA hairpin (pre-miR), which is then exported to the cytoplasm via exportin-5. Here, the hairpin is cleaved by Dicer and the resulting miRNA duplex loaded to the miRISC complex as one of its strands is degraded and the mature miRNA binds to miRNA-binding sites harboured in the 3'UTR of target mRNAs, leading to transcript degradation or translation repression. *Adapted from* Nguyen et al, 2017.

1.3 MicroRNAs in nervous system development

1.3.1 MicroRNAs in neuronal differentiation

The full biological functions of microRNAs are just being uncovered. Not surprisingly, recent research has largely highlighted their role in cell differentiation and development of various tissues (Sayed and Abdellatif 2011). MicroRNAs have been shown to control stem cell self-renewal ability by repressing the translation of selected mRNAs in stem cells and differentiating daughter cells (Gangaraju and Lin 2009) and appear to be involved in the pathways that trigger abnormal cell proliferation in cancer (Jansson and Lund 2012). Noticeably, neuronal differentiation and maturation during brain development share several of these mechanisms. In fact, microRNAs are particularly enriched in the nervous system (Fiore et al. 2011) and accumulating evidence supports their role in fine tuning cellular gene expression throughout the transition from progenitor cells to mature neurons (Sayed and Abdellatif 2011; Volvert et al. 2012).

The first *in vivo* evidence of microRNAs' role in nervous system development originated from a Dicer knockout in zebrafish. In effect, the absence of Dicer and the subsequent deficiency of mature microRNAs resulted in severe malformations in the brain and spinal cord (Giraldez et al. 2005). Furthermore, conditional Dicer knockout experiments performed in murine models led to impaired brain development, abnormal neuronal phenotype and early embryonic death (Huang et al. 2010; De Pietri Tonelli et al. 2008).

Dicer and the Argonaut-containing complexes are known to process other non-coding RNAs involved in gene silencing, such as small interference RNAs. However, the depletion of DGCR8, a Drosha binding protein part of the microprocessor complex specific to microRNAs production, resulted in diminished cognitive performance and deficit in dendritic arborisation in a mouse model of schizophrenia (Stark et al. 2008).

Although these and other studies involving the knockdown of microRNA biogenesis machinery components in the brain shed light on the neuronal function of microRNAs, they don't elucidate the role of specific microRNAs in neuronal differentiation. Brain-enriched miR-124 and miR-9 (Lagos-Quintana et al. 2002) are two of the most investigated microRNAs and their functions in neurogenesis and differentiation started to be unravelled in recent years. In a key study, Makeyev and co-workers correlated miR-124 to the transition of a non-neuronal to a neuronal-specific pattern of alternative splicing. miR-124 targets the splicing repressor PTBP1 mRNA leading to PTBP1 reduction and PTBP2 accumulation. This switch in the subpopulations of PTBP1 and PTBP2 triggers the initiation of a neuronal-specific splicing program that ultimately leads to neuronal differentiation (Makeyev et al. 2007).

MiR-124 has also been implicated in adult neuronal differentiation. Cheng and co-authors found that miR-124 knockdown in cells extracted from the subventricular zone, a neurogenic area in the adult brain, maintained the non-neuronal phenotype (Cheng et al. 2009). Conversely, the overexpression of miR-124 induced neuron formation. Functional studies with Sox9, identified as a target for miR-124, corroborated these findings, confirming that repression of Sox9 by miR-124 seems to mediate subventricular zone neurogenesis (Cheng et al. 2009).

In the case of miR-9, several studies have shown its role as a major player in the regulation of neurogenesis. Gain-of-function experiments in zebrafish embryo (Leucht et al. 2008) and mice embryonic brain (Zhao et al. 2009) showed the depletion of neural progenitor proliferation, accompanied by the early onset of progenitor neuronal differentiation. In an *in vivo* model of miR-9 loss-of-function, mice embryos lacking miR-9-2 and miR-9-3 exhibited multiple defects in the telencephalic structures related to enhanced proliferation of neural progenitors and development abnormalities, including the suppression of basal ganglia development (Shibata et al. 2011). Additionally, specific inhibition of endogenous miR-9 in the cortex of mouse embryos caused severe disruption of neuronal migration and differentiation (Dajas-Bailador et al. 2012).

Several studies suggest that miR-9-5p and its counterpart miR-9-3p are involved in the repression of a number of pathways leading to progenitor cells

differentiation towards a neuronal phenotype (Coolen, Katz, and Bally-Cuif 2013; Shibata et al. 2011; Yoo et al. 2009; Zhao et al. 2009). In double mutant miR-9-2/3 mice, Shibata and co-workers demonstrated that miR-9 negatively regulates multiple transcription factors linked to neuronal differentiation processes (Shibata et al. 2011).

In neural stem cells, miR-9 supressed TLX, a crucial inducer of stem cell self-renewal ability, resulting in stem cell proliferation deficiency and accelerated differentiation (Zhao et al. 2009). Yoo and colleagues found that miR-9, miR-9a* and miR-124 mediated the conversion of ATP-dependant chromatin remodelling complexes that occur with the end of mitotic ability in progenitor cells. This switch comprises the exchange of protein subunits part of neural-progenitor-specific BAF complex (npBAF) for their homologues, originating neural-specific BAF. Concomitant, but not individual, overexpression of the three microRNAs in neural progenitor cells led to decreased differentiation, in a process mediated by repression of BAF53a expression, a protein part of the npBAF, causing a shift towards neural-specific mechanisms (Yoo et al. 2009). This study hints at the fact that miR-9 alone might not be sufficient to induce neuronal differentiation. Nevertheless, taken together these discoveries indicate that miR-9 regulation favours the transition from a non-neuronal to a neuronal program.

1.3.2 MicroRNAs in the Axon

Neuronal microRNAs were initially implicated in early stages of nervous system development, but only recently their functions in post mitotic neurons have started to be investigated. The compartmentalized nature of neurons with their dendrites, axons and growth cones/presynaptic terminals supports the rationale for the presence of distinct local mRNA subpopulations in these specialized neuronal sub-compartments (Jung et al. 2012). This provides neurons with the ability to regulate protein synthesis with temporal and spatial resolution in a number of important neuronal processes, such as neurite outgrowth, axon guidance, synapse formation, and, ultimately cognitive brain function (McNeill and Van Vactor 2012).

Axonal regulation of protein synthesis modulates axon specification, maintenance of neuronal polarity and axon outgrowth and branching during axon development (Kaplan et al. 2013; Yoon et al. 2009). In effect, axons and growth cones are equipped with the translation machinery that enables rapid response to chemotropic guiding cues during axon pathfinding and outgrowth (Archana N. Iyer, Bellon, and Baudet 2014). This is particularly important in the peripheral nervous system, where growth cones can be a long distance from the cell body. Not surprisingly, recent research underlines a pivotal role of microRNAs in fine tuning axonal translation through local mRNAs expression regulation over various stages of axon development (Archana N. Iyer et al. 2014; McNeill and Van Vactor 2012).

Early experimental evidence on the dendritic localization of proteins that are part of the microRNA biogenesis pathway in mature neurons (Lugli et al. 2005) suggested the presence of microRNAs in neuronal sub-compartments. In fact, the investigation of the microRNA expression profile in axons and growth cones of sympathetic neurons identified around 130 microRNAs in distal axons, from which four were found to be highly enriched in the axon in comparison to the cell body (Natera-Naranjo et al. 2010). In an elegant experiment, the authors cultured superior cervical ganglia neurons in a compartmentalised Campenot culture chamber in which axons are isolated from their soma, microRNAs were further identified from the pure axonal RNA fraction by microarray analysis and quantified by quantitative PCR (Natera-Naranjo et al. 2010). In other study, an analysis of the axonal microRNA population in cortical neurons pinpointed seven axon-enriched microRNAs localized to distal axons and growth cones, when a "neuron ball" culture model was used (Sasaki et al. 2014). Although these findings highlight the diversity of axonal microRNA subpopulation, it is very likely that employing more sensitive and reliable molecular biology techniques for microRNA identification, such as deep sequencing, will add new layers of complexity to the current axonal microRNA landscape.

Very little is known about the function of specific microRNAs in the developing axon. MiR-16, a brain and axon-enriched microRNA (Natera-Naranjo et al. 2010) seems to be involved in the regulation of the local protein synthesis machinery in distal axons, by controlling the axonal expression of translation

initiation factors eIF2B2 and eIF4G2 (Kar et al. 2013). MiR-16 overexpression in the axon decreased both mRNA and protein levels of eIF2B2 and eIF4G2. Remarkably, following metabolic labelling, downregulation of axonal eIF2B2 and eIF4G2 inhibited local axonal protein synthesis. This pathway also seems to be involved in miR-16-mediated modulation of axon outgrowth (Kar et al. 2013).

Since the outgrowth and branching of the developing axon during navigation towards its neuronal target constitutes a fundamental aspect of neuron connectivity, the recent evidence described above points to a crucial role of microRNAs in wiring mechanisms within the nervous system.

Axon and growth cone response to attractant and repellent environmental cues guides the navigation of the axon during pathfinding. Recently, miR-124 has been proposed as a molecular timer of growth cone responsiveness to Sema3a in *X. laevis* retinal ganglion cell (RGC). The mechanism involves miR-124 mediated repression of the coREST/REST complex, leading to upregulation of NRP1, which encodes for Sema3a receptor synthesis and onsets growth cone sensibility to Sema3A (Baudet et al. 2011).

Other microRNAs have shown a role in outgrowth modulation of developing axons. In particular, Zhang and co-workers reported that overexpression of the cluster miR-17-92 in microfluidic compartmentalised axons of embryonic cortical neurons promoted axonal outgrowth, whereas axonal inhibition of endogenous miR-19a, a key component of this cluster, substantially supressed outgrowth in a process modulated by miR-19a control of local expression levels of PTEN, a peptide part of the mTOR pathway reportedly implicated in spinal cord regeneration (Zhang et al. 2013).

microRNAs have also been implicated in the regulation of axon branching. Of interest, studies in retinal primary cultures have shown that miR-132 targets p250GAP, a GTPase-activating protein for Rho family proteins, to promote axon branching (Marler et al. 2014). This interaction axis is in turn controlled by BDNF, which upregulates miR-132 to induce branching. The involvement of miR-132 in axon branching of retinal ganglion cells was further confirmed *in vivo*, where it was shown to be required for the proper branching of retinal RGC axon terminals in the mouse superior colliculus (Marler et al. 2014).

microRNAs have been reported to locally modulate the translation of cytoskeletal-associated proteins in the developing axon. Dajas-Bailador and colleagues were the first to describe that the expression of MAP1b, a key regulator of microtubule dynamics, is locally repressed in the axon by miR-9 (Dajas-Bailador et al. 2012). Moreover, miR-9 mediated regulation of MAP1b levels modulates axon growth and branching in cortical neuronal cultures. Experiments in compartmentalized microfluidic cultures suggested that BDNF modulates axonal outgrowth and branching via the miR-9 mediated control of MAP1b expression (Dajas-Bailador et al. 2012). More recently, another study described that axonal-enriched miR-132 locally targets the mRNA encoding for Rasa1, a cytoskeletal regulator protein, promoting axonal growth in dorsal root ganglia neurons (DRG; Hancock et al. 2014). Importantly, the local actions of microRNAs in axonal development are not only reserved for axon growth. In a recent study, miR-182 was reported to modulate growth cone responsiveness to Slit-2 in *X. laevis* RCGs. In vitro and in vivo experiments revealed that miR-182 acts, at least in part, by locally repressing the axonal translation of cofilin-1, a key mediator of growth cone repulsion mediated by Slit-2. Accordingly loss of miR-182 caused RGC axon targeting defects in vivo and impaired Slit2-induced growth cone repulsion (Bellon et al. 2017).

1.3.3 MicroRNAs at the Synapse

As see in the axon compartment, microRNAs are also reportedly enriched in dendrites relative to cell soma, indicated by a comparative analysis by laser capture multiplex RT-qPCR (Kye et al. 2007). In other studies, the synaptoneurosome, a biochemical fraction highly enriched in synaptic proteins and membranes, extracted from *in vitro* hippocampal cultures (Siegel et al. 2009) and the adult rat brain (Pichardo-Casas et al. 2012) was used to identify the microRNAs potentially involved in the synapse. Interestingly, Pichardo-Casas and colleagues found that a subset of microRNAs are differentially expressed in specific regions of the rat brain, suggesting that a particular microRNA might exert diverse roles in synaptic plasticity depending on its structural location in the brain (Pichardo-Casas et al. 2012).

Brain-specific miR-134 is the most extensively studied microRNA for its role in synapse formation and plasticity (Schratt 2009b). MiR-134 regulates the formation of dendritic spines by repressing the translation of Limk1, thereby reducing the polymerization of filamentous actin and leading to spine shrinkage. Remarkably, this effect is activity dependant, and following extracellular BDNF stimuli, Limk1 repression is disrupted (Schratt et al. 2006). Later, an antagonistic role in spine formation was found for miR-132 (Wayman et al. 2008). miR-132 negatively regulates the synthesis of Rac-inactivating protein p250RhoGAP and the subsequent increase in Rac activity promotes spine growth (Wayman et al. 2008). microRNA-dependant control of spinal size provides a mechanism for regulation of synapse formation (Schratt et al. 2006).

Contrarily to dendritic microRNAs, the roles of axonal/presynaptic microRNAs in synapse formation and plasticity are yet to be unveiled. In fact, microRNAs' ability to control local axonal signalling pathways in diverse axon development processes strongly supports the notion that future investigations may reveal many new functions for microRNAs in presynaptic terminal assembly, regulation of synapse formation and plasticity. Very recently, Cohen's laboratory reported *Drosophila melanogaster* miR-1000 as a regulator of neurotransmitter release from presynaptic terminals (Verma et al. 2015). Following a functional study using a library of mutants for 130 Drosophila microRNAs (Chen et al. 2014), further investigation of miR-1000 function revealed its role in the expression regulation of the vesicular glutamate transport into synaptic vesicles, a mechanism that could control synaptic transmission (Verma et al. 2015).

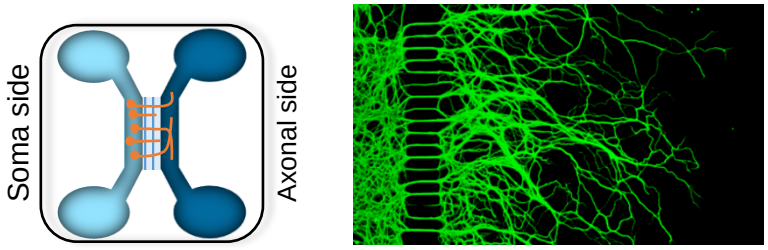
1.4 Axon-enriched microRNAs in developing cortical axons

Despite growing evidence indicating that microRNAs localise to axons, where they regulate local protein synthesis to exert axonal functions during development, the current knowledge on the specific set of microRNAs and microRNA regulatory networks modulating these processes is still very limited. Previous work by us had identified miR-9 as a local regulator of Map1b in cortical axons, which raised the question of what other microRNAs may

comprise the axonal microRNA population. This section will briefly describe the preliminary results of the approach taken by our lab to identify microRNAs potentially involved in the regulation of axonal function over development. This preliminary study acted as a starting point of the work presented in this thesis, in which the roles of axon-enriched microRNAs were further investigated.

In order to profile axonal microRNAs, cortical neurons were cultured in compartmentalized microfluidic devices (Taylor et al. 2005) to separate of the axons from the cells bodies (figure 1.2.a), thus allowing for the collection of a pure axonal RNA fraction. Identification of microRNAs present in both the axonal and the cell body fractions was further conducted by next generation sequencing, revealing a complex axonal microRNA subpopulation of over 100 microRNAs. As an approach to select microRNAs with a potential role in axonal development, an axon enrichment analysis was performed, resulting in a hierarchical list based on axonal enrichment in relation to cell body (figure 1.2.b).

(a)



(b)

Top 20 Axon-encriched microRNAs			
miRNA	**Ax/Cb**	**miRNA**	**Ax/Cb**
miR-434-3p	1.429	*miR-151-3p*	0.070
miR-3470b	0.857	*miR-191-5p*	0.067
miR-125-3p	0.750	*miR-30a-5p*	0.059
miR-182-5p	0.500	*miR-9-5p*	0.056
miR-181c-5p	0.375	*miR-27-3p*	0.054
miR-99a-5p	0.192	*miR-143-3p*	0.051
miR-134-5p	0.125	*miR-146a-5p*	0.043
miR-16-5p	0.115	*miR-25-3p*	0.040
miR-181b-5p	0.077	*miR-26a-5p*	0.039
miR-146b-5p	0.071	*miR-708-5p*	0.037

Figure 1.2. miRNAs enriched in developing cortical axons identified by axon enrichment. (a) Microfluidic devices were used to culture mouse cortical neurons with the goal to separate axons from cell bodies and, this way, obtain a pure axonal fraction free of contamination by neuronal cell bodies or dendrites (extraction performed at DIV8; see methods). Immunofluorescence of acetylated tubulin illustrates the compartmentalisation of the culture, showing axons on the righ-hand side compartment. **(b)** Hierarchical list of the top 20 miRNAs most enriched in the axons as compared to the cell body fraction and respective Axon/Cell body ratio (Ax/Cb).

This subset of 20 microRNAs included miR-9 and miR-16, two microRNAs with a previously described role in axon outgrowth (Dajas-Bailador et al. 2012; Kar et al. 2013). Further validation of the axon-enriched microRNAs was conducted by quantitative PCR (data not shown).

Interestingly, a bioinformatics prediction analysis of the pathways targeted by the top 20 axon-enriched microRNAs shows that various microRNAs are expected to target pathways related neuronal function and cellular growth and

development, as shown in figure 3. This adds to evidence from axon-enrichment and provides further indication of the relevance of the identified microRNAs in axonal processes. Moreover, several microRNAs from this subset target are predicted to target the same pathway, with "AMPK signalling", "Hippo signalling" being targeted by 10 and "Neurotrophin signalling" being targeted by 9 of the 20 axon-enriched microRNAs. These observations are in accordance with the prevalent notion that subsets of microRNAs act in a coordinate manner to regulate signalling pathways in control of specific cellular programs.

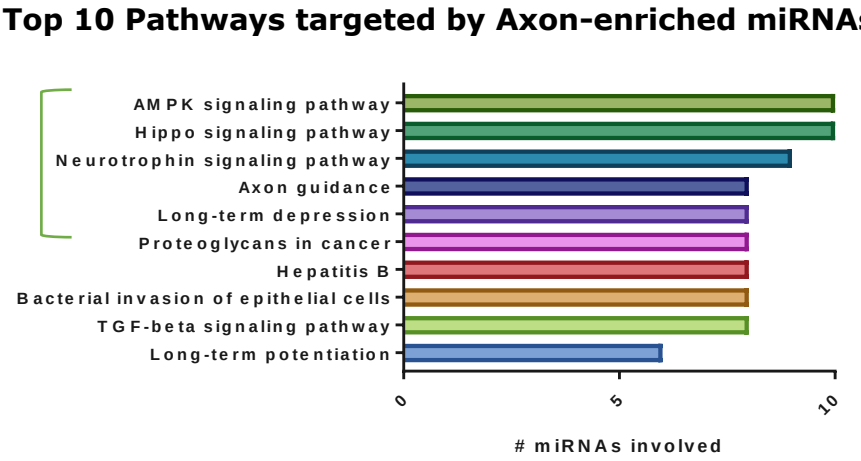


Figure 3. Molecular pathways predicted to be regulated by axon-enriched miRNAs. A bioinformatics analysis was performed to identify molecular pathways regulated by axonal miRNAs. This was conducted with miRPath v3 (part of DIANA Tools suit) by creating an overlap of the pathways predicted to be targeted by each individual miRNA. The graph shows the number of axon-enriched miRNAs predicted to regulate each pathway.

Following the identification of axon-enriched microRNAs, a functional screening was conducted to pinpoint microRNAs with functional roles in axonal development. For this, individual microRNAs were inhibited in cortical neurons and axon outgrowth was measured. Results suggested that miR-26a-5p, miR-708-5p, miR-434-3p, miR-151-3p, miR-99a-5p and miR-3470b are positive regulators of axon growth, whereas miR-16 acted as a negative regulator of axon growth, as previously described in rat sympathetic neurons (Kar et al. 2013). Conversely, miR-25 inhibition produced no effects on axon length (data not shown). Because we pinpointed axon-enriched microRNAs isolated from

developing axons growing in compartmentalised devices, it is possible that this approach is biased to the identification of growth promoting microRNAs.

Of interest, in a study conducted in parallel, Sasaki et al. used a neuron ball explant technique to quantify 375 microRNAs in axon and cell body fractions by RT-qPCR (Sasaki et al. 2014). A comparison of the subsets of axon-enriched microRNAs from both studies show little overlap. From those identified in Sasaki et al., miR-361, miR-532, miR-685, miR-720, miR-134, miR-181a-1, and miR-709, only miR-134 has been found by both studies. This reflects one of the major pitfalls of microRNA profiling, the lack of reproducibility resultant from different sample preparation and detection methods, making the unification of results a seemingly impossible task. In this specific case, the discrepancies might be due to the detection method, as although RT-qPCR is very sensitive and a more accessible detection method, its strength is limited by the number of microRNAs probed. Conversely, next generation sequencing allows for unbiased detection of all microRNAs present in the sample.

The preliminary study leading to the work in this thesis had some technical limitations related to the low number of biological replicates (only two were assayed), which prevented a more robust analysis of statistical significance. However, the data obtained proved to be very successful at identifying microRNAs with axonal actions, as demonstrated by our functional screen. Nevertheless, it is worth noting that each biological replicate is obtained from ~40 microfluidic cultures and thus variability across different axons and different cultures has been accounted for in each biological replicate.

Work in this thesis will focus in two of the two of the top axon-enriched microRNAs identified by this preliminary study, miR-99a and miR-3470b.

1.5 Exploring brain networks: How to investigate neuronal connectivity

The axon enrichment and functional studies that led to the work presented in this thesis suggested an important role for axonal microRNAs in the modulation of neuron connectivity via the control of axon growth. Thus, beyond the well characterised techniques for the identification of microRNA targets, and functional mechanisms, it was also important to identify relevant experimental approaches that would permit the investigation of functional neuronal networks.

1.5.1 Network activity

Cortical neurons in culture form neuronal networks over development that achieve a high level of complexity and, as they mature, exhibit intricate activity patterns (Luhmann et al. 2016).

The experimental platforms discussed in this section present several advantages in the study of neuronal networks. They allow entire networks of neurons to be monitored simultaneously, rather than in isolation, and thus enable the investigation of neuronal network dynamics. Despite representing a far simpler model in comparison to rodent brain slice cultures and *in vivo* preparations, cortical cultures have been successfully used to the study of network connectivity. Here, the experimental approaches employed later on in this thesis, will be described.

1.5.2 Microelectrode arrays

Microelectrode array technology uses microelectrode array devices (MEAs) for the detection of extracellular electric activity of neuronal networks *in vitro.* This platform consists of an array of 8x8 planar electrodes (figure 4) that allows for the non-invasive recording of neuronal activity in several sites of the culture simultaneously, providing insights on the spontaneous electrical neuronal activity at the network level (Jimbo 2007). Specifically, each electrode records the extracellular potentials of neurons located to its vicinity. In addition to spontaneous activity, MEAs allow for the stimulation of each

particular electrode of the array whilst recording the response of the network through the remaining electrodes. This feature has been successfully used to study the behaviour of the network in response to stimuli (Hales et al. 2012).

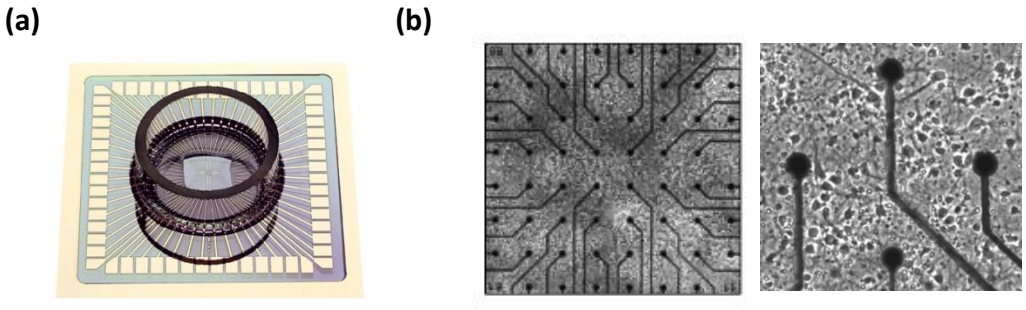


Figure 4. Cortical culture on microelectrode array. (a) Microelectrode array with 8x8 planar electrodes, cortical neurons are cultured on the central region of the glass ring (image adapted from Multichannel Systems). **(b)** Cortical primary culture on the microelectrode array. Overview of the culture on the full electrode array (left image) and a more detailed image of population of neurons cultured on microelectrode (right image).

Among several applications, including pharmacological and neurotoxicity *in vitro* studies (Chiappalone et al. 2003), this approach has been widely used to investigate neuronal communication within a network (Obien et al. 2014) and recently, Ito et al correlated the formation of dendritic synaptic densities with the electric activity of neuronal populations in long-term primary cultures (Ito et al. 2014).

Importantly, Chiappalone et al. investigated the profile of spontaneous network activity of primary cortical cultures on microelectrode arrays at different developmental stages, describing an increase of spontaneous network activity from day 5 and up to the third week in culture (Chiappalone et al. 2006). It takes neurons approximately one week in culture to start displaying electrical activity consistent with the establishment of functionally active synapses. The activity of the neuronal network increases and during the second and third week in vitro, the culture develops synchronization and bursting patterns that have been linked to network maturation and synaptic efficacy (Chiappalone et al. 2006; D. A. Wagenaar, Pine, and Potter 2006).

1.5.3 Calcium imaging

Calcium imaging of cortical networks can provide powerful insights into neuronal network function as intracellular calcium oscillations have been shown to be a reliable readout of neuronal electrical activity (Smetters, Majewska, and Yuste 1999; Takayama et al. 2009a). Calcium is an important second messenger, and following a burst of action potentials, depolarization of the neuron opens different voltage-gated channels, including voltage-gated calcium channels, resulting in a transient calcium influx. Such calcium transients can be monitored over time by using fluorescent calcium indicators, such as Fluo-5 AM, coupled with live cell microscopy (Grienberger and Konnerth 2012).

Over development in culture, primary cortical and, equally, hippocampal neurons display increasingly complex calcium oscillation patterns that correlate with network maturation (Blankenship and Feller 2010; Opitz 2002; Takayama et al. 2009a). Initially, cortical cultures show spontaneous oscillations in intracellular calcium concentration, without any synchronicity, and which appear within the first week of development *in vitro.* After the second week in culture, these evolve into periodic synchronised bursts of interconnected neurons, characterised by network-wide calcium waves (Maeda, Robinson, and Kawana 1995; Opitz 2002).

These synchronised calcium events are due to the periodic spontaneous generation of bursts of action potentials that propagate across the network (Kamioka et al. 1996; Maeda, Robinson, and Kawana 1995). This relies on underlying cellular processes such as neuronal survival, dendritic and axonal outgrowth and synapse formation and maintenance. In fact, the frequency of synchronous network-wide calcium events has been correlated to the increase in the number of synapses of the network (Muramoto, Ichikawa, Kawahara, Kobayashi, et al. 1993).

An important feature of spontaneous synchronous calcium events is their periodicity, intercalated by long mostly quiescent states between events, with tendentially stable frequency. Thus, this model provides a useful platform to study the basic mechanisms of network connectivity. It has been used to investigate the mechanisms underlying the emergence of spontaneous

network activity and synchronisation over development (Dravid and Murray 2004; Maeda et al. 1995; Verstraelen et al. 2014). Moreover, it offers an approach to study the effects pharmacological treatments, acute or chronically applied to the culture, and/or genetic manipulations in the formation and maintenance of network activity (Z. Cao et al. 2017; Cornelissen et al. 2013a).

1.6 Scope and Aims

This thesis attempts to extend the current knowledge of the factors in control of axon function as axons grow to establish precise neuronal connections during neuronal development. Work described here is centred on a class of such factors, microRNAs, small non coding RNAs with the ability to regulate gene networks that modulate the molecular signalling programs underlying axon development.

Following from previous investigations, this work explores the potential axonal roles of microRNAs recently identified in the axons of cultured mouse cortical neurons. In particular, it investigates how two axon-enriched microRNAs, miR-3470b and miR-99a, can modulate axonal function in developing axons, using primary mouse cortical cultures as a model. Furthermore, this work aims at exploring the impact of axonal microRNAs in the development of functional connectivity of cortical networks.

Specifically, Chapter 3 discusses the evolutionary implications of axonal microRNAs originated from repetitive elements embedded in mammalian genomes and focuses on the effects of miR-3470b, a mouse-specific microRNA, in axon outgrowth and in the electrical activity of cortical neuronal networks.

The role of the broadly conserved miR-99a in axonal outgrowth is investigated in Chapter 4. Moreover, this chapter examines the localised actions of miR-99a in cortical axons and identifies a novel miR-99a – target interaction mediating miR-99a effects in axonal development. Finally, the relevance of miR-99a function for the development of spontaneous calcium transient patterns is evaluated.

2. Methods

2.1. Animals and primary cortical cultures

All animal studies within this thesis were conducted in compliance with the ethics and animal welfare in place in the University, in accordance to the 1986 Animals (Scientific Procedures) act.

C57/BL6 mouse embryos in E16-E17 developmental stage were culled and their brains removed. The brain cortices were dissected and the meninges separated under a dissection microscope. The tissue was further incubated in Hanks Balanced Salt Solution (HBSS, Ca^{2+} and Mg^{2+}-free; Gibco) with 1mg/ml trypsin and 5mg/ml DNAseI (both Sigma) at 37°C/5% CO_2 for 30 min. Following treatment with 0.05% (v/v) trypsin inhibitor (Life Technologies), the tissue was washed in Neurobasal media (Gibco) and 5mg/ml DNAseI was added before mechanical dissociation of the tissue. The cells were finally washed in Neurobasal media and spun down at 250x g for 5 min. Dissociated cells were further resuspended and plated in Neurobasal media supplemented with 1x GlutaMax and 2% (v/v) B-27 (both Gibco), in accordance to experimental requirements. The procedure was conducted under sterile conditions and, whenever feasible, inside a class II cabinet.

2.1.1 Dissociated cortical cultures

Cortical cells obtained by the aforementioned procedure were resuspended in supplemented Neurobasal media to a final density of $10.0x10^6$ cells/ml. For functional assays (chapters 3 and 4), the cortical cell suspension was diluted down and plated in 6-well plates (Corning) containing 22x22mm glass coverslips (Menzel Glaser) at a final plating density of $1.75x10^5$ cells/cm^2 and incubated at 37^0C, 5% CO_2. Glass coverslips were previously coated with 50ug/ml poly-L-ornithine (PLO; Sigma-Aldrich) and washed twice with sterile distilled water. For immunofluorescence studies, cortical cells were seeded on PLO-coated coverslips at a density of $3.5x10^4$ cells/cm^2. For calcium imaging studies (Chapter 4), cortical cells were plated in PLO-coated Nunc dishes (8.8cm^2, Thermo Fisher), at a final plating density of $1.1x10^5$ cells/cm^2. For

long experiments (over 7 days in culture) the culture media was replenished with ¼ of its volume every 2-3 days.

2.1.2. Microfluidic cortical cultures

Two-channel microfluidic devices with a 150µm microgroove barrier across channels (SND150; Xona microfluidics) were used to compartmentalise axons of cortical neurons from their somato-dendritic compartment, in culture (chapters 3 and 4). The devices were prepared according to the procedure described in Garcez, Guillemot and Dajas-Bailador, 2016. Briefly, the devices were sterilised in 70% (v/v) ethanol, incubated in HBSS media overnight for removal of potentially toxic manufacturing by-products, washed in sterile water, and mounted onto well-dried PLO-coated (0.005% (w/v), overnight) glass coverslips (22mmx50mm) or Nunc dishes (8.8cm^2). Supplemented Neurobasal media was then added to both channels and the devices were left to equilibrate at 37^{o}C, 5% CO_2 for 1h. Following collection of excess media from the devices' reservoirs, the cortical neuronal suspension was added onto to the designated *soma channel* at a seeding density of 4.0x10^6 cells/ml and incubated for 30 min (37^{o}C, 5%CO_2) to allow for cell attachment to the substrate. The devices' reservoirs were then topped up with supplemented Neurobasal media and incubated at 37^{o}C, 5% CO_2. Culture media was

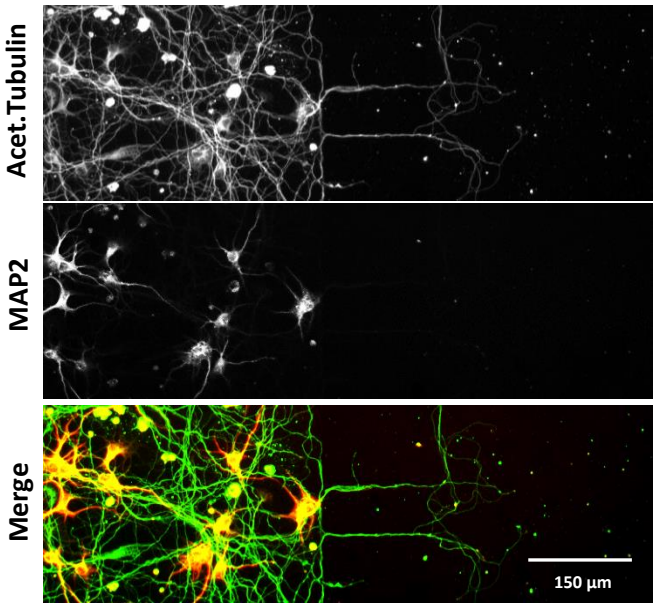


Figure 2.1 Map2 staining (red) of dendrites in microfluidic cultures at DIV8 shows that dendrites are restricted to the soma compartment. Axons extend to the axonal compartment (green, acetylated tubulin).

replenished 24h after plating and every 3 days thereafter. Axons were allowed to extend and cross the microgrooves to the side channel. Experiments were performed between 5-8 days *in vitro.*

2.2. Mammalian cell lines

Neuro2a and HEK293T cell lines were a kind gift from Prof. Robert Layfield lab. Cells were maintained and grown in Dulbecco's modified Eagle's medium (DMEM; Sigma) supplemented with 10% (v/v) fetal calf serum and 1% (v/v) Pen-Strep (both Sigma). For each experiment, cells were detached with 1x trypsin-EDTA (Sigma) and washed with supplemented DMEM. In all experiments, cells did not exceed passage 25 to prevent alterations in morphology (*in house* data).

2.3. RNA extraction

2.3.1. Dissociated cortical cultures

Primary cortical cultures were seeded at a density of $1.75x10^5/cm^2$ in 6-well plates and cultured as described above. Total RNA was isolated from cortical cultures at 4h, 24h after plating and then at day in vitro (DIV) 5, 9 and 12 by the phenol-chloroform extraction method using TRIzol Reagent (Invitrogen) for extraction of total RNA, in accordance to manufacturer's instructions. Briefly, culture media was removed and the cells washed with ice cold PBS (ThermoFisher), the cells were then scrapped and collected to 250µL of TRIzol (per well) into LoBind tubes (Eppendorf), homogenised and mixed with 1/5 volume of chloroform (ThermoFisher). Following centrifugation at 12000x g/ 4°C for 15 min, the aqueous phase was mixed with equal volume of isopropanol (ThermoFisher) and incubated at -20°C overnight. Total RNA was precipitated at 12000x g/ 4°C for 30 min and the pellet further washed twice in 75% (v/v) ethanol (12000x g/ 4°C, for 30 min; ThermoFisher). RNA pellet was left to dry until gel-like appearance and resuspended in Hyclone nuclease-free water (GE Healthcare).

All steps were conducted in an RNAse-free environment, using nuclease-free tubes and reagents, filtered pipette tips and, where adequate, on ice to

minimise the rapid RNAse-dependant degradation of the samples. All materials, equipment and surfaces were decontaminated with RNAZap solution (Sigma) before commencing the procedure. Quantification and quality of the RNA samples was assessed by UV spectrophotometry on a NanoDrop 2000 (ThermoFisher). Samples used for qPCR studies in this work showed a A280/260 ratio of 1.7-1.95 and the majority of the samples had a A260/230 ratio >2.0, consistent with low levels of protein or solvent contaminants.

To assess the quality of the total RNA obtained by this procedure, the Tapestation system (Agilent) was used to examine the integrity of the extracted RNA in representative samples. The RNA Integrity Number (RIN), a routinely used quality control parameter, results from an algorithm applied to the distribution and intensity of the peaks obtained by capillary gel electrophoresis and attributes a value within a 1-10 scale where 10 corresponds to highest integrity (Schroeder et al. 2006). RIN greater or equal to 7.5 is generally considered good by Agilent guidelines, all the samples evaluated showed a RIN>9.

2.2.2. Axonal RNA from microfluidic cultures

Total RNA was isolated from the axons and cell bodies of cortical microfluidic cultures at DIV8. At this time in development, the average length of the dendrites in similar density dissociated cortical cultures was 91.5 ± 50.23 µm (dendrite length of >120 neurons, not shown), which adds to previous evidence (figure 2.1) indicating that dendrites are not long enough to cross the 150µm microgroove barrier between the soma and axonal channels. The extraction procedure of purely axonal RNA is similar to described above for dissociated cultures, with some modifications to the sample collection step (figure 2.2). Culture media was removed from all four reservoirs and both channels were washed with ice cold PBS. TRIzol was added to the axonal channel for 2mins (20µL in each reservoir) and immediately collected to a LoBind tube, whilst PBS was kept in the *soma channel* (100µL/reservoir) to produce hydrostatic pressure and prevent backflow from TRIzol in the axonal channel to the soma channel, potentially causing contamination with RNA from the cell bodies. This process was then repeated for the soma channel. Both axonal and cell body samples followed the TRIzol method for extraction of

total RNA described above. Of note, total RNA isolated from ~40 microfluidic cultures was pooled together to form one biological replicate due to the inherent low input of biological material obtained with these devices, in particular from the axonal channel.

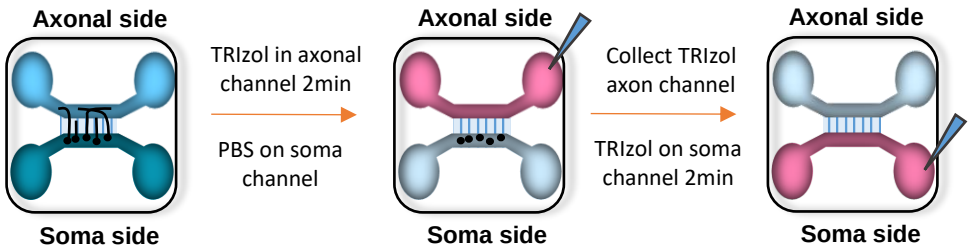


Figure 2.2 Schematic representation of the method to obtain axonal RNA from compartmentalised microfluidic cultures.

2.4. Quantification by real time qPCR

2.4.1. Real-Time qPCR of mature microRNAs

Reverse transcription of microRNAs was conducted using the miRCURY Universal cDNA synthesis kit (Qiagen) which adds a poly-A tail to mature microRNAs and uses a poly-T primer with a 3 mins degenerate anchor and a 5' universal tag to enable reverse transcription (RT) of ~21 nucleotide-long mature microRNAs. Real-time quantitative PCR (RT-qPCR) was performed using ExILENT SYBR Green Mastermix (Qiagen) using template cDNA or nuclease free water (non-template control; HyClone, ThermoFisher) on a 96-well plate layout. RT and amplification reactions were carried out as bellow:

RT reaction (10 µL)	
5x RT buffer	2µL
Hyclone water	4.5 µL
Enzyme mix	1 µL
Total RNA (5ng/µl)	2 µL
Spike in sp6	0.5 µL
RT reaction	42°C, 60min
Polymerase inactivation	95°C, 5min

PCR reaction (10 µL)	
SYBR master mix	5 µL
Primer set	1 µL
80x diluted cDNA	4 µL

PCR amplification	
Polymerase activation	95°C, 10min
Amplification	40 cycles 95°C, 10s 60°C, 1min

Table 2.1 microRNA RT-qPCR reaction composition and PCR amplification program

microRNA individual primer sets were acquired from the validated catalogue provided by Qiagen. ROX passive reference dye was incorporated in all reactions (1:50) to control for instrument born non-PCR related fluorescence fluctuations. UniSp6 RNA spike-in (Exiqon), a synthetic control template, was included in all RT-qPCR runs for quality control of cDNA synthesis and PCR reactions and as an inter-plate calibrator; runs were considered comparable when spike-in readings were <5% apart between plates. The amplification reactions were run on a StepOne Plus Real-Time PCR System (Applied Biosciences). A melting curve analysis of the PCR products was conducted in standard instrument conditions, at the end of each run, in order to verify the absence of primer dimers and the specificity of the amplification reaction for each target microRNA.

2.4.2. Real-Time qPCR of mRNA targets

cDNA was synthesised from 100ng of total RNA (10-30ng for axonal RNA) using SuperScript IV reverse transcriptase and Oligo(dT)$_{20}$ primer (both Invitrogen) as described in the table below. PCR amplification was undertaken using PowerUp SYBR Green (Applied Biosystems) as per manufacturer's instructions, using 1.5µL (5µl for axonal RNA) of template cDNA or nuclease free water (non-template control) per amplification reaction. As for microRNA RT-qPCR, amplification reactions were run on a StepOne Plus Real-Time PCR and also here melting curve analysis was conducted in standard instrument conditions, showing single melt curves for all primer pairs.

RT reaction (20 µL)	
Oligo d(T)20 primer	1 µL
10 mM dNTP mix	1 µL
RNA (20ng/uL)	5 µL
Hyclone water	6 µL
Primer annealing	65°C, 5min
5× Buffer	4 µL
100 mM DTT	1 µL
RNaseOUT RNase Inhibitor	1 µL
SuperScript IV	1 µL
RT reaction	50°C, 10min
Heat inactivation	80°C, 10min

PCR reaction (10 µL)	
SYBR master mix	10 µL
Primer set	0.8 µL
Template cDNA	5/1.5 µL
Hyclone water	7.7 µL

PCR amplification	
UDG Activation	50°C, 2min
Polymerase activation	95°C, 2min
Amplification	40 cycles 95°C, 3s 60°C, 30s

Table 2.2 mRNA RT-qPCR reaction composition and PCR amplification program

2.4.3. Real-Time qPCR analysis

Threshold was manually set to the same level for all targets and comparable plates and Ct (Cycle threshold) values were acquired using SDS2.3 software (Applied Biosystems). Data was analysed using the comparative $2^{-\Delta\Delta Ct}$ method to calculate relative expression of each target gene/microRNA (Bustin et al. 2009; Livak and Schmittgen 2001), according to the general formula:

$$Expression\ (geneX)\ in\ A\ relative\ to\ B = 2\ \hat{}\ -\ [\ (Ct_B - Ct_{Ref}) - (Ct_A - Ct_{Ref})\ ]$$

Where A and B represent two different conditions and Ct_{Ref} corresponds to the reference gene or set of microRNAs/genes used as internal control for data normalisation. The selection of internal controls followed specific criteria according to the individual characteristics of the different sample types.

microRNAs

Unlike RT-qPCR of mRNAs, there are no established reference candidates for microRNA RT-qPCR normalisation. Small nuclear RNAs, such as U6, were largely considered the gold standard for normalisation of microRNA data and their use is still widespread in the literature. However, growing evidence shows that these snRNAs are not stable in several biological processes (Gee et al. 2011; Peltier and Latham 2008), including cortical neuronal development (in house data, not shown). Although classified as small RNAs, snRNAs differ substantially from microRNAs in their transcription process, subcellular localisation and tissue/cell-specific expression patterns (Valadkhan and Gunawardane 2013), making them unsuitable as reference genes for microRNA data. Recent reports suggest the use of microRNAs as reference genes as they outperform snRNA normalisation. Global normalisation, where the mean expression of all microRNAs probed is used as reference value, has been suggested as the most reliable strategy. Where experiments focused on the expression of few microRNAs, a set of microRNAs was assessed for stability in the specific samples and experimental conditions assayed. The geometric mean of selected microRNAs deemed stable across conditions ($\Delta Ct < 1.5$, based in Mestdagh et al. 2009) was used as reference value for relative

expression calculation with the $2^{-\Delta\Delta Ct}$ method (Mestdagh et al. 2009; Peltier and Latham 2008; Schwarzenbach et al. 2015).

In studies of microRNA expression in cortical culture development, the choice of reference microRNA genes was advised by pilot RT-qPCR studies previously conducted in the lab. Of those, five candidate microRNAs were assessed over the five timepoints for this study (DIV1, 2, 5, 9, 12). Let-7a and miR-100-5p were selected as reference genes due to their stable expression across developmental stages (Bustin et al. 2009). The geometric mean of let-7a and miR-100 Ct values was used as reference value for normalisation and all data was analysed as relative expression to DIV1 (4h after plating), using the formula above (DIV1 = *condition A)*. Samples for each timepoint were collected from 5 independent experiments and each qPCR reaction performed in duplicate.

For axonal microRNA studies, the geometric mean of Ct values for the 25 axon-enriched microRNAs, as determined by miRNA-seq analysis available in the lab, was used as reference value for global normalisation. microRNA expression was calculated and presented as relative to the global mean, formula is as follows:

$$Relative\ expression\ miRNA = 2\ \hat{}\ -(Ct_{miRNA} - GeoMean_{all\ miRNAs})$$

Two independent axonal samples were used, each pooled from ~40 microfluidic devices, qPCR reactions were ran in duplicate.

mRNAs

In cortical culture development studies, of the candidate genes assessed as potential reference genes, GAPDH and UBE2 were found to be stably expressed across developmental stages and the geometric mean of both transcripts was used as reference value. Relative expression of HS3ST2 at different timepoints in relation to DIV1(4h) was calculated using the comparative $2^{-\Delta\Delta Ct}$ method as described above, where DIV1 = *condition A* (Vandesompele et al. 2002). This experiment was performed with the same total RNA samples used for microRNA cortical timecourse studies, a total of 5 independent biological samples, each read in duplicate.

For studies of *Hs3st2* expression in axonal RNA, *Hs3st2* levels were normalised to the levels of *Gapdh* using the formula in 2.4.3, both for axonal RNA and in RNA obtained from cell bodies in the soma channel (see 2.2.2). Total RNA from axon and cell body fractions were obtained from two different preparations, each read in duplicate.

2.5. microRNA functional analysis tools

Manipulating microRNA activity through the use molecular biology tools is a challenging task due to microRNA length (~20 nucleotides) and the sequence similarity within microRNA families, often differing by only one nucleotide. Widely used approaches include the use of plasmid-based overexpression of microRNA precursors for gain-of-function experiments and plasmids expressing transcripts carrying multiple microRNA complementary binding sites designed to sequester a specific microRNA for loss-of-function, termed microRNA sponges. Although successfully implemented by many groups, the efficacy of these plasmid-based strategies relies on the processing efficiency and resistance to degradation of the microRNA precursor or sponge transcripts designed, which are often difficult to predict and verify (Zhang, Shykind, and Sun 2012).

In this work as in previous studies from our lab (Dajas-Bailador et al. 2012), commercially available microRNA mimics and inhibitors (miRCURY LNA microRNA Mimics and Inhibitors, Qiagen) were used to manipulate the activity of specific microRNAs, miR-3470b (chapter 3) and miR-99a (chapter 4), in order to investigate microRNA-mediated effects in axon development. These are oligonucleotides that incorporate locked nucleic acid monomers, modified RNA analogs containing a 2'-O, 4'-C methylene bridge that locks the ribose in a rigid conformation, this significantly enhances their binding specificity and makes them resistant to nuclease degradation (Kaur et al. 2006).

MicroRNA mimics are used in gain-of-function studies to replicate the silencing activity of the mature microRNA of interest. These oligos bear a three-stranded RNA-LNA design in which one strand is identical to the endogenous mature microRNA and is complemented by two shorter passenger strands that

allow for incorporation to the RISC complex without non-specific star-like effects from the passenger strands (Bramsen et al. 2007). Thus, cellular internalisation of microRNA mimics increases the proportion of RISC complexes bearing the microRNA of interest thus potentiating its actions on target mRNAs.

microRNA loss-of-function was achieved using microRNA inhibitors, LNA antisense oligonucleotides bearing the perfect complementary sequence to the particular mature microRNA. LNA-based microRNA inhibitors strongly bind to and sequester the endogenous microRNA of interest thus blocking normal microRNA-mediated silencing in the cell (Naguibneva et al. 2006). Also used in this work were cell-permeable microRNA inhibitors that carry phosphorothioate modifications to their LNA backbone (miRCURY LNA microRNA Power inhibitors, Qiagen; chapter 4) which markedly improves their stability in culture, allowing for transfection-free incorporation into the cell. Another class of cell-permeable microRNA inhibitors used in this study are peptide nucleic acids (PNAs), high-affinity modified nucleic acids conjugated with a cell penetrating peptide to enable PNA delivery (PNA microRNA inhibitors, Panagene; Chapter 3).

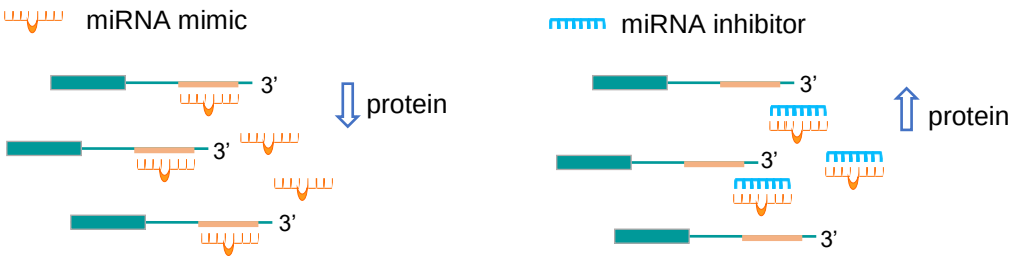


Figure 2.3 Mechanism of action of miRNA mimics and inhibitors.

All microRNA functional assays were controlled with the correspondent microRNA negative control, a non-targeting oligonucleotide (no homology to any known mouse, rat or human microRNA or mRNA sequence) with identical length and design to the microRNA-specific mimic or inhibitor. This control accounts for potential non-specific effects related to inherent oligo

cytotoxicity, transfection procedure or overload of the RISC complex in the case of microRNA mimics.

2.6. Functional assays on axonal growth

For all functional experiments, cortical primary cultures ($1.75x10^5$ cells/cm^2) were transfected 24h after plating using 5µL/well of Lipofectamine 2000 (LF 2000; Life Technologies) and 250ul/well of Opti-MEM reduced serum media (Life Technologies), in accordance to manufacturer instructions. Briefly, LF 2000 was incubated with 125ul/well of Opti-MEM for 15 min and, in parallel, plasmid DNA, siRNA and/or microRNA inhibitors/mimics were incubated with 125ul/well of Opti-MEM. These reactions were then mixed together and incubated for 30' at RT to allow for particle formation and, finally, loaded to the cells.

For experiments with microRNA mimics and inhibitors, miRCURY LNA microRNA inhibitors and inhibitor control or miRCURY LNA microRNA mimics and mimic control (all Qiagen) of miR-99a and miR-3470b at a final concentration of 25nM and/or 50nM were co-transfected with 1µg pmaxFP (Lonza, hereafter referred to as pGFP in all chapters).

In silencing experiments (chapter 5), a pool of siRNA specifically targeting HS3ST2, siHS3ST2 (mouse; siGENOME SMARTpool Dharmacon) or siRNA non-targeting control (mouse; siGENOME SMARTpool #2 Dharmacon) were cotransfected at final concentrations of 25 and 50nM with 1µg pGFP. For overexpression experiments (Chapter 5), 1µg of pcDNA3.1(+)-Zeo or pcDNA-HS3ST2 (see 2.7.2) were cotransfected with 1µg pGFP.

To rescue of the effects of miR-99a inhibition (chapter 5), cortical neurons were co-transfected with 1µg pGFP and 25nM inhibitor control or miR-99a inhibitor 25nM plus 35nM siRNA control or siHS3ST2. To test the rescue of miR-99a ectopic expression, cortical cultures were co-transfected with 1µg pGFP and either 25nM mimic control or miR-99a mimic plus 1µg of pcDNA3.1(+)-Zeo or 1µg of pcDNA-HS3ST2. pGFP was cotransfected in all functional experiments for detection of transfected neurons and visualisation of their morphology.

In all the aforementioned experiments, cortical neurons were fixed in 4% (w/v) paraformaldehyde (ThermoFisher) 72h after transfection (96h in culture), washed in PBS and either followed an additional immunofluorescence staining protocol (see 2.9) or were immediately mounted with Vectashield Hardset with Dapi mounting media (Vectorlabs) and further visualized under a 20x or 10x objective of a widefield fluorescence microscope (Axiovert 200M, Zeiss), using a CCD camera (Retiga 3000, QImaging) and Micro-Manager software (Edelstein et al. 2010).

2.6.1. Measurement of axon length in dissociated cortical cultures

Per condition, axons of 50 to 80 GFP-positive neurons where the axon was defined as the neurite with at least 3 times the length of any other neurite were measured using Fiji software (Schindelin et al. 2012). Axons were traced from the soma to the tip of the longest branch that is parallel to the principal projection (Figure 2.4, Dajas-Bailador et al. 2012). The data set of 4 to 6 individual experiments was later normalised to the respective control, with each condition corresponding to the length measurements of >200 axons.

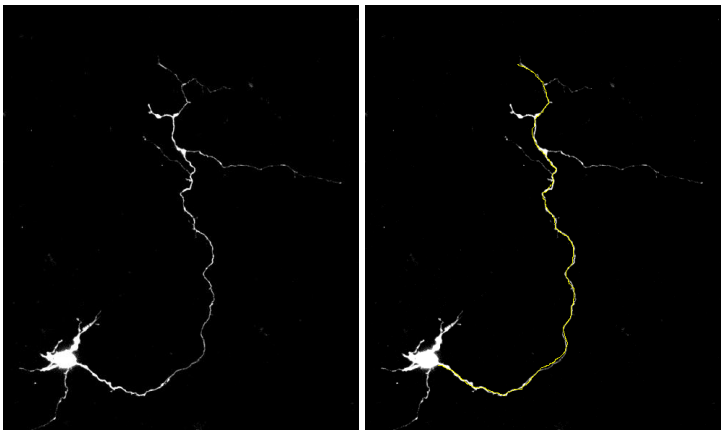


Figure 2.4 Measurement of axonal projection in ImageJ.
Axons were traced from the axon initial segment to the tip of the growth cone of the longest branch parallel to the direction of growth.

2.6.2. Measurement of axon length in microfluidic cortical cultures

Microfluidic cortical cultures were cultured for 5 days until the axons crossed the microgroove barrier to the *axonal channel*. The axonal channel was treated with cell-permeable Power inhibitor miR-99a or Power inhibitor control (Qiagen) at a final concentration of 100nM. A difference of volume of 50µl was maintained between the soma and axonal channels for fluidic isolation purposes. The same experimental setup was repeated for the soma channel to control for non-local effects. Live imaging of the axons in the axonal channel was performed immediately before treatment (time 0), 24h and 48h treatment, on Axiovert 200M microscope (Zeiss) under a 10x phase contrast lens. The whole area occupied by axons was imaged and the length of the axons was further measured in Fiji by tracing at least 50 axons per condition; each axon was traced from the start of microgrooves to the growth cone of the longest axonal branch. Due to the great variability between individual microfluidic cortical cultures, the data for the different timepoints of each microfluidic culture were normalized to time 0. At least 5 cultures were performed per condition and results were expressed as percentage of time 0.

2.6.3. HS3ST2 mRNA levels after RNAi transfections

In experiments of siRNA-mediated knockdown of HS3ST2, primary cortical cultures (seeding density $1.75x10^5$ cells/cm^2 in 6-well plates) were transfected with either 50nM siRNA control or siHS3ST2, as described section 2.6.1, this time without pGFP. Neuro2A cells were selected to determine the effects of miR-99a in HS3ST2 mRNA levels due to being an "easy-to-transfect" neuronal cell line (figure 2.5), in contrast with primary neurons. Neuro2A cells were seeded at $1.5x10^5$ cells/well in 12-well plates (Greiner) and transfected with miR-99a mimic or mimic negative control (to final concentration of 50nM), 1.5µL of Lipofectamine 2000 and 200µL of Opti-MEM. In both sets of experiments, 72h after transfection total RNA was extracted as described in 2.3.1, using 250µL/well of TRIzol for cortical cultures and 150 µL/well for Neuro2A cultures. HS3ST2 and GAPDH mRNA levels were quantified by RT-qPCR as in 2.4.2 using 5µL of template cDNA. Relative expression of *Hs3st2* was calculated as compared to control by the $2^{-\Delta\Delta Ct}$ method, using *Gapdh* as

reference gene. A total of three independent experiments were performed and each sample was quantified in duplicate readings.

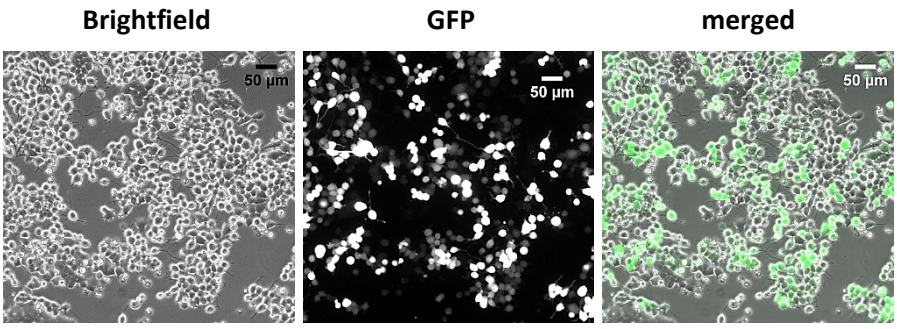


Figure 2.5 Neuro2A cells transfected with pGFP showing a high level of transfectability (10x magnification, GFP in green).

2.7 Cloning

2.7.1. Luciferase reporter constructs

Luciferase assays were carried out using reporter constructs with the dual-luciferase pmirGLO vector (Promega), which carries a firefly luciferase as the reporter of microRNA regulation and a renilla luciferase acting as an internal control for signal normalisation. The putative microRNA binding sites were synthesised as complementary oligonucleotides bearing the appropriate restriction site overhang with a 5'-phospho modification (~30bp oligos containing the putative microRNA binding site; Integrated DNA Technologies). Oligonucleotides used for Hs3st2 reporter assay were: Fwd – 5' CTAGCAT GCGGCCGCGACAAAAGCACATAATCTGCTGTTACGGGTAC and Rev – 5' TCGAC GTACCCGTAACAGCAGATTATGTGCTTTTGTCGCGGCCGCAT.

The complementary oligos annealed for 5min at 95°C followed by 15 min 37°C in annealing buffer (Promega) on the thermocycler (MasterCycle Eppendorf). The pmirGLO vector was digested with XhoI and NheI restriction enzymes in Cutsmart buffer and dephophorylated for 1h at 37°C (CIP, all NEB). Annealed

oligos were then ligated into pmiGLO XhoI/NheI restriction sites at 16°C, overnight using T4 ligase (NEB), transformed into XL10 Gold chemically competent E.coli (produced in house) and plated onto LB agar plates containing 0.1 mg/ml ampicillin. A NotI site included in the oligos design allowed for further screening of positive colonies by NotI digestion (37°C, 1h; NEB) of colony-derived plasmid DNA, which was purified by silica spin columns (Miniprep, Qiagen) and later visualised by DNA electrophoresis on a 1% (w/v) agarose gel (Sigma).

The mutated pmirGLO-HS3ST2 construct was obtained by site-directed mutagenesis using primer pairs bearing a mutated seed sequence (positions 2-5) and Phusion HF DNA polymerase (ThermoFisher) for PCR amplification of the full-length pmirGLO-HS3ST2 construct (Initial denaturation 95°C, 30s; 18 cycles: denaturation 95°C, 30s / annealing 55°C 1min / extension 68°C 8min). Oligonucleotides used for site-directed mutagenesis of Hs3st2 were Fwd - 5' GCA CAT AAT CTG CTG TTA TAA ATA CGT CGA CCT GCA GGC ATG and Rev - 5' GCA TGC CTG CAG GTC GAC GTA TTT ATA ACA GCA GAT TAT GT GC. After DpnI (NEB) digestion of the dam methylated parental plasmid, the dsDNA containing the seed-mutation was recircularised by T4 ligation and transformed into XL10 Gold cells, as described above. Colonies were screened for the presence of the mutation by Sanger sequencing (DeepSeq lab, University of Nottingham) using pmirGLO sequencing primer.

2.7.2. HS3ST2 expression construct

To build the pcDNA-HS3ST2 construct, HS3ST2 cDNA was PCR-amplified (table 2.3), Q5 High-Fidelity DNA Polymerase purchased from NEB) from the bacterial construct pGEM-HS3ST2 (Stratech) with primers designed to contain the entire HS3ST2 ORF and the appropriate flanking restriction sites (NheI/XbaI), compatible with subcloning of the amplicon into pcDNA3.1(+)-Zeo vector plasmid (a kind gift of Dr. Simon Dawson, University of Nottingham). Primer sequence as follows: Fwd-5' GCG CGC TAG CAT GGC CTA TAG GGT CC and Rev - 5' GCG CCT CGA GTC ACT CCC ACC GG. Both PCR product and pcDNA3.1(+)-Zeo were double-digested with NheI-HF and XbaI (NEB) at 37°C overnight and then purified by gel extraction (QIAquick Gel

Extraction kit, Qiagen) following manufacturer's instructions. The HS3ST2 amplicon was next ligated to the linearised plasmid with T4 ligase at 16°C overnight and transformed into competent XL10 gold cells, as described above. Colonies were screened by colony PCR using a standard taq polymerase PCR amplification and primers CMV-fwd and HS3ST2-rev. Positive colonies had their sequence confirmed by Sanger sequencing using BGH-rev and CMV-fwd sequencing primers.

PCR reaction (50 µL)	
5x Q5 buffer	10 µL
Hyclone water	4.5 µL
Q5 DNA polymerase	0.5 µL
Template DNA (100ng/µl)	0.5 µL
10µM Fwd primer	2.5 µL
10µM Rev primer	2.5 µL
10mM dNTPs	1 µL

PCR amplification	
Initial denaturation	98°C, 30s
Amplification	35 cycles 98°C, 10s 60°C, 30s 72°C, 30s
Extension	72°C, 2min

Table 2.3 PCR reaction and amplification program of HS3ST2 cDNA.

2.8. In vitro target validation: luciferase reporter assay

HEK-293T cells were seeded in 24-well plates (Greiner) at a seeding density of $1.0x10^4$ cells/mL. After 24h, cotransfection of 100ng/well of wild-type or mutated luciferase reporter construct and either microRNA mimic or mimic negative control at a final concentration of 100nM was performed in triplicate, using 1µL of Lipofectamine 2000 reagent and 100µL of Opti-MEM reduced serum media per well. Cells were harvested 48h after transfection in passive lysis buffer (Promega) for 30mins and further read with Dual Luciferase assay system (Promega) in the GloMax Multidetection System (Promega), following the manufacturer's instructions. Each sample was read in duplicate and the firefly luciferase/renilla expression ratios were obtained. A total of three independent experiments were conducted with three technical replicates per condition. Per experiment, firefly luciferase/renilla expression ratios from each condition were normalised to respective control.

2.9 Immunofluorescence

Cortical neurons cultured on coverslips or microfluidic devices were fixed in 4% (w/v) paraformaldehyde (3.6% sucrose (w/v), 1x PBS, 5mM $MgCl_2$, pH 7.4; ThermoFisher) for 30 min at RT, washed with 10mM Glycine in PBS and further permeabilised in PBS/Glycine-Triton (1x PBS, 10mM glycine, 0.2% (v/v) Triton X-100; Sigma) for 20 min. The cultures were then blocked for 1h at RT (overnight at 4°C for HS3ST2) with 3% (w/v) BSA in PBS (Sigma) and incubated with the following primary antibodies as appropriate, diluted in 3% BSA-PBS at 4°C overnight: anti-βIII tubulin (1:100; Abcam), anti-acetylated tubulin (1:300; clone 611B-1, Sigma), anti-synaptophysin (1:100; Dako clone SY38), anit-Map2 (1:100; Abcam), anti-HS3ST2 (1:100, incubation for 48h; Abcam). After 3x 5 min PBS-Triton 0.1% (v/v) washes, secondary antibodies Alexa Fluor 488 and 568 (1:300; Molecular Probes), were incubated where appropriate for 1h, washed 3x 5 min with PBS-Triton 0.1% and finally mounted with Vectashield Hardset mounting media with Dapi or without Dapi.

2.9.1. Quantitation of immunofluorescence signal

Neurons stained for HS3ST2 were imaged at 10x or 20x magnification and images were further processed with Fiji software. Cell bodies were manually selected and the parameters area, mean grey value and integrated density were measured. In order to correct for background in each image, 3 areas were selected around every cell. Total cell fluorescence (C.F.) per cell was given by the measured integrated density corrected for background, according to the formula:

$$\text{C. F.} = \text{Integ. Density} - [\text{Area of cell body X Average (mean grey value of background)}]$$

For quantification of endogenous HS3ST2 over development in culture, a minimum of 20 images were randomly acquired and >60 neurons measured in each timepoint, DIV 2, 5 and 12. In each experiment, data from all timepoints was normalised to the average of C.F. at DIV2 and a total of three independent experiments were conducted.

For quantification of HS3ST2 levels after miR-99a mimic transfection, >50 GFP-positive neurons were imaged per condition and HS3ST2 C.F. analysed as above. A total of four independent experiments were conducted, in each set of data obtained for C.F with miR-99a mimic, this was normalised to the average C.F. of control.

2.10. Primary cortical cultures on microelectrode arrays

Primary cortical neurons were prepared as described above and 20µL of the suspension was plated in microelectrode arrays (Multichannel Systems) at a plating density of $2.5x10^6$ cells/ml, left to attach to the substrate for 20 min and later toped up with 1mL of media (Neurobasal supplemented with 1% (v/v) Glutamax, 2% (v/v) B27, Life Technologies). The cortical cultures were incubated at 37ºC, 5%CO_2 for 21 days and approximately 30% of the media replenished with fresh media every 3-5 days. The extracellular electrical activity of the cultures was recorded at DIV5, 9, 13, 14, 15, 16, 17, 18, 19 and 21. For studies of miR-3470b function, transfection was performed by application of 75nM cell-permeable PNA-miR-3470b inhibitor (Panagene) or PNA inhibitor control. The signal was processed using MCRack software (Multichannel Systems) and further analysed with Matlab using workflows developed in house. This work was done is collaboration with Nitzan Herzog, Noah Russell lab, who performed the analysis with an *in house* script developed in Matlab.

2.11. Calcium imaging of cortical cultures

2.11.1. Loading of Fluo-5 and measurement of calcium transients

Fluo-5 AM (Molecular Probes), a fluorescent calcium indicator, was used to monitor intracellular calcium transients in cortical networks at DIV9 after silencing of miR-99a with a cell-permeable miR-99a inhibitor (LNA miR-99a Power inhibitor) or correspondent inhibitor negative control (LNA Power inhibitor control) at DIV6. Fluo-5 AM was mixed to equal volume of 20% Pluronic F-127 (Molecular Probes) to help disperse the non polar ester in imaging buffer (135mM NaCl, 3mM KCl, 10mM HEPES, 15 mM glucose, 1mM

$MgSO_4$, 2mM $CaCl_2$, pH 7.4). Primary cortical cultures were incubated with the 1µM Fluo-5 AM in imaging buffer for 30 min at RT for dye loading, washed twice with imaging buffer and next incubated with imaging buffer for 30 min at RT for de-esterification of intracellular AM esters. Spontaneous activity was recorded for 900s at which point 100mM KCL was added by buffer exchange and activity recorded for further 60s. Cultures were imaged at 10x magnification on a Nikon Elipse Ti microscope equipped with Cool LED pE excitation system and ANDOR Zyla sCMOS camera; images were acquired at 1 frame/sec over 960s with Micro-Manager 1.4. Data was obtained from a total of five independent experiments.

2.11.2. Image analysis

Images were pre-processed using Fiji software. Briefly, cells in the field of view were automatically detected using the maximum intensity z-projection of the images after KCl depolarization to define the regions of interest (ROI) correspondent to each cell. Selections were then adjusted using binary mask tools and only cells showing a sustained response to KCl depolarization at the end of each recording were considered for further analysis (Pickering et al. 2008). Average cell fluorescence was measured for each set of images (mean grey value; >100 cells per condition, 900 frames). Analysis of calcium transients was conducted using the Matlab package developed by the Meaney lab (Patel et al. 2015) termed Fluorescence single neuron and network analysis package (FluoroSNNAP), in Matlab 2015b.

The baseline fluorescence (F_0) was calculated as the average of the lower 50% of the previous 60s for every frame, to adjust for photobleaching artefacts over the time of recording. Additionally, background fluorescence was measured in all frames and subtracted from all ROIs in each frame. $\Delta F/F_0$ was calculated by subtracting each value of the average fluorescence of the pixels within a ROI in every frame with the value of F_0 and dividing it by F_0, obtaining this way, a calcium trace for each cell over time. Spontaneous calcium events were called when $\Delta F/F_0$ exceeded the threshold of 15% above the baseline ($\Delta F/F_0 > 0.15$), thus obtaining the calcium trace for each cell over time. The number of calcium events per cell was calculated by averaging the number of

detected calcium events for every neuron in each condition; the mean amplitude per cell was calculated by averaging the mean fluorescence signal ($\Delta F/F_0$) at the peak of a calcium event for every neuron, in each condition; the mean interspike interval (ISI) was obtained by the averaging the mean interval, in seconds, between two subsequent calcium events obtained per neuron, for all neurons of each condition. Synchronised events were defined as a synchronous network event in which >80% of the cells show a calcium event within a 2s window before and after the peak of the synchronised event. Asynchronous events were all calcium events that were not included within a synchronised event and the number of asynchronous events per cell was given by the averaging the mean number of asynchronous events per cell, for all neurons in each condition. Cells with calcium events lasting >5s were removed from the analysis as it is glia rather than neurons that often show such lengthy transients (Cao et al. 2013). Raster plots and single cell transient kinetics were obtained in FluoroSNAPP; calcium traces were plotted in Graphpad Prism 7.0.

2.12. Synaptosomes (Appendix I.1)

The isolation of synaptic fractions, termed synaptosomes, from the mouse brain (C57/BL6 strain) was conducted by subcellular fractionation, in accordance to the method detailed in Smalla, Klemmer, and Wyneken 2013. Briefly, cortical tissue of P14 or P21 mice were homogeneised at 10mL/g tissue using a dounce homogeneiser in suspension buffer (320mM sucrose, 5mM HEPES, 0.1mM EDTA, 1mM DTT pH 7.4) supplemented with protease inhibitors cocktail (mammalian; Sigma) and RNAse inhibitors (Sigma) and centrifuged at 1000xg/20 min to pellet down nuclei and cell debris; this was repeated twice. Supernatants were combined, spun for 20 min at 12000xg twice to separate the crude synaptosome fraction (pellet) from the cytosol fractions. The crude synaptosome fraction was next resuspended at 1.5mL/g tissue in gradient buffer (320mM Sucrose, 5mM Tris-HCl, pH 8.1) and loaded onto a sucrose gradient composed of G1 (1.2M sucrose in 5mM Tris-HCl, pH 8.1) and G2 (1.0M sucrose in 5mM Tris-HCl, pH 8.1). After ultracentrifigation at 100,000xg for 2h (Optima LE-80K, Beckam), the purified synaptosome fraction was collected from the interphase of G1 and G2.

For RNA isolation, 150µL of the purified synaptosome fraction was homogeneised with 300µL TRIzol and the total RNA extracted following the procedure described in 2.3.1. RT-qPCR detection of microRNAs was conducted as outlined in 2.4.1 in two independent synaptosome preparations of P14 and P21 pups and later analysed with the comparative method described in 2.4.3 for global normalisation. For western blot analysis, protein in the synaptosome fraction was extracted with 150µL of RIPA buffer (150mM NaCl, 5mM EDTA, 10mM Tris, 1% (v/v) NP-40, 5% (v/v) sodium deoxycholate, 1% (w/v) SDS) and centrifuged for 20 min at 12,000xg; the supernatants were collected and run on a 12% SDS-PAGE gel. Following protein transfer to a polyvinylidene difluoride membrane (Merk-Milipore), the blots were blocked with 5% skimmed milk in TBS-T (0.1% (v/v) Tween, 150 mM NaCl, 50mM Tris-HCl, pH 7.5) for 1h and further probed with anti-synaptophysin (1:1000, Dako clone SY38) and anti-p53 (1:1000) in 1% skimmed milk in TBS-T overnight at 4^{o}C, followed by 3h incubation with horse peroxidase-conjugated secondary antibody in 1% skimmed milk in TBS-T (1:4000, Pierce). The signals were developed with ECL substrate (SuperSignal West Femto Maximum Sensitivity Substrate, ThermoFisher) and imaged on a Fujifilm LAS-3000 Imager Mini.

2.13. microRNA expression in human samples of frontal cortex (Appendix I.2)

Human brain samples of frontal cortex were provided by the Bristol Brain Bank through Brains for Dementia Research, UK. The cohort comprised 8 Alzheimer's disease (AD) patients and 8 age and gender matched control subjects. Patient data and Braak tangle stage is depicted in table 2.4. Samples originate from the BA9 area of the frontal cortex by flash-freezing at the post-mortem delay times indicated in table 2.4. Frozen brain samples (~20mg of tissue) were homogeneised in 500µL TRIzol with a dounce homogeneiser, followed by a standard total RNA extraction procedure as described in 2.3.1. Quantification of miR-99a expression levels by RT-qPCR was performed as outlined in 2.4.1. Expression of miR-99a was calculated relative to control samples by the $2^{-\Delta\Delta Ct}$ method, using the geometric mean of miR-125b-5p and miR-100-5p as reference (see 2.4.3).

	Sex	Age	PM delay (h)	Braak tangle stage
Healthy individuals	F	86	38.5	I
	F	94	29.5	II
	F	82	36	II
	F	89	26.5	II
	M	96	21	II
	M	78	51.5	II
	M	92	56.5	I
	M	86	44.25	II
AD patients	F	85	14	V
	F	82	22	V
	F	57	63	VI
	F	90	21.25	VI
	M	91	43	VI
	M	92	30.5	V
	M	70	32.25	V
	M	63	21.25	VI

Table 2.4. Patient cohort demographics and clinical data. Table shows age, sex, post-mortem delay (PM delay in hours) from time of death to sample collection, and Braak tangle stage for the AD patients and healthy subjects selected for this study. Braak staging identifies plaque and tangle distribution at different stages of Alzheimer's disease progression. Stages V and VI refer to extensive cortical involvement of neurofibrillary tangles. AD: Alzheimer's disease.

2.14. Statistical analysis

All data analysis and statistical evaluation were carried out in Graphpad Prism (version 7.00 for Windows, GraphPad Software, La Jolla California USA, *www.graphpad.com*). All data was tested for the assumption of normal distribution (Shapiro-Wilk normality test). In axon outgrowth experiments, the inter-experimental variability of the absolute values of length distribution is a confounding factor for analysis. To account for this, length data was normalised to the mean length of the control neurons within each experiment, therefore the mean of the control length becomes 100% for all biological replicates. Statistical evaluation between two groups was performed using One-Sample Student's t-test, considering a hypothetical value of 100. Analysis of more than two groups were carried out using One-way ANOVA with Tukey's or Dunnett's *post hoc* analysis. All data are presented as mean ± standard

deviation (mean±S.D.) or mean ± standard error of the mean (mean±S.E.M.), as appropriate.

3. Axonal microRNAs derived from repetitive elements

3.1 Introduction

3.1.1 Evolution of microRNAs

MicroRNAs have the intrinsic capacity to affect the expression of hundreds of genes, with the potential to have a high impact in gene regulatory networks and, importantly, in the diversification of phenotypes during the evolution of different species (França et al. 2017; Meunier et al. 2013).

In metazoans, the bigger waves of microRNA expansion throughout animal genomes occurred at times of great evolutionary innovation, with several studies supporting the contribution of microRNA-dependant regulatory networks to organism complexity (Heimberg et al. 2008; Meunier et al. 2013). Indeed, accelerated rates of microRNA generation coincide with periods of dramatic changes in body plan, tissue organization and specialisation associated with the bilateral split, emergence of vertebrates, early stages of placental mammals radiation and later, the rodent-primate split (Iwama et al. 2013, Berezikov 2011). These findings are consistent with the observed correlation between the number of microRNAs and organism complexity (Meunier et al. 2013, França et al. 2017).

The current count on genes encoding for human microRNAs annotated in miRBase is near the 2000 figure (miRBase release 22, March 2018), a number comparable to other classes of trans-regulators of gene expression, such as transcription factors. However, an important advantage of microRNAs is that, unlike transcription factors, their genes appear to undergo fast turnover and can be easily acquired and lost in the course of evolution (Iwama et al. 2013; Lu et al. 2008; Meunier et al. 2013) In fact, microRNAs are known for their rapid evolutionary dynamics and equally high rates of novel microRNA formation and degeneration, with newly formed families being lost soon after formation (Meunier et al. 2013). Still, microRNAs have accumulated through evolutionary time and are constantly added to metazoan genomes, with newly formed microRNAs being rarely lost once they have find a function (Hertel et al. 2006; Meunier et al. 2013) This leads to a seemingly paradoxal feature of microRNAs, where despite their relatively rapid and dynamic evolution, are

frequently fixed in the common ancestor genome and tend to be kept throughout their clade, with several microRNAs being conserved amongst vertebrates. These characteristics place microRNAs in a privileged position that provides them with a significant capacity for the modulation of regulatory networks during species diversification (Berezikov 2011; França et al. 2017).

When investigating the evolutionary origins of human microRNAs, Iwama et al reported that just over half of all human microRNAs emerged in the simian lineage to human, whereas 28% originated in the early stages of placental radiation and only 15% of all human microRNAs are found beyond placental mammals. An appealing hypotheses for the emergence of human-specific microRNAs has been explored by Somel et al where, by comparing microRNA expression data from macaque, chimpanzee and human brains, the authors proposed that microRNAs may have played a crucial role in shaping the gene expression patterns underlying cognitive evolution (Santpere et al. 2016; Somel et al. 2011)

The genomic sources of novel microRNAs can be varied, with introns being a major genomic donor of new microRNAs (Berezikov 2011). Indeed, hairpins that rise in intronic regions of coding genes bear the added value of an existing promoter, allowing novel microRNA gene sequences to link their expression to their host's transcription regulation (Rodriguez et al. 2004). Gene duplication is another important mechanism for the generation of new microRNAs, and microRNA families in particular tend to be formed by gene duplication events in the same (tandem) or in different chromosomes (non-local), giving rise to paralogous microRNAs. These duplicated sequences may then evolve through independent mutations to generate a new microRNA with novel functions (Hertel et al. 2006; Shabalina and Koonin 2008). The work presented here will focus on a third important genomic source for novel microRNA formation: transposable elements.

3.1.2 Transposable elements: the Good, the Bad and the Evolutionary

The completion of the human genome project at the turn of the century revealed that nearly half the size of the human genome derives from

transposable elements, so-called "jumping genes", which are able to replicate and mobilise from site to site within genomes (Lander et al. 2001; Smit 1999). This is not limited to humans, as transposable elements (TEs) comprise half the size of most mammalian genomes, which is particularly remarkable when we consider that protein coding regions account for less than 1.5% of the mammalian genome (de Koning et al. 2011). Overall, these findings demonstrate the potential impact of TEs on their host genomes.

TEs fall into two major classes, based on their replication mechanism. Class II TEs are DNA transposons that mobilise via a "cut-and-paste" mechanism involving DNA intermediates, whereas Class I TEs are called retrotransposons and use a "copy-and-paste" strategy involving RNA intermediates (Chuong, Elde, and Feschotte 2017; Cordaux and Batzer 2009; Feschotte 2008). In this process, these RNA intermediates are transcribed from the retrotransposons and serve as a template for the synthesis of cDNA that can then be inserted into new locations in the genome, originating new copies (Kramerov and Vassetky, 2005).

3.1.3 Retrotransposons

Retrotransposons are by far the most abundant class of TEs found in mammalian genomes, including mice and humans (Kramerov and Vassetzky, 2011). Unlike currently inactive DNA transposons, some retrotransposons are still capable of retrotransposition in humans and mice (Kramerov and Vassetzky, 2011; Mita and Boeke, 2016). Retrotransposons can be further classified into long terminal repeat (LTR), which are similar to retroviruses both in terms of their structure and mechanism, and non-LTR. This latter group includes long interspersed nuclear elements (LINE) and short interspersed nuclear elements (SINE), and are non-autonomous retrotransposons which rely on LINE machinery (specifically L1 elements) for retrotransposition (Kramerov and Vassetzky, 2011).

Although their discovery dates back to the work of Mcklinton on maize transposons in the 1940s (McClintock, 1951), nearly four decades had to pass for us to begin to understand the ways in which TEs interact with their genomic environment (Feschotte 2008; Krayev et al. 1980; Muotri et al. 2007). TE insertions into the genome often disturb gene expression and have deleterious

consequences, as documented by the extensive catalogue of disease-causing *de novo* insertions (Scarfò et al. 2016), particularly in the nervous system (Larsen et al. 2018; Reilly et al. 2013). On the plus side, TEs are also an extraordinary source of sequence innovation and genomic plasticity and are now widely regarded as important drivers of evolution (Cordaux and Batzer 2009; Feschotte 2008; Göke and Ng 2016; Lu et al. 2017).

Once inserted into a genome, TEs can acquire novel functions and change regulatory gene expression networks (Chuong et al. 2017; Mita and Boeke 2016). In particular, retrotransposons have been involved in the generation of new cis-regulatory elements such as enhancers and promoters of neighbouring genes and contributed to isoform diversity when integrated into protein coding genes (alternative splicing) (Häsler and Strub 2006; Polak and Domany 2006). As LINEs and SINEs sequences bear Pol II and Pol III promoters respectively (Kramerov and Vassetzky, 2011), new insertions can even originate novel genes (Perrat et al. 2013). Indeed, retrotransposons are thought to underlie the formation of lncRNA, circRNAs and microRNAs (Cartault et al. 2012; Hadjiargyrou and Delihas 2013)(see below, section 3.1.5) and TEs as a whole have contributed significantly to transcriptional diversity among different organisms (Erwin, Marchetto, and Gage 2014; Perrat et al. 2013; Polak and Domany 2006). Additionally, due to their mechanism of colonization, TEs are much less conserved when compared to protein-coding sequences and are often lineage and species specific, which supports their role in species diversification during evolution (Göke and Ng 2016).

Alu and B1 elements are the most abundant SINEs in humans and mice, constituting 11% and 7% of the human and mouse genomes, respectively (Quentin, 1989; Kramerov and Vassetzky, 2011; Dridi, 2012). Both originated from the common ancestor small RNA 7SL RNA, which colonized mammalian genomes before the primate-rodent split approximately 80 million years ago (Kass, Raynor, and Williams 2000). These TEs continued to be active in each germline and regulator factors/genes arising from them are normally evolutionarily new in their germline and not conserved (Cordaux and Batzer, 2009; Kramerov and Vassetzky, 2011). As a result, copies of Alu and B1 elements have amplified and duplicated independently in the two genomes, while simultaneously accumulating mutations which frequently result in loci with little resemblance to the original 7SLRNA sequence (Umylny et al. 2007).

It is therefore possible that the true impact of Alu/B1 colonisation in the human and mouse genomes is underestimated (Cordaux and Batzer 2009; Tsirigos and Rigoutsos 2009). As in other SINES, Alu and B1 sequences contain a PolIII promotor and a poly-A tale, but rodent B1 elements are approximately half the length (~135bp) of primate Alus (~300bps) and resemble the left arm of Alus (Deininger 2011; Quentin 1989; Veniaminova, Vassetzky, and Kramerov 2007). Nevertheless some lines of evidence show that B1 elements might have taken much similar functional paths to Alu elements over the course of rodent evolution (Tsirigos and Rigoutsos 2009).

3.1.4 Relevance of SINEs as motors of novelty in the evolution and function of the nervous system

Growing evidence suggest SINEs (as other TE classes) may have a significant role in the evolution and function of the mammalian brain (Erwin et al. 2014; Garcia-Perez, Widmann, and Adams 2016; Linker et al. 2017). SINEs were found to act as enhancers for host genes with neuronal function, particularly those associated with neurodevelopment (Santangelo et al. 2007). In effect, one of the first reports of a functional TE insertion in the nervous system describes an ancient SINE insertion in tetrapods that drives the expression of LIM homeodomain transcription factor Islet1, a gene required for specification of spinal cord motor neurons (Bejerano et al., 2006). Similarly, an ancient SINE integrated into the proopiomelanocortin gene functions as a tissue-specific enhancer in the mouse ventral hypothalamus and is conserved in humans (Santangelo et al. 2007). Another example is the mammalian-specific AmnSINE1 insertions associated with fibroblast growth factor 8 (FGF8), which act as neural-specific enhancers in transgenic mice and regulate FGF8-dependant forebrain patterning during brain development (Sasaki et al. 2008). Moreover, TE insertions have originated novel genes relevant for neuronal function, one of the most notable examples is Arc, well known for its role in synaptic functions and long-term memory formation, and which derives from a Ty3/Gypsy LTR insertion (W. Zhang et al. 2015).

Of the SINEs class of TEs, primate Alu and mice B1 elements are present in neural tissue and are expressed in neuronal progenitors in early stages of

embryonic development (Ohnishi et al. 2012; Smalheiser 2014). However, the function of the majority of these transcripts remains unknown (Garcia-Perez et al. 2016; Ohnishi et al. 2012).

Expression of Alu/B1 transcripts was found to be induced by stress insults to cells, such as heat shock and viral infection (Dunker et al. 2017; Li et al. 1999; Liu et al. 1995), presumably acting to repress mRNA transcription in response to heat shock (Ponicsan, Kugel, and Goodrich 2010). Of note, B1 and B2 elements were induced in CA1 hippocampus of gerbils one day after global ischemia, suggesting these transcripts can also be stress-inducible in the adult brain (Kalkkila et al. 2004). In age-related macular degeneration, accumulated Alu/B1 transcripts appear to be pathological to retinal pigment epithelial cells. Interestingly, degradation of the deleterious Alu/B1 transcripts is mediated by Dicer1 (Kaneko et al. 2011).

BC200 and G22 are two of the better known functional Alu transcripts found in the nervous system of primates where they act as inhibitors of translation initiation (Khanam et al. 2007). These neuronal small non-coding RNAs are enriched in dendrites where they have been suggested to aid local protein synthesis and, in transgenic mice overexpressing either transcripts, they are actively transported to the dendritic compartment (Eom et al. 2011; Khanam et al. 2007; Tiedge, Chen, and Brosius 1993). In rodents, the brain specific repeat-derived con-coding RNA, BC1, exhibits a similar dendritic localisation and function as its primate analogous (Smalheiser 2014; Tiedge et al. 1991), and is regulated by synaptic activity (Zhong et al. 2009).

Overall, TEs are now recognised to underlie the formation of several non-coding RNAs with relevance to the evolution, development and function of the nervous system, including lncRNAs, circRNAs enriched at the synapses (Hadjiargyrou and Delihas 2013; Larsen et al. 2018) and, importantly in this work, microRNAs (Qin et al. 2015; Roberts, Cardin, and Borchert 2014).

3.1.5 The birth of microRNAs from transposable elements

Transposable elements were long overlooked as a potential mechanism for the origin of microRNAs, as computational analysis of microRNA genomic context

often excluded repetitive elements, which were, until recently, considered non-functional parasitic genomic sequences (see sections above). The realisation that TEs are rapidly evolving sequences with functional and, importantly, regulatory potential (Feschotte 2008; Ponicsan et al. 2010) spiked the interest of researchers on the possible contribution of these mobile sequences to the origin of novel microRNAs in the course of evolution. Indeed, Smalheiser and Trovik were the first to propose this idea and the first to model a generation mechanism of novel microRNAs from TEs, in which two TEs insert to the genome (within introns of coding genes, for example) in adjacent positions but opposite orientations (Smalheiser and Torvik 2005). Subsequent transcription can lead to the formation of a new hairpin that may be further processed by drosha and the microRNA biogenesis machinery, resulting in a putative mature microRNA sequence with regulatory potential. Later, several studies corroborated these observations (Borchert et al. 2011; Jittima Piriyapongsa, Mariño-Ramírez, and Jordan 2007; Roberts et al. 2014; Yuan et al. 2011) and showed that microRNAs can also originate from the whole or partial sequence of a unique TE. This is due to the intrinsically palindromic sequence of some TEs, such as Alu elements, which make them good sequence donors for novel hairpin formation (Qin et al. 2015). Available evidence from independent studies indicates that approximately 15% of microRNAs in human and mouse originate from TEs (Borchert et al. 2011). Although this proportion seems lower than expected when considering that TEs occupy nearly half of the human and mouse genomes, it is likely a low estimation, as the rate of evolution in older TE insertions is expected to render them unrecognisable to current computational approaches. Also, many uncharacterized microRNAs probably remain to be identified.

The genomic novelty introduced by TE sequences could also provide a mechanism for the generation of microRNAs that are specific to a lineage or species and could exert diversifying effects in evolving organisms (Yuan et al. 2010). In an attempt to evaluate the contribution of TEs to human microRNA using a computational approach, Piriyapongsa et al. identified several TE-derived microRNAs that are poorly conserved and unique to the taxa (J Piriyapongsa, Marino-Ramirez, and Jordan 2007).

Importantly, Alu/B1 elements can be responsible for *de novo* microRNA-mRNA target interactions (Smalheiser and Torvik 2006). Several computational studies revealed that TE elements embedded in regulatory regions of coding genes show complementarity to TE-derived microRNAs (Daskalova et al. 2007; Filshtein et al. 2012; Smalheiser and Torvik 2006). More recently, a few reports validated these findings experimentally. For example, the human miR-1285-1 is an Alu-derived microRNA and was shown to target Alu-derived microRNA binding sites within the 3'UTR of its putative targets, EIF2S3, CHST6 and CBFA2T2, by luciferase reporter assays (Spengler, Oakley, and Davidson 2014).

The observation that TE-derived microRNAs tend to be evolutionary new and regulate correspondent TE-derived regions within their target mRNAs serves to show the relevance of TEs in the establishment of microRNA-regulatory networks in the course of evolution. Indeed, TE-derived microRNAs are thought to co-evolve with their targets (Lehnert et al. 2009).

From a neurodevelopmental perspective, as the fundamental mechanisms of axon growth, guidance and synaptic transmission have deep evolutionary roots and are well-conserved across animals, one could hypothesise that evolutionarily new microRNAs have no relevance to these processes. However, the formation of neuronal circuitry isn't a binary system, instead it is modulated by a plethora of gene networks that account for differences between species. As these gene networks are under microRNA-dependant regulation, the emergence of new microRNA-target interactions can contribute to the evolution of neuronal connectivity.

3.1.6 Aims

In light of the potential relevance of evolutionarily new microRNAs to neuronal processes, this chapter analyses the genomic context and conservation of the top 20 axonally enriched microRNAs previously identified in our lab by enrichment analysis of axonal vs cell body miRNA-seq data (described in section 1.7). In particular, this study focus on the axon-enriched miR-3470b, a mouse-specific microRNA, and aims at dissecting its genomic context and

ascertain whether this evolutionarily recent microRNA may have acquired functions in the development of the axon and formation of neuronal network activity in developing primary cortical cultures.

In brief, the specific experimental aims of this chapter are:

- Conduct a computational comparative analysis of the genomic origin of non-conserved microRNAs enriched in cortical axons;
- Define the genomic origin of miR-3470b from TEs;
- Examine the effect of miR-3470b in axonal outgrowth of developing cortical neurons and its regulation over development of cortical cultures;
- Evaluate the impact of miR-3470b inhibition on the development of spontaneous network activity using cortical neurons cultured on microelectrode arrays.

3.2. Results and Discussion

3.2.1 Genomic context of axonal miRs

After establishing the microRNAs that are present in the axon of developing cortical neurons, it was important to analyse their genomic context and conservation. The investigation was focused on the top 20 axon-enriched microRNAs, and in order to examine microRNA conservation within animals, their respective orthologs in the Metazoa taxa, namely in the worm, fly, fish, rodents, primates and human were identified. For this, a database of annotated microRNAs (miRBase) that have been confirmed by published microRNA sequences and not just predicted by genomic studies was employed. Of the top 20 axon-enriched microRNAs only 3 have orthologs reportedly expressed in the fly but not in *C.elegans*, whereas 12 have been found within vertebrates and 5 are restricted to rodents and/or placental mammals (Table 1). Interestingly, Lugli and colleagues observed that microRNAs enriched in synaptic fractions of the mouse hippocampus have the tendency to be evolutionarily new (Lugli et al. 2008a).

	Chr start/end Pre-miR	Host gene	TE class	Length TE (% Coverage)	Lineage	Conservation (PhasCons)
Mir-151	Chr15: 73,254,815-73,254,882 [-] **68bp**	Ptk2 intronic [-]	LINE/L2a [-]	58bp **(72.4%)**	Placental mammals	0.995
Mir-708	Chr7: 96,249,430-96,249,538 [+] **109bp**	Tenm4-intronic [+]	LINE/L2a [-] LINE/L2c [+]	37bp 49bp **(66.1%)**	Placental mammals	.0.996
Mir-434 **UUUGAACCAUCACUCGACUCCU**	Chr12: 109594506-109594599 [+] **96bp**	Rtl1-exon 2 [-]	Long terminal repeat (LTR) [+]	352bp **(100%)**	Rodentia	0.076
Mir-3470b **UCACUCUGUAGACCAGGCUGG**	Chr16: 44,013,852-44,013,977 [+] **126 bp**	Gramd1c – intron 1 [-]	SINE/Alu - B1_Mus1	152bp **(100%)**	Mouse-specific	0.003
Mir3470a **UCACUUUGUAGACCAGGCUGG**	Chr6: 83,090,311-83,090,387 [-] **77bp**	intergenic	SINE/Alu - B1_Mur3	145bp **(100%)**	Mouse-specific	0.217

Table 1 Repeat-derived microRNAs present in the axon of cortical neurons. Genomic location and class of transposable element (TE) associated with microRNA precursor (Pre-miR) sequences of miR-434, miR-3470a and 3470b.

As discussed previously in this chapter, transposable elements are thought to play an important part in the formation of new microRNAs during evolution (Meunier et al. 2013; Roberts et al. 2014), which prompted the search for

repeat-derived microRNAs within the subset of axon-enriched microRNAs. By comparing the microRNA precursor transcripts of the top 20 axonal microRNAs with the genomic locations of all classes of transposable elements annotated by RepeatMasker (Smit, Hubley, and Green 2013) in the UCSC Genome Browser (Kent et al. 2002), it was found that four microRNAs aligned partially or completely with repetitive elements in the mouse genome, these being miR-151, miR-434, miR-708, miR-3470b (Table 1). In this analysis, microRNAs were considered of TE origin when the overlap between genomic positions of the repetitive element and microRNA precursor genomic covered at least 50% of the pre-microRNA sequence or 100% of the microRNA mature sequence (See Table 1 - coverage) (J Piriyapongsa et al. 2007). The intersection of the subset of repeat-derived microRNAs with the subset of lineage-specific microRNAs (rodent and placental mammals lineage) present in the top 20 axon-enriched indicates that all lineage-specific microRNAs but one (miR-134) originated from a transposable element (Figure 3.1). The observation that most lineage-specific microRNAs are originated from transposable elements is in line with the emerging concept that repeat-derived microRNAs tend to be younger and lineage- or species-specific (Iwama et al. 2013; Meunier et al. 2013; Qin et al. 2015; Roberts et al. 2014).

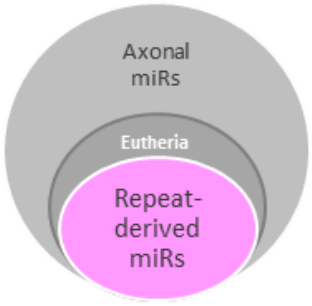


Figure 3.1 Venn diagram showing the intersection between repeat-derived miRNAs and miRNAs specific to the lineage of placental mammals (Eutheria) found within the top 20 axon enriched microRNAs. Five of the top 20 axonal microRNAs are lineage-specific in Euthera (placental mammals), within these five, four are repeat-derived microRNAs.

Additionally, comparative genomics data obtained from the UCSC Table Browser was used to estimate the evolutionary conservation of the repeat-derived microRNAs. This analysis was based on whole genome sequence alignment data from 60 vertebrates, and the average conservation score for each pre-microRNA sequence in the 60way multiple alignment was calculated using the PhastCons method in UCSC Genome Browser (Siepel et al. 2005). The average PhastCons scores represent the probability of evolutionary conservation within a given phylogenetic tree, Vertebrata in our analysis. The conservation scores obtained by the PhastCons method range between 0 and

1, with higher values corresponding to higher conservation. As depicted in table 1, the average conservation scores of miR-151 (0.995) and miR-708 (0.996) are in accordance with a previous study where, by analysing conservation for human microRNAs derived from several TE classes, Piriyapongsa and colleagues found that L2 elements contribute for far more microRNAs with higher conservation scores than nonconserved microRNAs (J Piriyapongsa et al. 2007). Both microRNAs derive from the long interspersed nuclear element 2 (LINE2) family, a relatively old family of TEs that is thought to have expanded in organisms' genomes in the 180 million years since eutherian mammals diverged from marsupials and appears to have found evolutionary pressures in this clade that lead to an abnormally high rate of conservation (Silva et al. 2003). These observations support the conservation of miR-151 and miR-708 within the placental mammals' lineage leading to human. Despite the very similar TE from which they derive, the genomic positioning of the repetitive element suggests different mechanisms of origin, with the entire miR-151 gene deriving from a L2c element sequence and miR-708 hairpin arising from a double insertion of two LINE2 elements into opposite strands of neighbouring positions (see 3.1.3 for mechanisms of microRNA formation from TEs).

Unlike miR-151 and miR-708, rodent-specific miR-434 and mouse-specific miR-3470b showed very low average conservation scores, 0.076 and 0.003 respectively (Table 1), which are similar to the results found by others for species-specific microRNAs (J Piriyapongsa et al. 2007; Yuan et al. 2010). In the case of miR-434, it is derived from a LTR repeat and its expression in rat and mouse is suggestive of a lineage-specific expansion in the genome of rodents.

3.2.2 Species-specific miR-3470b

To get further insight into the genomic origin of miR-3470b in the mouse genome, the genomic region flanking the microRNA hairpin sequence was analysed in more detail. Firstly, the analysis of multiple genomic alignments of miR-3470b gene across placental mammals and respective PhastCons track in UCSC genome browser, including rat and human, (Figure 3.2), showed that not only miR-3470b gene but also the neighbouring genomic sites occur

exclusively in the mouse genome. A closer look at the pairwise alignment between the sequences of the specific B1 element identified in the region of miR-3470b precursor by the Repeat Masker (B1_Mus1, opposite strand; Table 1) and the miR-3470b precursor gene showed that miR-3470b precursor sequence overlaps completely with the B1 element. Notably, this B1 element itself (B1_Mus1, Table1 and figure 3.2) is constituted, nearly exclusively, by the sequence of the miR-3470b precursor (figure 3.3).

The sequence similarity and genomic region of the repeat B1_Mus1 and miR-3470b precursor suggest that miR-3470b originated from a phylogenetically recent insertion (in the mouse genome) of the B1_Mus1 element into intron 2 of Gramdc1 gene (antisense strand) that gave rise to a newly formed hairpin in the opposite strand (sense strand) and eventually generated the miR-3470b gene. Notably, the nearly total sequence similarity between miR-3470b precursor and the repetitive element that originated it (figure 3.3) suggests that miR-3470b genomic sequence hasn't suffered significant evolutionary diversion from the B1 element consensus sequence. This lack of sequence drift might be suggestive of evolutionary pressures to fixate it in the mouse genome. It is, thus, possible that the repeat-derived microRNA sequence could have acquired a function (Berezikov 2011).

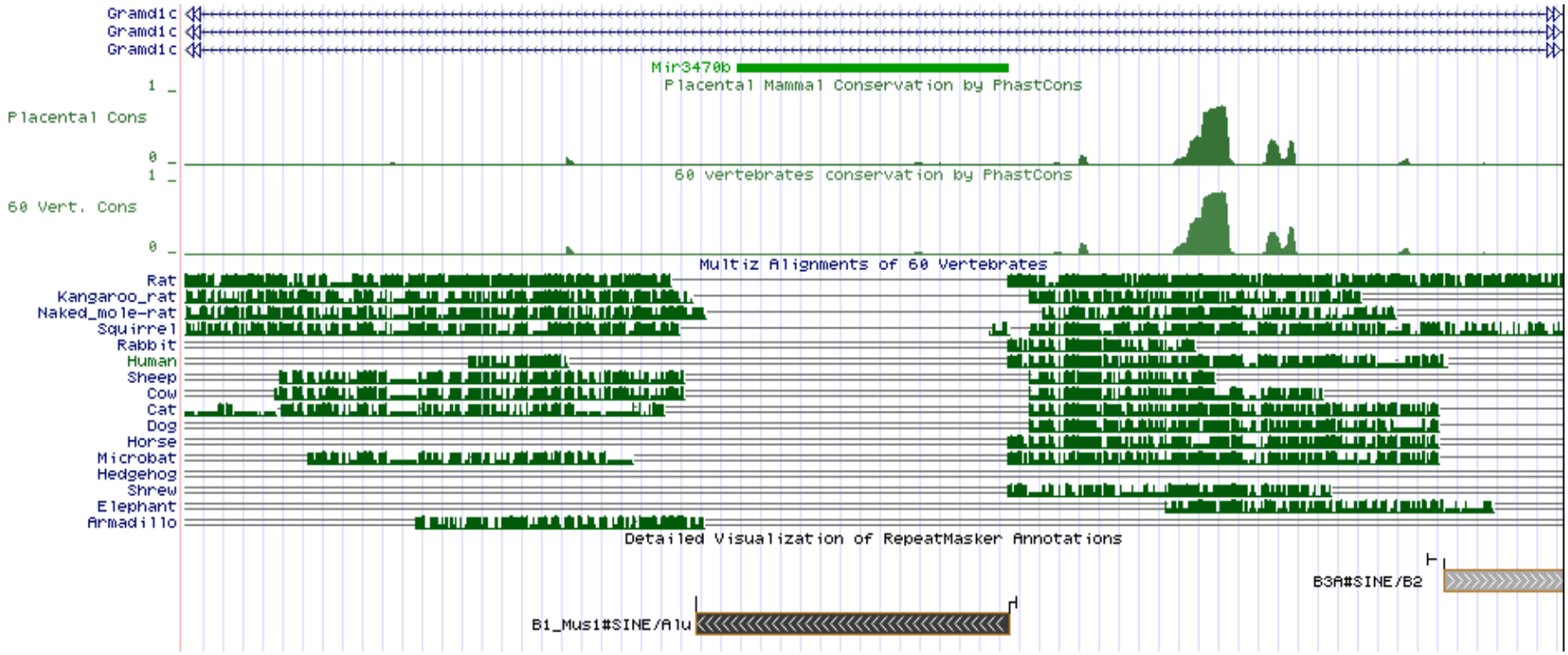


Figure 3.2 Multiple genomic alignments of miR-3470b in placental mammals. Alignment of miR-3470b genomic region across placental mammals shows no conservation of the mouse miR-370b precursor sequence, while flanking regions show alignments in various placental mammals, including rodent and human. Multi-Z alignment of 60 vertebrates track in UCSC genome browser, only placental mammals are shown. RepeatMasker track shows the B1_Mus1 element insertion in the mouse genomic region correspondent to miR-3470b precursor sequence.

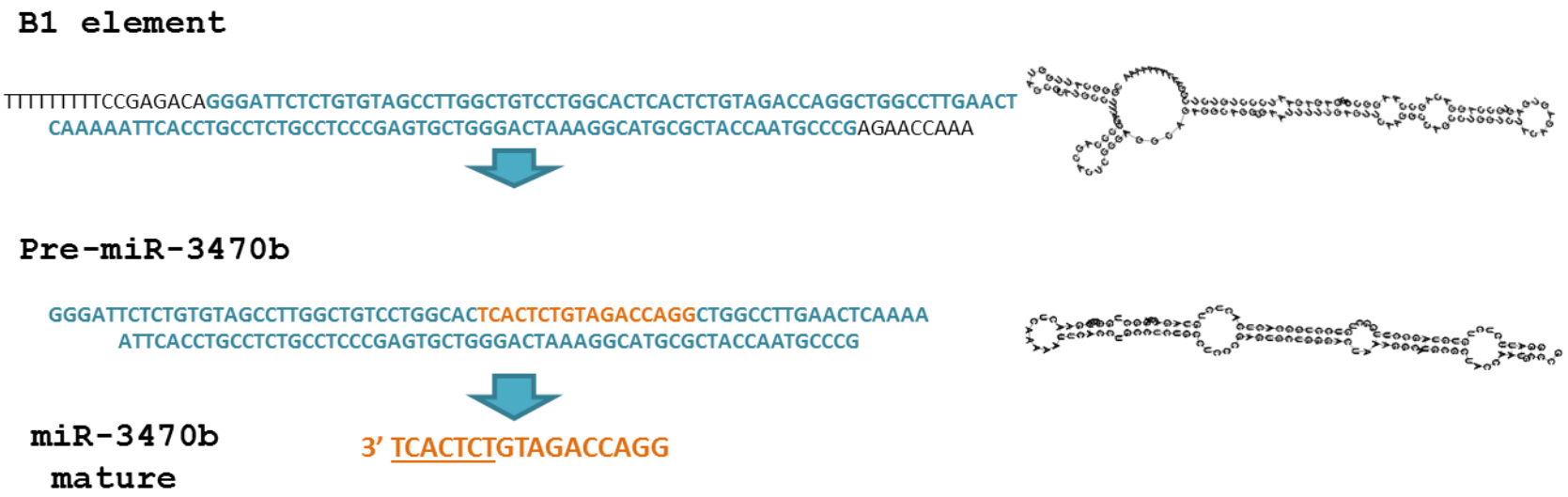


Figure 3.3 Comparison of the B1 element and miR-3470b precursor sequences. Pairwise alignment of B1_Mus1 element and miR-3470b precursor revealed that the B1 element covers the totality of pre-miR-3470b sequence (blue). Conversely, pre-miR-3470b constitutes ~83% of the B1 element sequence. RNAfold models of B1 element and pre-miR-3470b secondary structures (on the right) show the formation of miR-3470b hairpin. miR-3470b mature sequence is shown in orange.

MiR-3470b is part of the 3470 microRNA family consisting of miR-3470b and miR-3470a, which are both mouse-specific (Yuan et al. 2011, and our data). In order to get further insight into miR-3470b origin, the miR-3470a gene was analysed in the same manner as described above for the four repeat-derived microRNAs discussed in this section. The summary of our findings can be found in Table 1, last row. Not surprisingly, the analysis demonstrated that miR-3470a is also derived from a B1 element, although in this case it is B1_Mus3. Average PhastCons score (0.21) and multiple genomic alignments in placental mammals suggest an evolutionarily older B1 insertion, compared to miR-3470b (B1_Mus1). The miR-3470a gene aligns partially with the genomic sequences of a few members of the rodentia lineage, with particularly significant similarity to rat (figure 3.4). Despite this apparent genomic conservation, to date miR-3470a expression has only been reported in mouse (miRBase release 22: March 2018). In rats, expression has been predicted by miRviewer, an algorithm that combines conservation scores and probability of hairpin formation for prediction of novel microRNA homologs (Kiezun et al. 2012).

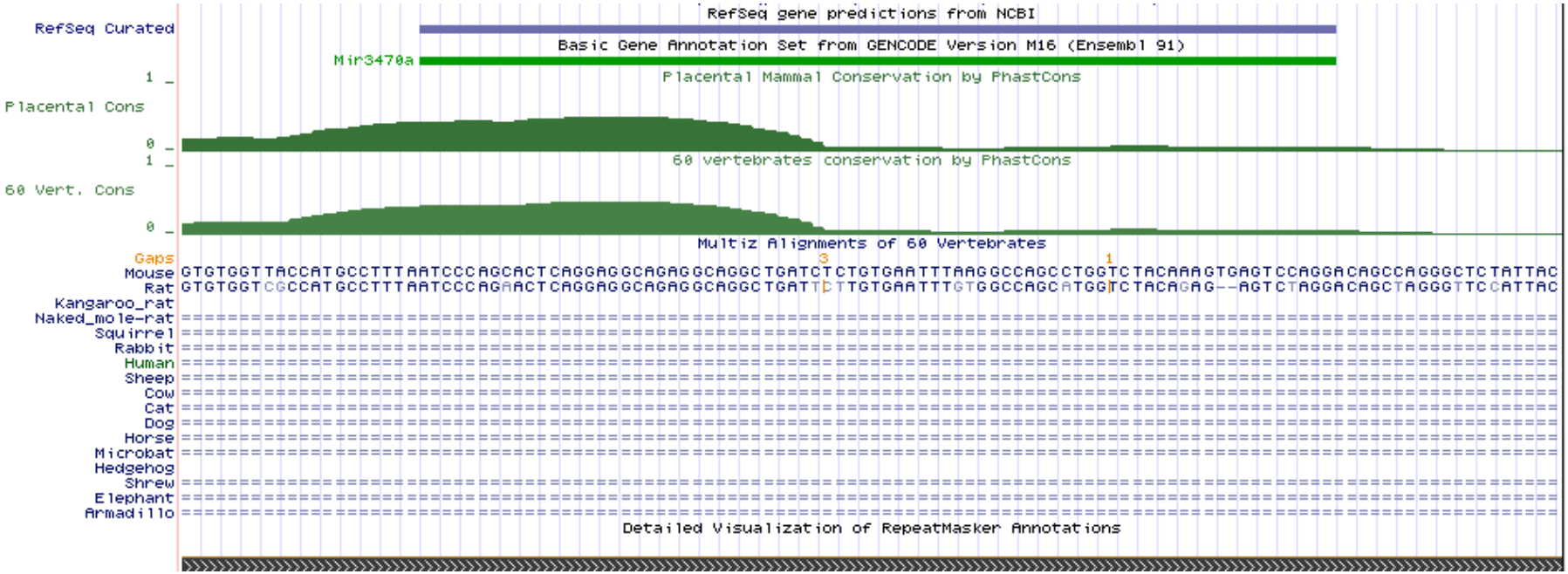


Figure 3.4 Multiple genomic alignments of miR-3470a in placental mammals. Alignment of miR-3470a genomic region across placental mammals shows that the sequence of miR-3470a precursor is highly conserved in rat despite the fact that the expression of this miRNA has not been identified in rat. Multi-Z alignment of 60 vertebrates track in UCSC genome browser, only placental mammals are shown (blue track). PhastCons conservation track in placental mammals and vertebrates shows the histogram of Phastcons scores (green). RepeatMasker track shows the B1_Mus3 element insertion in the mouse genomic region correspondent to miR-3470a precursor sequence (bottom, grey track).

Taken together, the studies carried out indicate that the miR-3470 family is an example of rapid TE evolution giving rise to new microRNAs that are not present in closely related species such as rat. However, unlike miR-3470b, miR-3470a was not detected by miRNA-seq in cortical neurons during our pilot study on axon-enriched microRNAs. For this reason, further studies on the functional role gained by newly originated microRNAs on neuron development focused exclusively on miR-3470b.

B1 elements are TEs only found in rodent species that originated in an initial duplication of the common ancestor 7SLRNA gene prior to the primate-rodent split ~80million years ago and account for a significant fraction of the mouse genome (3.6%) (Tsirigos and Rigoutsos 2009). These B1 elements belong to the same repeat family as Alu elements that have also descended from the 7SL RNA and spread in the genomes of primates at the beginning of the primate radiation (see 3.1.2). Although B1 and Alu elements expanded independently in the mouse and human genomes, a fascinating observation was made in a study by Tsirigous & Rigoutsos whereby genome-wide alignment analysis suggests that Alu and B1 element insertions have been selectively retained in genes belonging to similar functional classes across both genomes (Tsirigos and Rigoutsos 2009). It isn't unreasonable to hypothesise that B1 and Alu elements suffer similar evolutionary pressures, thus making the study of B1-derived microRNAs a potentially relevant model for the investigation of the function of Alu/B1-derived microRNAs in settings where human functional studies are challenging, such as the nervous system.

Although there are several comprehensive studies on the genomic origins of repeat-derived microRNAs in mammals and specifically human (Gim et al. 2014; J Piriyapongsa et al. 2007; Qin et al. 2015; Roberts et al. 2014; Yuan et al. 2011), there is limited evidence for their biological function, with only few reports suggesting an enrichment in growth- and development- related pathways (Hu et al. 2012; Spengler et al. 2014; Yuan et al. 2010). Notably, Hu et al describe a microRNA derived from a tandem repeat specific to human, miR-941, which is expressed in the brain and targets transcripts involved in neurotransmitter signalling (Hu et al. 2012). Thus, the study of B1-derived

miR-3470b builds on the current knowledge of species-specific microRNAs in neuronal function.

3.2.3 Role of miR-3470b in axonal development

3.2.3.1 Function of miR-3470b in axonal outgrowth

Following from the identification of miR-3470b among the axon-enriched microRNAs in cortical neurons, it was important to test its potential role in axonal outgrowth in vitro. For this, the functional outputs of miR-3470b were manipulated within the cell by transfecting cortical neurons with specific microRNA inhibitors or mimics. In brief, these are short oligonucleotides with a locked nucleic acid (LNA) backbone that either binds to endogenous miR-3470b, thus inhibiting the function (microRNA inhibitor) or LNA oligos that bear the same sequence as miR-3470b and act as an overexpression system (microRNA mimic) within the cell (See Methods).

The effect of specific miR-3470b inhibitors and mimics in axonal outgrowth of cortical primary neurons was examined after co-transfection of these oligos with a GFP expression plasmid. Inhibition of endogenous miR-3470b led to a significant decrease in the mean axon length of 24.1±2.9% in comparison to LNA-control, when 50nM of LNA-miR-3470b inhibitor was transfected, respectively to cortical neurons (figure 3.5.a).

To further test the role of miR-3470b in the elongation of developing axons, we examined whether a specific microRNA mimic influenced axonal outgrowth. Accordingly, transfection of cortical neurons with LNA-miR-3470b mimic exhibited an increase in axonal outgrowth (approximately 20% with LNA-miR-3470b mimic in comparison to control; Fig 3.5.b).

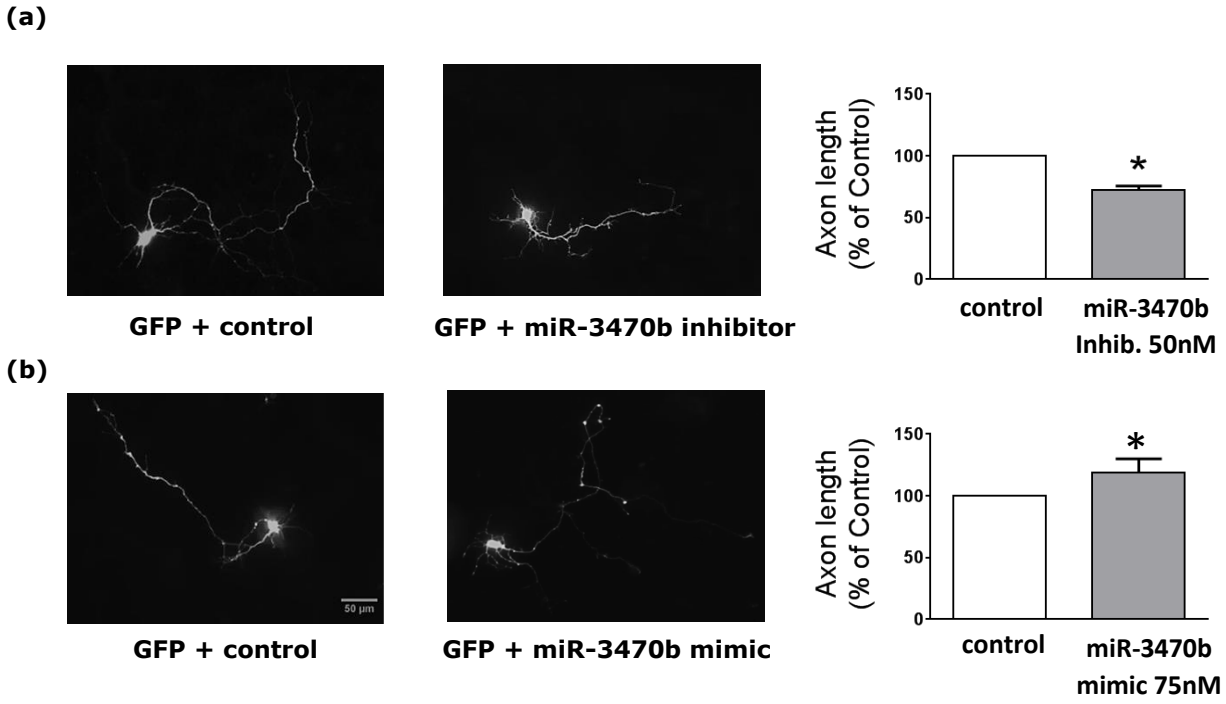


Figure 3.5 miR-3470b controls axonal outgrowth in cortical neurons. Quantification of neuronal axon length after co-transfection with GFP and an inhibitor **(a)** or a mimic **(b)** of miR-3470b. Inhibition of miR-3470b led to a 23.2% decrease in axon length when compared to a non-targeting control **(a)**, whereas co-transfection with a miR-3470b mimic resulted in axons 19.8% longer in comparison to those co-transfected with a non-targeting control **(b)**. Transfections were performed 24h after plating and imaged at DIV5. Data is expressed as mean ± SEM of measurements conducted in n=5 independent experiments, each normalised to the mean length of the respective non-targeting control; * $p<0.05$, One-sample t-test.

Overall, the analysis of axon length measurements in GFP positive cortical neurons upon manipulation of miR-3470b activity suggests a role for this axon-enriched microRNA in axonal outgrowth. The apparent subtle effects of ectopic expression and inhibition of miR-3470b on axon outgrowth can be explained by the multiple mechanisms at interplay during axonal development. It is in fact remarkable that the modulation of a single microRNA bears the potential to impact such tightly regulated biological processes, and suggests that relevant signalling pathways are being regulated by miR-3470b (Schratt 2009a).

Likewise, similar effects have been found for other microRNAs comprehensively investigated for their roles in neuronal function and, specifically, axonal outgrowth. Mir-9 and the cluster miR-17-92a are such

cases, where manipulation of microRNA levels resulted in changes of approximately a quarter of total axonal length (Dajas-Bailador et al. 2012; Zhang et al. 2013). Of note, the power of experiments performed with microRNA mimics is likely to be limited by off target effects of the exogenous microRNA and its interference with the biomechanisms of the miRISC complex (Jin et al. 2015).

3.2.3.2 Regulation of miR-3470b over development

As miR-3470b can control axonal outgrowth in cortical neurons, it was important to determine if the levels of this microRNA were dynamically regulated during the development of cultured primary cortical neurons (see Chapter1). For this, miR-3470b was quantified by qPCR at different stages of the development of neurons in culture (Fig 5). In these experiments, total RNA was extracted 24h after neuronal plating (DIV2), when minor processes are forming and axon specification occurs, at DIV5, to coincide with active axon outgrowth at high rates, and finally at DIV12 where axonal outgrowth slows down, neurons mature and synaptogenesis takes place (Dotti et al. 1988; Lewis et al. 2013) (figure 3.6). As seen in Figure 3.6, miR-3470b levels increase rapidly in cortical neurons from DIV2 to DIV5, with a 3.5 fold increase. Later in development, at DIV12, miR-3470b levels were 6-fold higher in relation to DIV2 (figure 3.6).

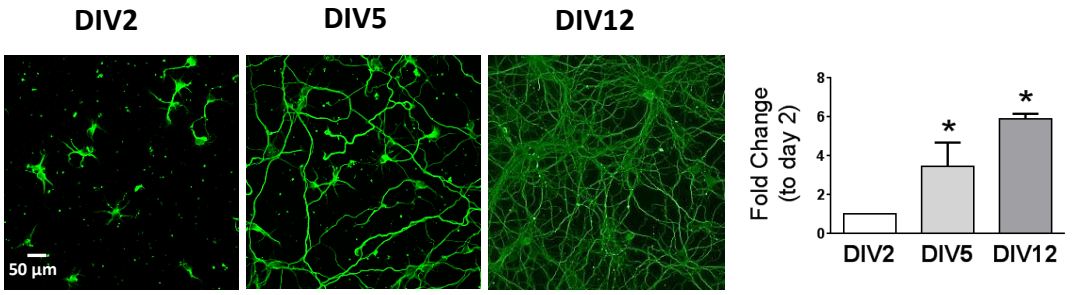


Figure 3.6 miR-3470b increases over development in culture. Acetylated tubulin staining (green) reveals the increasing complexity of the cortical culture over development. Real-time qPCR quantification of miR-3470b of cortical neurons at day in vitro 2, 5 and 12 shows increase in miR-3470b levels over development in vitro, particularly at DIV12, a period associated with the beginning of culture maturation.

Although neuron numbers remain constant, total cytoplasmic volume increases greatly in cortical neurons over development, mainly as a function of overall axonal growth. Despite this, microRNA levels don't necessarily follow the same trend (Yao et al. 2012). As a result, the high levels of miR-3470b at DIV12 in comparison to DIV2 might indicate the need to fulfil an important function in network development. In our hands, changes in endogenous levels of several microRNAs over the same time-points tend to be less pronounced, with some microRNAs decreasing and others maintaining stable levels over cortical culture development (qPCR array, data not shown).

Despite its axonal localisation, as demonstrated by our sequencing data in isolated axons (section 1.7), the levels of miR-3470b in cortical neurons as measured by qPCR are relatively low (Ct>28, not shown), when compared to other microRNAs found in cultured neurons by us and others (Natera-Naranjo et al. 2010; Sasaki et al. 2014). Interestingly, in a genome-wide study of the evolution of human microRNAs, Iwama and colleagues found that expression levels of microRNAs tend to correlate with their evolutionary history, with the younger microRNAs being less expressed. This was simultaneously corroborated in a miRNA-seq study in mammalian lineages (Iwama et al. 2013; Meunier et al. 2013), and supports the hypothesis that the relatively low levels of this species-specific microRNA reflects its origin from a recent B1 element insertion. Nevertheless, it is important to mention that despite its low expression levels, miR-3470b was detected in cortical neurons and has a dynamic regulation over the development of neuronal network complexity in culture.

It was then relevant to investigate the regulatory networks that are potentially targeted by the evolutionarily new miR-3470b, and that could mediate its actions in axon development.

3.2.4. Pathways potentially targeted by miR-3470b

A regular next step after finding a function for a specific microRNA is to identify the regulatory networks being targeted. For this, a standard bioinformatics workflow was carried-out (Peterson et al. 2014; Riffo-Campos, Riquelme, and Brebi-Mieville 2016). First, two of the most widely used microRNA target

prediction tools, TargetScan (Agarwal et al. 2015) and DIANA-microT-CDS (Paraskevopoulou et al. 2013), were employed to create a computational prediction of the potential transcript targets of miR-3470b. Both tools produced a ranked list of genes scored by strength of predicted miR-3470b-mRNA site interaction: 5360 targets in TargetScan (TargetScanMouse 7.1) and 492 targets DIANA-microT-CDS (miTG score threshold >0.7, see Methods). To increase the likelihood of identifying biologically valid target candidates, an overlap of the two gene datasets was produced, obtaining a subset of 486 targets genes common to both TargetScan and Diana prediction analysis (Sethupathy, Megraw, and Hatzigeorgiou 2006) (Riffo-Campos et al. 2016) (Figure 3.7).

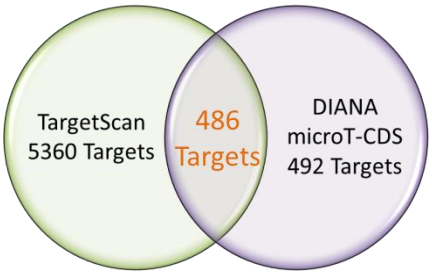
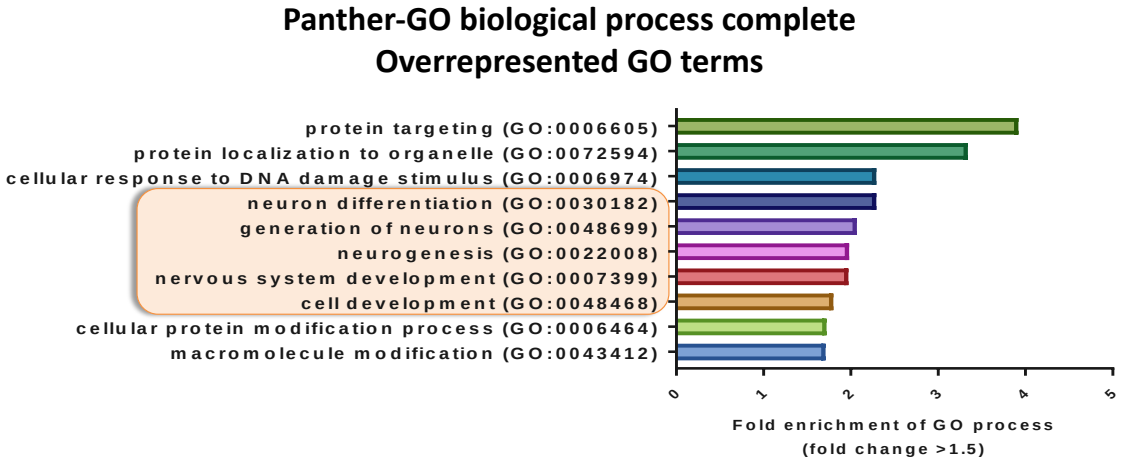


Figure 3.7. miR-3470b predicted target genes. Venn diagram representing the number of common targets between TargetScan and DIANA micro-T-CDS lists of predicted targets.

After this step, a functional classification analysis of the 486 genes predicted to be targeted by miR-3470b was made using the PANTHER Classification System tool (PANTHER13.1 release) (Mi et al. 2017, 2013). To investigate the functional gene ontology (GO) classes that are enriched in the gene list an overrepresentation analysis of GO terms related to biological process was conducted (GO-Biological process complete, Fisher's Exact with FDR multiple test correction, p-value<0.05). The data referring to number of genes observed/expected for each GO category and its correspondent statistical analysis is detailed in figure 3.8. As shown in Fig 3.8.a) and b), the targets of miR-3470b that are associated with protein targeting, cellular response to DNA damage and GO categories linked to neuronal differentiation and development are significantly higher than expected in a randomly chosen set of genes. Importantly, of the top 10 overrepresented GO terms, four are related to neuronal function and development: neuron differentiation (2.29 fold enrichment), generation of neurons (2.07 fold enrichment), neurogenesis (1.98 fold enrichment), nervous system development (1.97 fold enrichment) and one GO category is related to cell development (1.8 fold enrichment). These findings are consistent with a function of miR-3470b in the modulation

of gene networks relevant for neuronal development, and further support the axon growth effects observed in cortical primary neurons.



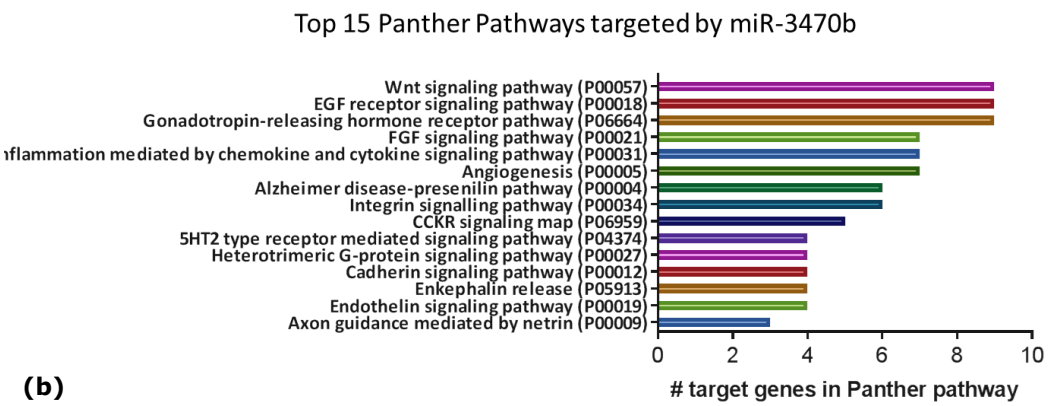
GO biological process complete	# genes in miR-3470b targets	# expected genes		Fold enrichment	P-value	False Discovery Rate <0.05
protein targeting (GO:0006605)	12	3.06	+	3.92	9.99E-05	3.49E-02
establishment of protein localization to organelle (GO:0072594)	16	4.79	+	3.34	4.62E-05	1.69E-02
cellular response to DNA damage stimulus (GO:0006974)	25	10.92	+	2.29	1.76E-04	4.92E-02
neuron differentiation (GO:0030182)	37	16.16	+	2.29	5.22E-06	3.21E-03
generation of neurons (GO:0048699)	53	25.56	+	2.07	9.27E-07	7.50E-04
neurogenesis (GO:0022008)	54	27.29	+	1.98	2.29E-06	1.53E-03
nervous system development (GO:0007399)	72	36.49	+	1.97	4.04E-08	7.77E-05
cell development (GO:0048468)	48	26.63	+	1.8	1.10E-04	3.74E-02
cellular protein modification process (GO:0006464)	67	38.93	+	1.72	1.35E-05	6.70E-03
protein modification process (GO:0036211)	67	38.93	+	1.72	1.35E-05	6.49E-03
macromolecule modification (GO:0043412)	74	43.33	+	1.71	7.06E-06	3.87E-03
transcription, DNA-templated (GO:0006351)	57	33.43	+	1.71	1.19E-04	3.97E-02
cellular protein metabolic process (GO:0044267)	82	48.11	+	1.7	1.91E-06	1.34E-03
nucleic acid-templated transcription (GO:0097659)	57	33.44	+	1.7	1.19E-04	3.90E-02

Figure 3.8. Gene ontology of miR-3470b targets. a. Overrepresentation analysis of GO biological process complete of genes potentially targeted by miR-3470b, bars represent fold enrichment of GO process in miR-3470b targets in relation to expected to be found by chance in the mouse genome. GO term with fold enrichment > 1.5 were considered. Highlighted are GO terms directly related to neuron function and development. **b.** Table showing the analysis parameters including number of genes belonging to each GO term found within miR-3470b targets and number of expected genes by random sampling of the mouse genome. Analysis conducted in PANTHER-Biological process complete, overrepresentation test p>0.05 with Bonferroni correction.

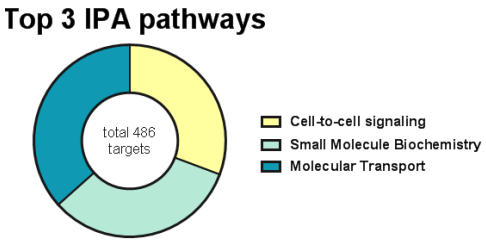
To further elucidate the involvement of miR-3470b in neuronal function, examination of the molecular pathways potentially targeted by miR-3470b was carried-out by performing a pathway analysis of the 486 putative target genes. For this, PANTHER-Pathways, a bioinformatics tool for analysis of curated pathways, was employed (See Methods) (Mi et al. 2017; Mi and Thomas 2009). As shown in figure 3.9.a, the top 15 pathways resulting from

the analysis include some of the most well studied pathways in neuronal function: tropic and growth factor signalling including EGF, GnRH and FGF; Wnt signalling crucial to cell fate determination and polarity; cell adhesion and inter-cellular communication through integrin and cadherin signalling and neurotransmitter/neuropeptide signalling (5-HT2, enkephalins) and netrin-dependent axon guidance through (Goldberg 2003; Polleux and Snider 2010).

(a)



(b)



(c)

No. predicted targets MicroT-CDS	Synaptic genes	Expected synaptic genes	Fold enrichment	P-value
486	47	9.11±5.56	1.62	p<0.001

Figure 3.9. Pathway analysis of miR-3470b regulatory networks. (a) Top 15 pathways targeted by miR-3470b obtained from PANTHER Pathway analysis of miR-340b predicted target genes. Pathways were ranked by number of target genes (bars) belonging to each Panther pathway depicted in the graph. **(b)** Ingenuity Pathway Analysis (IPA) Top 3 pathways in Biofunction category **(c)** Overrepresentation analysis of synapse-related genes given by IPA within miR-3470b targets list, showing a fold enrichment of 1.62 (Monte Carlo simulation, n=100000).

In parallel and to validate our findings, a functional classification analysis of miR-3470b 486 predicted targets was carried out in Ingenuity pathway Analysis (IPA), another widely used software for gene classification and pathway analysis in gene lists, which allows to query gene lists included in functional categories relevant to a particular phenotype of interest, such as "biological function - Biofunction" (Krämer et al. 2014). The top 3 gene

networks in the "Biofunction" category in IPA include Cell-to-Cell Signalling and Interaction, a category that contains genes involved in synaptic contact and neuronal cell adhesion (figure 3.9.b). A comparison between the number of miR-3470b targets related to synaptic maturation and transmission (47 targets) and the total number of synaptic-related molecules included in Cell-To-Cell interaction and signalling, revealed an overrepresentation of genes related to synapse contact in the list of miR-3470b targets (Monte Carlo simulation n=100 000; figure 3.9.c).

Taken together, the functional classification and pathway analysis data, combined with the effect of miR-3470b in axonal outgrowth of cortical neurons places miR-3470b at the centre of regulatory networks related to neuronal development.

In an attempt to further explore miR-3470b-mediated regulation in cortical development, we decided to investigate the specific target genes that might be mediating the action of miR-3470b in axonal outgrowth. Therefore, we devised a strategy to pinpoint candidate target genes whose repression could explain the observed functional effect of miR-3470b in axon development. A subset of putative targets belonging to GO categories and pathways related neuronal function were ranked according to DIANA-microT-CDS and TargetScan prediction scores and further manually curated in NCBI for expression in nervous system and function in growth/development, resulting in a shortlist of 4 candidate genes: *Slitrk*, *Ephrin-A receptor 4*, *IL-1 receptor 1, Neuroendocrin secretory protein 55*. As a next step, we sought to experimentally validate this subset of candidate targets *in vitro* by means of luciferase reporter assays, whereby the binding of miR-3470b-mRNA target site is probed by measuring the capacity of miR-3470b sequence to repress activity of luciferase linked to the mRNA binding site (See methods). Contrary to our expectations, none of the miR-3470b-mRNA pairs were successfully validated (data not shown).

This illustrates a well acknowledged problem in the microRNA field, which is the accurate identification of biologically functional microRNA targets. Despite the vast number of publications dissecting the nuts and bolts of microRNA binding mechanisms in the past decade, due to incomplete knowledge of the rules governing effective microRNA-mediated repression of gene expression,

the algorithms for prediction of microRNA-mRNA interactions still struggle to produce biologically valid predictions, with high numbers of false negatives (elimination of true targets) and false positives (too permissive), even when multiple prediction tools are combined to increase accuracy (Riffo-Campos et al. 2016)(Chevalier and Borchert 2017). Recently, the use of more comprehensive approaches to target prediction have been proposed as a way to improve accuracy in microRNA target identification, including machine learning algorithms directly trained on experimental data and the combination of computational prediction analysis and experimental approaches (Ref). A limitation of these approaches is their reliance on either the availability of extensive experimentally validated data on microRNA-target interactions, which is limited (machine learning algorithms), or on the execution of costly laboratory techniques that require a great deal of technical expertise and can be time-consuming (transcriptomic, proteomic and RNA immunoprecipitation approaches) (Chevalier and Borchert 2017).

Another potentially useful approach takes into account the genomic origins of microRNAs and their potential targets. Accordingly, some computational and experimental studies suggest that repeat-derived microRNAs could target mRNAs that express the same repeat within 3'UTR in antisense orientation, thus providing a complementary binding sequence to the microRNA (Filshtein et al. 2012; Lehnert et al. 2009; Piriyapongsa and Jordan 2007; Spengler et al. 2014). In fact, many microRNAs have been found to target a conserved site within Alu and B1 repeats existent in the 3'UTR of protein genes (Daskalova et al. 2007; Smalheiser and Torvik 2006) and a few cases where repeat-derived microRNAs target repeat related sites embedded in the 3'UTRs of protein coding genes have been experimentally validated (Shin et al. 2010; Spengler et al. 2014). For instance, miR-28, a placental specific microRNA derived from the relatively ancient insertion of a L2 element, regulates the expression of LYPD3 and E2F transcription factor 6 (E2F6) through 3' UTR-resident LINE2 sequences (Shin et al. 2010; Spengler et al. 2014). In the same study, evolutionarily recent miR-1285-1 derived from the B1 primate equivalent Alu element was shown to regulate Alu-derived target sites within the 3'UTRs of its target genes, using luciferase reporter assays. With this in mind, Filshtein and colleagues proposed that limiting miR target searches to transcripts containing a miR's progenitor TE can facilitate accurate target

identification (Filshtein et al. 2012). This approach could be specially relevant for repeat-derived microRNAs due not only to their origin, but also because they tend to be evolutionary young and the level of conservation of microRNA-target interactions is an important parameter in most microRNA target prediction tools, including the ones used in our study, TargetSCan and DIANA (Riffo-Campos et al. 2016).

Because miR-3470b is a species-specific B1-derived microRNA, future work could employ the aforementioned methodology proposed by Filshtein et al, 2012 the Origin-based identification of microRNA targets (OrBid), with adaptations to restrict the pool of potential miR-3470b targets to transcripts bearing murine B1-related sites capable of complementary binding to miR-3470b. Non-conservation based algorithms, such as RNA22 and RNAHybrid, could then be used to assess quality of seed matching, free energy of the interaction pairs and site accessibility to help pinpoint true microRNA targets. Additionally, as our data suggests that miR-3470b levels increase over development in cortical neurons, gene expression data during the development of the mouse brain could help inform miR-3470b target prediction. Therefore, publicly available transcriptome and proteome datasets at different stages of mouse brain development, specifically RNA-seq and microarray data, may be used to infer differentially expressed genes within the origin-based predicted targets of miR-3470b (Gonzalez-Lozano et al. 2016; Han et al. 2009; Hartl et al. 2008; Mody et al. 2001; Semeralul et al. 2006).

3.2.5 Development of network activity in cortical neurons cultured on microelectrode arrays

3.2.5.1 Microelectrode array model

Collectively, miR-3470b regulation over development, its effect in axonal elongation and its potential to be a modulator of regulatory networks related to neuron growth, development and synaptic maturation in the nervous system prompted us to question whether miR-3470b could have a role in the formation/regulation of cortical neuronal networks. To investigate this, we took advantage of microelectrode array culture systems.

As indicated in more detail in the methods section, primary cortical neurons were cultured on microelectrode arrays and the spontaneous electrical activity of the neuronal network over the development in culture was recorded at days 5, 9, 13, 14, 15, 16, 17, 18, 19 and 21. In accordance to previous reports (Chiappalone et al. 2006; D. A. Wagenaar et al. 2006), the extracellular electrical activity measured on the microelectrodes is very low or non-existent up to day 5, starts to develop richer patterns of activity after the first *in vitro*, which continues to augment over the first 3 weeks in culture (figure 3.10.a). When synaptic maturation starts developing, the neuronal networks undergo a striking transformation in their activity patterns, in which sporadic spikes progressively increase frequency and synchronized activity across the culture appears, with periods of bursting that are followed by short silent periods (D. A. Wagenaar et al. 2006).

3.2.5.2 Effect of miR-3470b in spontaneous network activity of neuronal cultures

Because miR-3470b levels are elevated in late stages of neuronal development (section 3.3.2) and the fact that this microRNA is predicted to target gene networks related to axonal growth, pathfinding and the formation of synaptic contacts, we hypothesized that miR-3470b would be necessary for the establishment of mature axonal growth and synaptic connectivity of cortical cultures.

To investigate this, a cell-permeable miR-3470b inhibitor or non-targeting negative control was applied to primary cortical neurons grown on microelectrode arrays at the end of the second week in culture, day 14. The network activity of cortical neurons was recorded every 24h after transfection for 5 days.

After application of the miR-3470b inhibitor, cortical cultures exhibited an arrest in the development of electrical activity of the network in comparison to the control group, particularly when the number of spikes/min channel was analysed (figure 3.11.b). A non-linear regression analysis of the spikes/min per channel data showed a significant difference between the miR-3470b inhibitor and the control groups as depicted in figure 3.11.c (slope comparison, $p<0.05$). This effect could be mediated by deregulation upon inhibition of miR-

3470b of target genes associated with the synaptic machinery. Nevertheless, it is also possible that the observed arrest in the network activity results from miR-3470b-dependant inhibition of axonal outgrowth, therefore affecting the normal establishment of neuronal network.

Although the microelectrode array culture model gives insights of the electrical activity at the network level in a non-invasive manner, the intrinsic variable nature of the cultures rise issues with the control and reproducibility of the experiments and results have to be interpreted with caution, as previously reported by Wagenaar et al (D. A. Wagenaar et al. 2006).

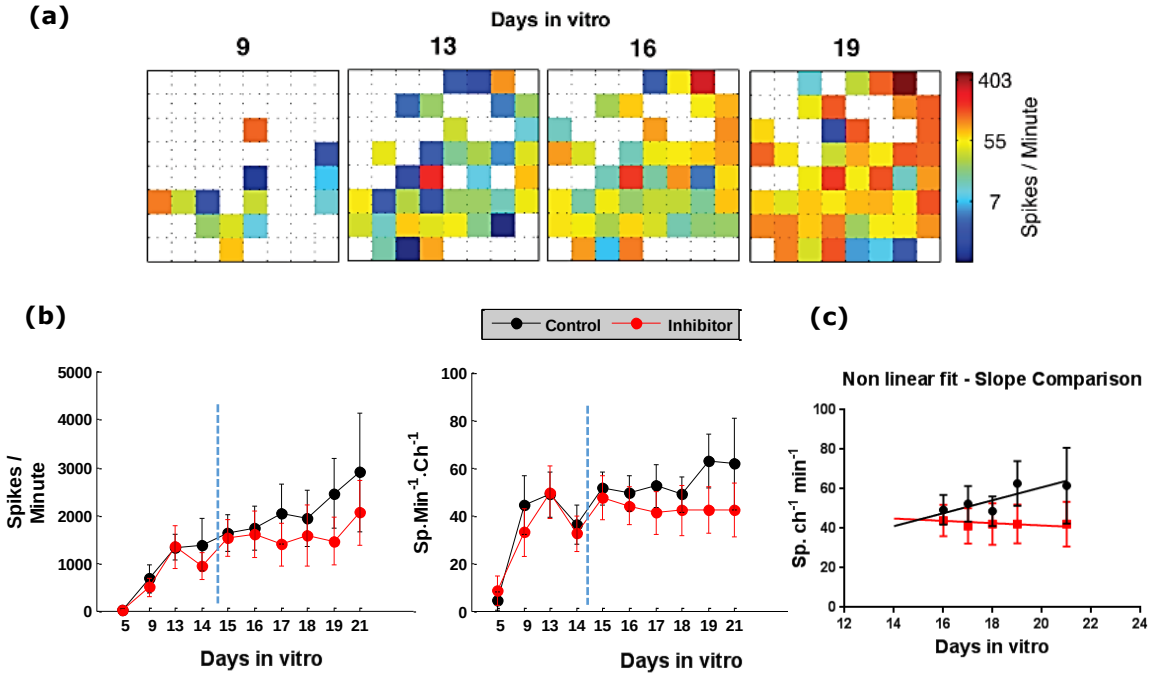


Fig. 3.10. Neuronal network activity after transfection with miR-3470b inhibitor
(a) Representation of the spikes obtained with extracellular recording of one microelectrode channel (left). Activity patterns of cortical cultures recorded by the microelectrode array after 5, 13, 16 and 19 days in culture (right). Heat map represents spikes/min. The network activity increases over the development of the culture. **(b)** Analysis of total number of spikes/min and spikes/min per channel recorded in different timepoints during development before and after transfection with miR-3470 inhibitor (red dots) or miR-control (black dots) on day in vitro 14. In both analysis the activity of culture tends to be lower than then the control when miR-3470 is inhibited. Data acquired from 8 individual cultures in each group and represented as mean±SD. **c.** Non linear regression fit of the spikes/min per channel data shows a significant difference in curve slopes of the miR-3470b inhibition dataset in relation to miR-control dataset (constrain data start at day 14, $p<0.05$).

3.6 Concluding remarks

The work presented in this chapter employed sequence identity and conservation analysis to study the genomic origin of axonally enriched microRNAs in cortical primary neurons (Introduction, section 1.7). The overall findings identified the axon-enriched miR-3470b as a murine-specific microRNA that has arose from an evolutionarily relatively recent insertion of a rodent-specific short interspersed B1 element, the mouse counterpart of primate-specific Alu element. Although this is not the first study that identified microRNAs originated from transposable sequences by genome context analysis (Roberts et al. 2014), the multidisciplinary approach outlined has provided a great opportunity to combine bioinformatics and evolutionary analysis with functional studies. In this way, it has been possible to explore the biological relevance of repeat-derived microRNAs.

The experimental data presented supports the notion that TEs can give rise to functional microRNAs with the capacity to regulate physiological processes. Here we show that mir-3470b is expressed in cortical neurons at levels compatible to its young evolutionary history (Meunier et al. 2013). Although it is theoretically possible to argue whether this repeat-derived microRNA is a true microRNA, the results presented throughout this chapter demonstrate that miR-3470b is positively regulated during in vitro development of cortical networks *in vitro* and promotes the growth of cortical axons over development in culture. Crucially, miR-3470b appears to be relevant for the development of network activity in cortical neurons, with the inhibition of endogenous miR-3470b function leading to an arrest in the development of normal electric activity of cortical neurons cultured on microelectrode arrays.

Species-specific TE insertions contribute to increase the repertoire of microRNAs of the host organism, introducing novel regulatory elements with the potential to impact on gene networks. Our data suggests that murine-specific miR-3470b could target pathways related to cell and nervous system development, neuron differentiation and synapse formation/transmission. Together, our functional data is in accordance with Meunier and colleagues who showed that in mammals, evolutionarily younger microRNAs tend to be predominantly expressed in cortex and cerebellum, whilst ancient microRNAs are predominantly expressed in heart and kidney (Meunier et al. 2013). How

exactly the introduction of evolutionary novel miR-3470b influences specific regulatory networks in the mouse brain is still to be determined, and further studies will use an origin-based approach whereby TE-derived microRNA binding sites are considered more probable true targets, as an attempt to increase the accuracy of the prediction of miR-3470b target transcripts (Filshtein et al. 2012).

TEs elements are known to be transcribed in response to stress, heat shock and in early stages of cell development (Fort et al. 2014; Ohnishi et al. 2012; Rudin and Thompson 2001; Williams, Tamburic, and Astell 2004). *De novo* TE insertions have been described in the brain (Muotri et al. 2005) and recent research shows mosaicism in neurons that can lead to genomic diversity in the brain and can be regulating formation of connections between neurons (Erwin et al. 2014; Maag et al. 2015). *De novo* insertions are, in fact, increased in the brain when compared to other tissues (Erwin et al. 2014). From a developmental perspective, *de novo* insertions have been implicated in neurogenesis, even in the adult hippocampus (Coufal et al. 2009; Kuwabara et al. 2009; Muotri et al. 2005). Could TEs, in particular SINE-B1 elements, be transcribed in neurons over development and have an action in differentiated neurons? In this study it was observed that the sequence of the B1 element B1-Mus1 embedded in intron 2 of the Gramd1c gene contributes almost exclusively to the generation of miR-3470b precursor transcript. This prompted the hypothesis of whether TEs, in particular B1 elements, may have a dual action over development and be transcribed as B1 or a microRNA. In the 90s Maraia and colleagues found that Alu/B1 elements can actually accumulate in the cytoplasm and interestingly, pre-mRNAs containing intronic ID elements, a mouse repeat also part of the SINE family, can be targeted to the dendrites through ID-mediated mechanisms (Buckley et al. 2011; Maraia 1991). The combination of these observations allows to speculate whether 1) B1/alu transcripts can have a function in axonal outgrowth in during neuronal development, 2) these transcripts can be transported to the axon and exert their function locally.

Transcription of microRNAs embedded in introns of coding genes is commonly driven by polII, with microRNA hairpins being further cleaved by drosha. In a study on synaptic fractions of the mouse brain, Smalheiser and colleagues found that both microRNA precursors and microRNA primary transcripts can

localise to synaptic fractions and both drosha and dicer were found in axons (Lugli et al. 2008a). Moreover, Alu sequences embedded in introns can be transcribed to exert regulatory functions on genes relevant for pluripotency (Garcia-Perez et al. 2016; Morales-Hernández et al. 2016). It is then possible that Gramd1c primary transcript is present in the axon and, if this is the case, the precursor or mature miR-3470b and even its host B1 element could be further processed locally in the axon. The Gramd1c host gene encodes for protein Aster-C in the mouse and comprises the Aster proteins, a family of proteins whose function remains largely unknown. Only recently, Aster proteins, including protein Aster-C, were found to locate to the endoplasmic reticulum and the plasma membrane. Recent findings suggest that Aster proteins facilitate non-vesicular transport of cholesterol from the plasma membrane to the endoplasmic reticulum in mammalian cells (Sandhu et al, 2018). Whether protein Aster-C and/or the Gramd1c transcript can localise to the plasma membrane in mammalian neurons and, importantly, in axons and growth cones, remains elusive. Future experiments will use axonal isolates from compartmentalised cultures to characterise the populations of B1-related transcripts present in developing axons of cortical primary cultures.

The investigation of microRNA evolution is important not only for phylogenetic classification studies, but also for the investigation of the relevance of microRNA expansions coincident to times of increasing organism complexity during evolution. Indeed, significant microRNA expansions could help explain the rapid emergence of species diversification at specific evolutionary times, such as the mammalian radiation (Iwama et al. 2013). Additionally, understanding microRNA evolution has strong implications for the study of microRNA biology and function as the evolutionary origin of microRNAs can help disentangle and identify the microRNA-dependent regulatory networks being targeted (Barbash, Shifman, and Soreq 2014; Lehnert et al. 2009; Spengler et al. 2014). Importantly, given that younger, lineage-specific microRNAs in human tend to be neuronal and target neuronal gene networks (Barbash et al. 2014; SALISBURY 1946), understanding the evolutionary origins of neuronal microRNAs can significantly aid the investigation of their function.

In conclusion, the work presented in this chapter has built from the identification of microRNAs enriched in the axon of cortical neurons and

performs a comprehensive analysis based on their evolutionary origin. It has identified miR-3470b as a prototypical example of a TE-derived microRNA that has rapidly evolved to target specific functional mechanisms with impact in the development of neuronal connectivity.

4. Role of axon-enriched miR-99a in axon development and network connectivity

4.1 Introduction

4.1.1 miR-99a, an old friend of metazoan genomes

In addition to lineage/species-specific microRNAs, deep sequencing profiling of microRNA population of cortical axons identified microRNAs widely conserved across vertebrates. One of such microRNAs is miR-99a, a younger distant relative of the miR-10 precursor family of microRNAs, a group of microRNAs that derive from the same common ancestor. The miR-10 family is the most evolutionarily ancient animal microRNA family known and it is thought to have arisen in a common ancestor of Eumetazoans, around 650 million years ago (Grimson et al. 2008; Tehler, Høyland-Kroghsbo, and Lund 2011; Wheeler et al. 2009). In particular, miR-99a shares a high level of sequence conservation across vertebrates, with the mature microRNA sequence displaying 100% identity conservation from human and mouse to zebrafish and xenopus.

In mouse and human, miR-99a is genomically encoded within a polycistron embedded in chromosome 16 and 21, respectively. Commonly known as megakaryocytic oncogenic non-coding RNA gene (MONC) in mouse, this tricistron encodes for mouse let7c, miR-99a and miR-125b-2 and is transcribed to a primary transcript that is later processed to multiple mature microRNAs. From the two mature microRNA sequences generated from the mmu-miR-99a precursor hairpin, mmu-miR-99a-3p and mmu-miR-99a-5p, the miR-99a-5p is the overwhelmingly most expressed strand (Kozomara and Griffiths-Jones 2014), and the one found to be enriched in axons in our miRNA-seq screen data (Chapter 1). Hereafter, mmu-miR-99a-5p will be referred to as miR-99a throughout this chapter.

4.1.2 miR-99a in neuronal development and function

MiR-99a function has been most explored in cancer biology with several studies implicating this microRNA in various cancer types including glioblastoma, breast, epithelial ovarian, bladder and gastric cancer, to name a few. miR-99a actions in cancer appear to be mainly tumour suppressive and some anti-tumour effects were linked to miR-99a regulation of mTOR and FGFR3 signalling pathways (Chakrabarti et al. 2013; Feng et al. 2014; Jiang et al. 2014; Yang et al. 2014).

In the nervous system, miR-99a has been identified as part of the subset of brain-enriched microRNAs in independent studies. Using a next-generation sequencing approach, Yao et al. profiled the global small RNA transcriptome of the rat cerebral cortex over development, from embryonic day 10 to postnatal day 28. From E13 onwards, miR-99a consistently ranked within the top 20 highly expressed microRNAs in the rat cerebral cortex (Yao et al. 2012). In an attempt to characterise microRNA expression during the transition from neuronal progenitors into the earliest differentiating cortical neurons, Nielsen et al. analysed the expression profiles of rat neuronal progenitors at embryonic day 11, 12 and 13 by microarray technology. miR-99a was found >10 fold upregulated in E13 vs E11 whereas the expression of miR-99a bioinformatics predicted targets was downregulated (Nielsen et al. 2009a).

In cultured neurons, our enrichment analysis of axon vs cell body RNA fractions indicates that miR-99a is enriched in cortical axons. Likewise, the same observation was made by Natera-Naranjo and colleagues in the axons of sympathetic neurons upon axon enrichment analysis using microRNA microarray data (Natera-Naranjo et al. 2010). In contrast, miR-99a was found depleted in dendrites of rat hippocampal neurons by RT-qPCR (Kye et al. 2007), which hints at potential axonal functions for miR-99a.

Despite being highly expressed and developmentally regulated in the brain, evidence of a function for this microRNA in the nervous system is largely lacking. In a few studies, miR-99a has been found within biochemical preparations enriched for synaptic terminals (Li et al. 2015; Lugli et al. 2008b) and was shown to be released from synaptosomes in a calcium dependent manner (Xu et al. 2013). Thus it is possible that miR-99a is involved in the

formation of synaptic connections. Recently, miR-99a regulation was implicated in neuroregeneration processes following spinal cord injury in mice. Specifically, miR-99a inhibition protected neurons from apoptosis after injury, likely via modulation of mTOR expression (F. Cao et al. 2017).

4.1.3 Aims

miR-99a is a well conserved microRNA with ancient evolutionary roots and, despite its high expression in the human and rodent brain, the potential roles of this microRNA in neuronal function, specifically neuronal development, remain undisclosed. Our preliminary findings identified miR-99a as one of the highly enriched microRNAs in developing axons, strengthening the case for its potential relevance in neuronal function. Experiments described in this chapter will explore the role of miR-99a in the development of neuronal connectivity in cultured mouse cortical neurons, with focus on its actions in the regulation of axonal outgrowth over development and the impact on the formation of neuronal networks.

The specific experimental aims of this chapter are as follows:

- Study the regulatory effects of miR-99a in outgrowth of developing cortical axons in culture, by manipulating its activity with microRNA mimics and inhibitors;
- Examine miR-99a expression regulation over development in growing cultured cortical neurons;
- Identify and validate the regulatory target gene that mediates miR-99a actions in axonal outgrowth;
- Investigate novel roles for the functional target gene of miR-99a in axonal development, using gain and loss-of-function approaches;
- Address the axonal localisation of miR-99a and its function in axon growth;
- Evaluate the functional consequences of miR-99a inhibition in the development of network activity patterns through the analysis of spontaneous calcium oscillations in developing cortical cultures.

4.2. Results and Discussion

4.2.1 Expression and regulation of miR-99a in developing cortical neurons

microRNA profiling of cortical axons identified miR-99a as part of the top 5 most enriched microRNAs in developing axons when compared to the cell body fraction, in neurons cultured on compartmentalised microfluidic devices (see introduction, section 1.7). In further experiments, the relative abundance of the top 25 axon-enriched microRNAs was measured in whole cortical cultures at day 2 in vitro (DIV2), by real time qPCR. As shown in figure 4.1.a., miR-99a was one of the microRNAs most highly expressed in neurons amongst the 25 axonal microRNAs, quantified using the delta Ct method (only the 10 most abundant axonal microRNAs are shown, data normalised to the global mean Ct of 25 microRNAs). Interestingly but perhaps unsurprisingly, microRNAs with known roles in the regulation of axonal outgrowth appear within the most abundant axon-enriched microRNAs in fast-growing DIV2 cortical cultures (Figure 4.1.a). miR-9 was reported by our group as a local regulator of axon growth through repression of axonal expression of Map1b in cortical axons (Dajas-Bailador et al. 2012). Likewise, in a recent study from our lab, miR-26a was found to mediate both neuronal polarity and axonal outgrowth by modulation of GSK3β at distinct developmental stages of cortical neuronal development *in vitro* (Lucci et al, manuscript in preparation). Furthermore, studies by the Kaplan lab showed that miR-16 is highly abundant in rat superior cervical ganglia axons and represses axon growth, at least in part, by regulating the local protein synthesis of eukaryotic translation initiation factors eIF2B2 and eIF4G2 in the axon (Kar et al. 2013; Natera-Naranjo et al. 2010). Hence, evidence from the literature further supports a possible role for miR-99a in axonal processes.

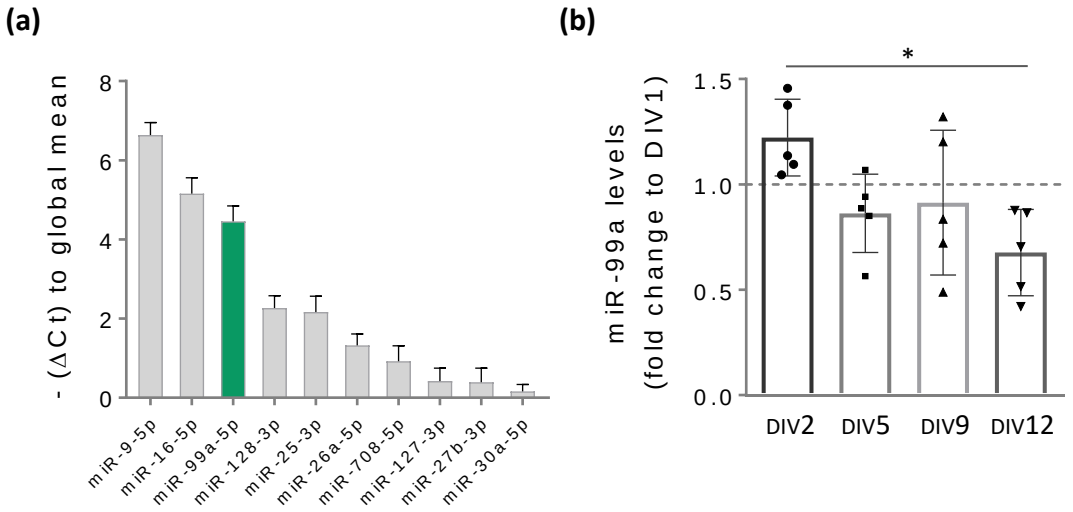


Figure 4.1. (a) Relative expression of axon-enriched miRNAs in primary cortical cultures at DIV2, showing miR-99a (green fill) amongst the highest expressing miRNAs (only the 10 most abundant miRNAs in axons are represented). Data is expressed as inverse ΔCt of each miRNA to the global mean of 25 miRNAs and is represented as mean±SEM of a minimum of two biological replicates, each read in duplicate. **(b)** miR-99a expression over development of cortical primary cultures relative to DIV1. Data expressed as fold change to DIV1 and normalized to miR-100 and let-7c reference genes using the ΔΔCt method; mean±SD of 5 independent experiments, each read in duplicate. One-way ANOVA with pos-hoc Tukey's test, **P<0.05.*

To investigate a potential role for miR-99a in the development of axonal connectivity in cortical cultures, miR-99a expression levels were quantified by real-time qPCR at different stages of cortical development *in vitro*. Levels of the mature miR-99a sequence (mmu-miR-99a-5p) were measured at DIV2, DIV5, DIV9 and DIV12 and the data analysed as relative expression to DIV1, correspondent to 4h after plating (figure 4.1.b). Relative expression at each timepoint was calculated following the comparative ΔΔCt method to expression at DIV1 (represented as fold change to DIV1). miR-100 and let-7a were selected as reference genes for normalisation since both microRNAs were found to be stable over the timepoints analysed (ΔCt < 1.5 between all timepoints). Moreover these two microRNAs showed similar Ct values and, consequently, expression levels, to miR-99a. For a detailed description of the ΔΔCt method and choice of reference genes please see Methods.

As depicted in figure 4.b, miR-99a levels show a slight increase at DIV2, when developing axons start to actively extend (Dotti et al. 1988; Polleux and Snider

2010). miR-99a expression shows a modest decreasing trend at DIV5 and DIV9 with a 0.86 and 0.91 fold change to DIV1, respectively. A more notable decrease of 0.68 fold was observed at a later stage of development, DIV12, a period when the rate of axon growth has slowed down and synaptic connectivity is maturing (Chiappalone et al. 2006). Despite the observed downregulation over the timepoints measured, in particular at later stages, miR-99a is consistently highly expressed in cortical neurons over the course of neuronal development in culture.

4.2.2 Effect of miR-99a in axonal outgrowth

As part of the functional screen of axonal microRNAs, loss and gain of function experiments were conducted to investigate whether there is a role for this microRNA in the outgrowth of cortical axons over neuronal development in culture.

As discussed for miR-3470b in the previous chapter (section 1.5), microRNA functional studies used locked nucleic acid (LNA) antisense nucleotides to specifically inhibit (LNA inhibitors) or mimic (LNA mimics) miR-99a function and thus assess the impact of this microRNA in the growth of cortical axons in a culture model of axon development using cortical primary neurons (see methods). Briefly, cortical neurons were cotransfected at DIV2 with either miR-99a inhibitors or mimics and GFP and later fixed 72h after transfection, at DIV5. Cotransfected GFP was used as a reporter to identify transfected neurons to be selected for analysis and, simultaneously, allow for adequate visualisation of neuronal morphology (Dajas-Bailador, Jones, and Whitmarsh 2008; Hancock et al. 2014). At this stage of neuronal development in culture, cortical axons have already specified and are at a period of intensive active growth (Dotti et al. 1988; Polleux and Snider 2010), making DIV2-DIV5 an ideal temporal window to study key players in axonal development and outgrowth. Furthermore, this experimental window was previously chosen and validated by our group to investigate the role of JNK interacting protein 1 (Jip1) and miR-9 in axon growth (Dajas-Bailador et al. 2014, 2008).

In cortical neurons, blocking miR-99a function by transfection of a miR-99a inhibitor resulted in significantly shorter axons. Indeed, in GFP-positive neurons transfected with miR-99a inhibitor, average axonal length showed a 21.5% and 27.3% decrease (for 25nM and 50nM of miR-99a inhibitor, respectively) when compared to neurons transfected with a non-targeting oligonucleotide as a control (Figure 4.2).

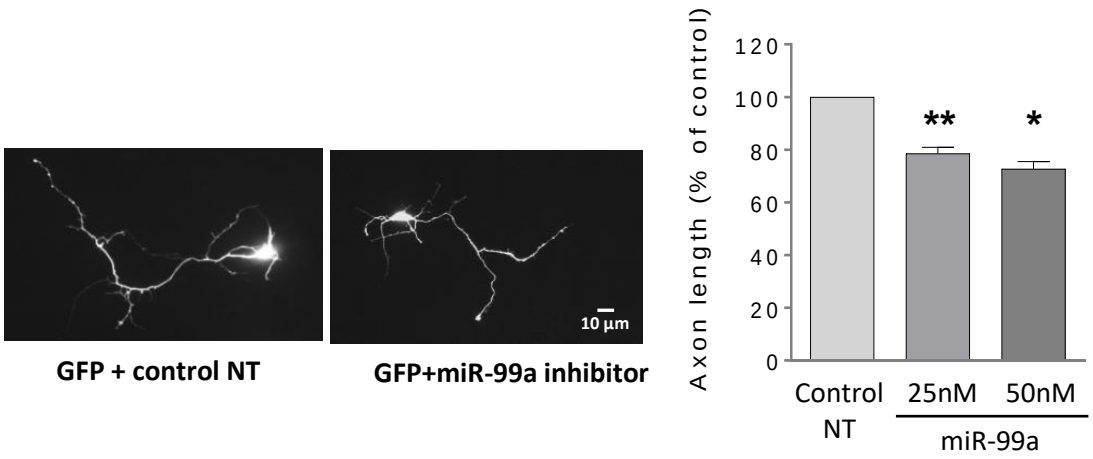


Figure 4.2. Inhibition of miR-99a function leads to shorter axons in cortical neurons. Developing cortical neurons were transfected with miR-99a inhibitor (DIV2), the length of axons of GFP-positive neurons measured 72h after transfection (DIV5) was 78.5% and 72.7% of the control, when 25nM and 50nM of miR-99a inhibitor, respectively, was used. Neurons were cotransfected with GFP for visualisation of transfected neurons. Control neurons were transfected with non-targeting oligonucleotides. Data are expressed as percentage of the average length of control axons and presented as mean±SEM from four independent experiments (>200 axons measured for each condition); Student's t-test *$P<0.05$, **$P<0.01$.

To further assess the role of miR-99a in the extension of axons, cortical neurons were cotransfected with miR-99a mimic and GFP to study the effect of increasing miR-99a levels in the outgrowth of developing axons (see Methods section for details on the mechanism of action of microRNA mimics). The same developmental window used to test miR-99a depletion was also used to investigate the effect of miR-99a mimic; indeed cortical neurons were cotransfected with GFP and miR-99a mimic or a non-targeting oligonucleotide control (mimic negative control) at DIV2 and axon length was measured at DIV5. As depicted in figure 4.3, ectopic expression of miR-99a led to an

increase in axon length relative to control of 16.5% when miR-99a mimic was transfected at 25nM and 22.5% when 50nM of mimic was used. This data complements the observations made for miR-99a inhibition, where the opposite effect, decrease of axonal length, was observed. Importantly, dendrite length did not alter in neurons transfected with miR-99a mimic in comparison to control (data not shown). Of note, the effects of miR-99a inhibitors and mimics in axonal length appear to be dose dependant, consistent with a biologically relevant function of miR-99a in axon extension over the development of the neuronal networks in vitro.

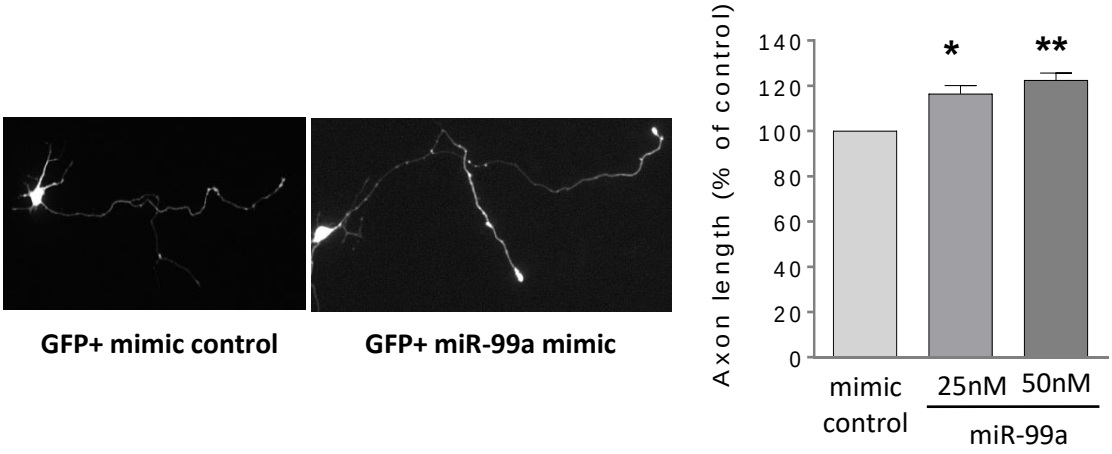


Figure 4.3. miR-99a promotes axon extension in cortical neurons. Ectopic expression of miR-99a in cortical neurons results in axons 16.5% (25nM miR-99a mimic) and 22.5% (50nM miR-99a mimic) longer than axons of neurons transfected with mimic negative control. Cortical primary cultures were cotransfected 24h after plating with GFP and miR-99a mimic or mimic negative control and imaged at DIV5, representative images of GFP-positive neurons for both conditions are shown on the left. Data are expressed as percentage of average length of control axons and presented as mean±SEM from five independent experiments (>250 axons measured for each condition); Student's t-test value *$P<0.05$, **$P<0.01$.

Collectively, these observations provide compelling evidence for a role of miR-99a in the regulation axonal outgrowth over development of cortical neurons *in vitro,* suggesting that miR-99a is necessary for the normal extension of the cortical axon as inhibition of its function disturbs outgrowth. Moreover, these functional data suggest miR-99a-dependant regulation favours axonal growth, making miR-99a a positive modulator of axon extension in developing cortical axons.

The recognition/identification of a function for miR-99a in axonal development supports the working hypothesis in our lab that microRNAs enriched in cortical axons appear to be more likely to have a role in inherently axonal processes, such as axon extension, as they navigate towards their post-synaptic partners. In the past few years, this hypothesis has been gaining strength with various studies, including work developed in our lab (Section 1.5 and Chapter 3), reporting axon-enriched microRNAs with relevant roles in the regulation of key players in cytoskeleton formation and axon guidance of different neuronal types, including mouse dorsal root ganglia, frog retinal ganglion cells, rat superior cervical ganglia and mouse cortical neurons (Aschrafi et al. 2008; Baudet et al. 2012; Bellon et al. 2017; Dajas-Bailador et al. 2012; Hancock et al. 2014; Zhang et al. 2013).

To better elucidate the role of miR-99a in cortical axon development, further experiments aimed at the investigation of genes potentially targeted by miR-99a that are capable of mediating the observed effect of this microRNA in axonal outgrowth. The following section focuses on the prediction strategy of miR-99a putative targets and the subsequent validation of one of such genes as a target of miR-99a.

4.2.3 In search of miR-99a regulatory pathway

As discussed in previous chapters, one challenging stage of microRNA research is the identification and investigation of microRNA-dependant regulatory pathways underlying the function of specific microRNAs in a biological process of interest. This project drew from published evidence to develop a bioinformatics workflow aiming at identifying candidate genes potentially targeted by miR-99a (Peterson et al. 2014; Riffo-Campos et al. 2016). Briefly, microRNA-mRNA interaction prediction algorithms generated a set of candidate miR-99a target genes that were further assessed for expression and function in the nervous system, in an attempt to select meaningful targets that could mediate/explain miR-99a actions in the cortical axon.

Firstly, two of the most widely used microRNA target prediction tools, TargetScan and DIANA-microT-CDS, were employed to create a computational

prediction of the transcripts potentially targeted by miR-99a. Both tools produced a ranked list of genes scored by strength of predicted miR-99a-mRNA site interaction: 52 targets in TargetScan (TargetScanMouse 7.1, genes with only poorly conserved sites were excluded; Agarwal et al. 2015) and 23 targets with DIANA microT-CDS v5.0 (miTG score threshold >0.7, Paraskevopoulou et al. 2013).

Interestingly, the list of putative targets produced by these tools is unusually short when compared to other microRNAs, including species-specific miR-3470b, investigated in chapter 3, which was predicted to target a much higher number of transcripts. Moreover, in one of the most recent updates of the TargetScan prediction tool, the Bartel lab describes that even widely conserved microRNA families are predicted to target over 400 conserved transcripts on average (Agarwal et al. 2015; Bartel 2009). An interesting line of research would be to investigate the biological significance of the low number of predicted targets for such broadly conserved and highly expressed microRNAs, such as miR-99a. Can the significantly lower number of targets have an impact in microRNA function? For example, due to the lack of buffering from other transcripts? Can an explanation be found in the specificity of processes controlled by these microRNAs?

Following a similar rationale to the one used for miR-3470b target prediction workflow (Section 3.4), and in order to increase the likelihood of identifying true targets, genes common to the two target lists were matched to obtain a final subset of 17 target genes (figure 4.3.a) given by both TargetScan and Diana microT-CDS prediction analysis (Riffo-Campos et al. 2016; Sethupathy et al. 2006). Despite the undeniable utility and convenience of these tools for microRNA binding prediction, the use of these algorithms alone cannot determine which predicted targets can truly be physiologically meaningful in any given biological process, such as in axonal development. In addition to effective binding, another important consideration in the search of relevant candidates is the simultaneous expression of a microRNA and its targets. MiR-99a biological targets must be expressed in the same place at the same time to allow regulation to occur, therefore targets mediating miR-99a regulatory action in axon development must be expressed in the developing brain.

The strategy devised to narrow down the list of predicted targets to determine the strongest candidates combined three main pillars (Figure 4.4): 1) score of targeting prediction; 2) expression levels of the candidate genes in the tissue of interest, the brain; and 3) known role in neuronal function and/or cell growth, with special relevance to neuronal/cell growth phenotypes that recapitulate/are in agreement to/with miR-99a function in axon growth.

Hence, the putative targets shortlisted for miR-99a were ordered according to the predicted efficacy of targeting, as determined by TargetScan Mouse 7.1 (Figure 4.4.b). This tool was found to yield lower number of false positives when compared to Diana microT-CDS and other microRNA target prediction tools (Peterson et al. 2014; Riffo-Campos et al. 2016). TargetScan's algorithm translates the efficacy of targeting into a score system representing the cumulative weighted *context scores* ++ of all the conserved 8mer, 7mer, and 6mer binding sites (site type classification based on the number and position of seed nucleotides involved in target binding) that match the seed region of a microRNA of interest within each target transcript. C*ontext scores* ++ for individual microRNA binding sites are a result of the contribution of several components relevant for microRNA binding probability such as site type, supplementary pairing of nucleotides outside the seed region and, importantly, conservation of the interaction pair (Agarwal et al. 2015). Figure 4.4.b) shows miR-99a putative targets ranked from high to low prediction strength, according to the cumulative *context scores* ++ calculated for each target transcript. Of note, in accordance to Targetscan's scoring system, a more negative score is associated with a more favourable site, therefore corresponding to a higher position in the ranking.

As a next step, the 17 candidate targets were examined for evidence of expression in the nervous system, more specifically in the brain, following the assumption that, in this study, relevant miR-99a-target interactions are conserved in human. Hence, RNA sequencing data available from the Human Protein Atlas database was used to rank candidate targets according to their expression in the human brain (figure 4.4.c). The Human Protein Atlas (HPA) aims at generating a map of all the proteins existent in human tissues and cells by integrating transcriptomics, proteomics and imaging data (Uhlén et al. 2015, www.proteinatlas.org). HPA Tissue Atlas database gathers RNA

sequencing data from 37 major different normal tissue types. Of those, mRNA expression data in *cortical cortex* was used to order the candidate targets within an arbitrary scale where higher and lower boundaries correspond to the predicted targets with the higher and lower median transcript per million (TPM) given by the HPA cortical cortex database (figure 4.3.c).

Finally, the role of each target in neuronal function and development was investigated by manual curation of the literature. This served two purposes, gather hints on the molecular pathways miR-99a could be regulating in neurons and, more importantly, allowed to select targets whose described function in the nervous system, nervous system development or in general cell growth match the phenotype of miR-99a in cortical axons. Functional data discussed in 4.2 suggests that miR-99a acts as a growth promoting factor in developing cortical neurons, therefore miR-99a regulation is expected to silence growth suppressor genes. This led to exclusion of arguably more classic neuronal genes such as *Fgf* receptor 3 and *mTor*, known to promote growth (Jaworski and Sheng 2006).

This strategy generated four final candidate targets: heparin sulfate-3-O-sulfotransferase 2 (*Hs3st2*), mothers against decapentaplegic homolog 7 (*Smad7*), CTD small phosphatase-like protein (*Ctdspl*) and frizzled class receptor 5 (*Fzd5*). The predicted miR-99a binding sites for these gene candidates and respective prediction score obtained via TargetScan analysis are depicted in table 4.1. Notably, miR-99a is predicted to target another member of the heparin sulphate sulfotransferase family, *Hs3st3b*, however its expression in the human brain and even other nervous system tissues appears to be negligible in the RNA-seq datasets explored in this study, thus this gene did not make to the final candidate shortlist.

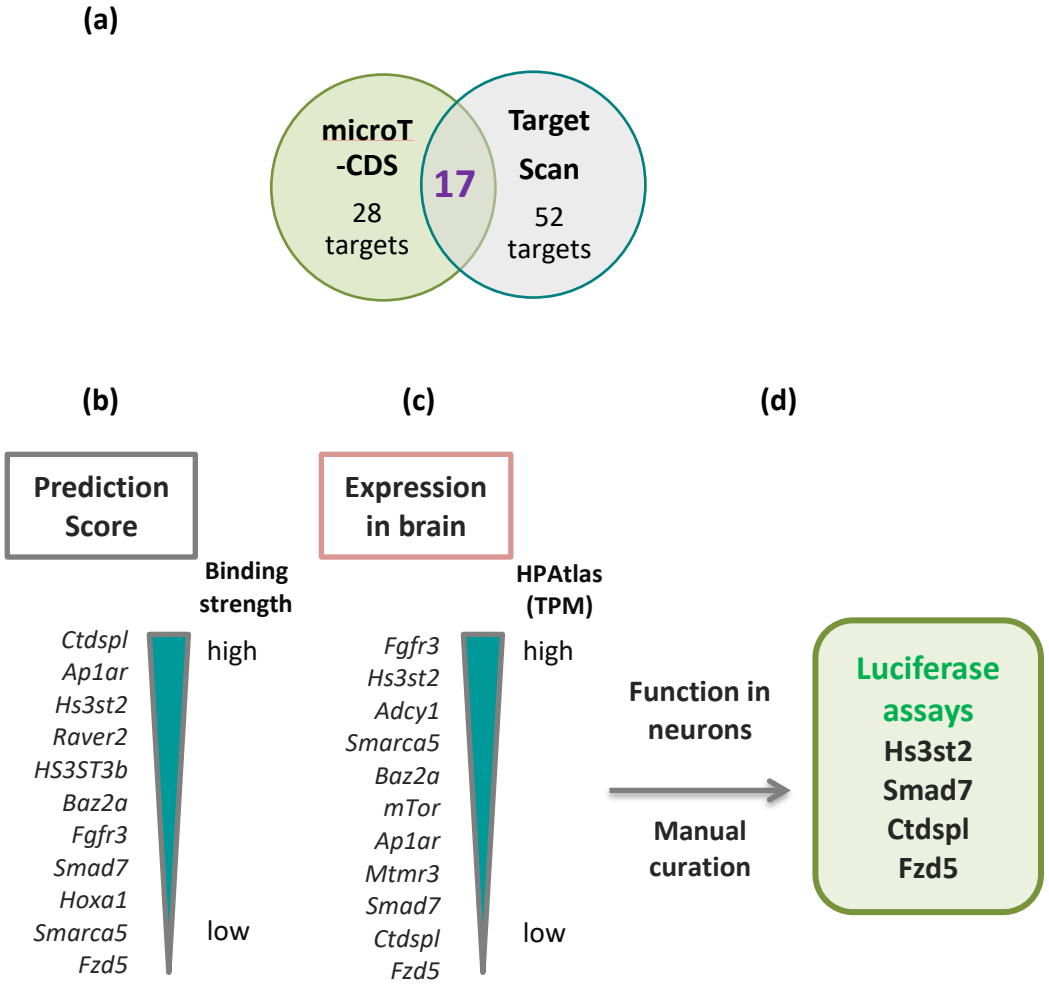


Figure 4.4. Strategy for prediction of miR-99a putative targets. (a) miR-99a targets were predicted computationally by overlapping target candidates obtained by DIANA microT-CDS v5.0 and TargetScanMouse 7.1 bioinformatic tools. **(b)** The subset of putative targets was ranked according to efficacy of binding given by TargetSCan's prediction score (Context score ++) and **(c)** to expression in the human brain according to the Human Protein Atlas gene expression database (TPM=reads per kilobase million). For clarity, only the top 10 transcripts are shown for both rankings. **(d)** These target genes were submitted extensive literature search for their roles in the nervous system. Targets with a high prediction score, expressed in the human brain and neuronal/cell growth function in agreement with miR-99a-dependant regulation of axon growth were selected for further binding assays using luciferase reporters.

Candidate target	Position on 3'UTR	Target site binding	Site type	Context score++
Hs3st2	Position 640-647	5' ...CACAUAAUCUGCUGUUACGGGUA ||| ||||||| 3' GUGUUCUAGCCUAG-AUGCCCAA	8mer	-0.76
Ctdspl	Position 2474-2481	5' ...UUUUCUUAAGGUAAAUACGGGUA ||||||| 3' GUGUUCUAGCCUAGAUGCCCAA	8mer	-0.69
Smad7	Position 44-50	5' ...GGUAGUUCUUUAAUUUACGGGUC ||||||| 3' GCGUUCCAGCCAAGAUGCCCAC	7mer	-0.4
Fzd5	Position 3721-3727	5' ...UUUAGUGACUUUUGAUACGGGUU ||||||| 3' GCGUUCCAGCCAAGAUGCCCAC	7mer	-0.25

Table 4.1. Predicted target sites of miR-99a for the gene candidates. The position of the binding site in the 3'UTR of the transcript, the putative microRNA binding site, site type and Context score++ obtained in TargetScan are shown for the candidate target genes. More negative Context score++ values indicate increased binding preference.

To validate miR-99a – target binding, the candidate genes were taken to an *in vitro* screening using dual firefly/renilla luciferase reporter assays conducted in HEK293T cells. The oligonucleotide corresponding to the predicted miR-99a site in the 3'UTR of each four candidates was cloned downstream the firefly luciferase to obtain dual luciferase reporters for mouse *Hs3st2*, *Smad7*, *Ctdspl* and *Fzd5* predicted sites. These reporter constructs were cotransfected into HEK293T cells, along with miR-99a mimic or negative mimic control, and the activity of both luciferases was measured. In this dual reporter system, the expression of renilla luciferase is independent of microRNA regulation, functioning as an internal control of cell number and transfection efficiency, whereas firefly luciferase expression and subsequent activity is dependent on target site regulation by miR-99a. miR-99a binding to a target site was assessed by the capacity of miR-99a mimic to induce a decrease in the ratio firefly/renilla activity. For three of the targets tested, Ctdspl, Smad7 and Fzd5, miR-99a expression was unable to repress firefly/renilla activity in HEK293T (data not shown). This data suggests that these three transcripts are not direct targets of miR-99a, at least not through binding to their predicted target site.

However, when the miR-99a mimic was transfected together with *Hs3st2*-site reporter construct, the firefly/renilla activity ratio underwent a decrease of 23.6% in comparison to the mimic negative control (Figure 4.5.b). To further verify the specificity of microRNA binding to target site, a mutated dual luciferase reporter was designed, *Hs3st2*-mut. Indeed, site directed mutagenesis of four nucleotides in the seed region of the predicted site blocked miR-99a-induced decrease of firefly/renilla activity (figure 4.5.b), thus confirming the importance of *Hs3st2*-site specific sequence for silencing. A diagram of the dual luciferase constructs designed for *Hs3st2*-site and *Hs3st2*-mut are shown in figure 4.5.b (only the site's sequence correspondent to miR-99a seed region is shown, see methods for full sequences of the oligonucleotides).

This assay validated that *Hs3st2* is a *bona fide* target of miR-99a. Indeed, it shows that miR-99a can directly target and regulate *Hs3st2* through its predicted binding site. Moreover, the seed sequence located at positions 640-647 is essential for this regulation to take place. Figure 4.5.a depicts the binding of miR-99a to its site, embedded in the 3'UTR of *Hs3st2* transcript. As shown, miR-99a binds to *Hs3st2* through an 8mer site, correspondent to an exact match to positions 2-8 of the mature microRNA (seed region 2-7 + position 8) followed by an 'A' (TargetScan nomenclature, Agarwal et al. 2015). 8mer sites were shown to mediate the strongest expression repression of all site types (Baek et al. 2008). Furthermore, miR-99a binding site on *Hs3st2* 3'UTR is broadly conserved across vertebrate families and fully conserved in human (figure 4.x.x), which further supports the biological relevance of the miR-99a – *Hs3st2* interaction.

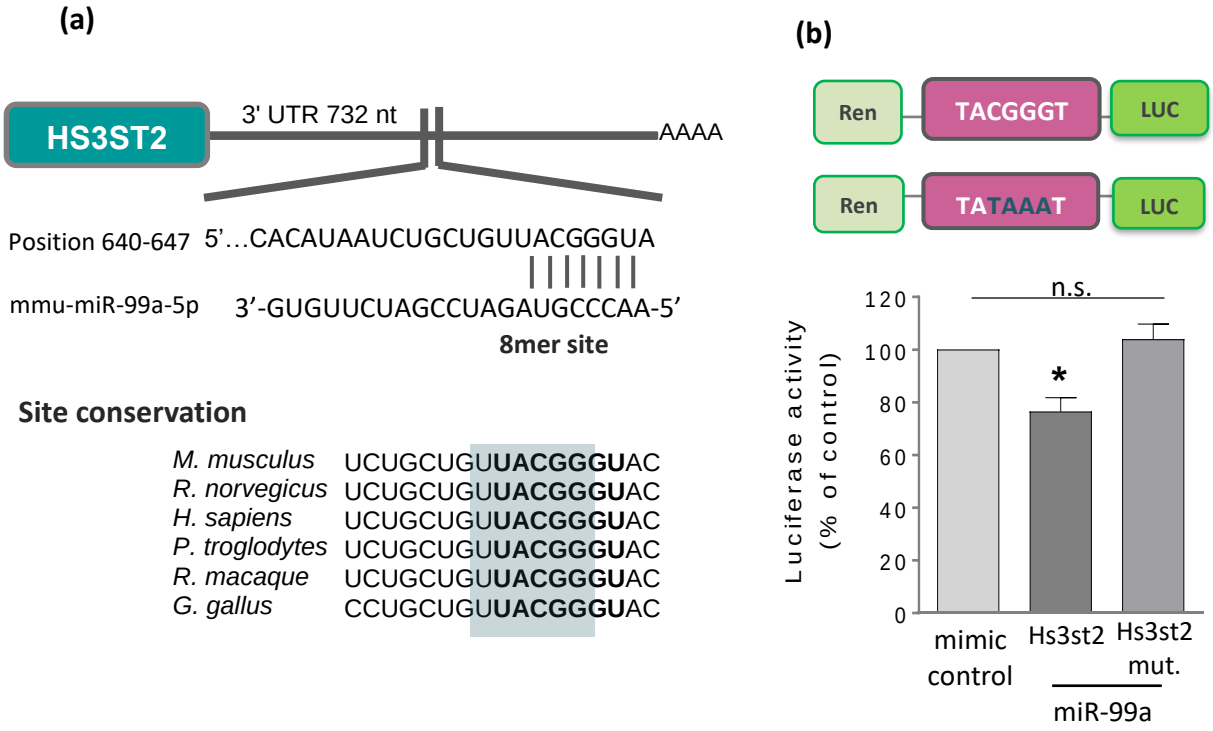


Figure 4.5 Hs3st2 is a target of miR-99a. (a) Schematic representation of mouse Hs3st2-site oligonucleotide cloned downstream the firefly luciferase in a dual firefly/renilla reporter (top). Hs3st2-mut reporter construct where four nucleotides complementary to the seed region of miR-99a were mutated (bottom). c) Diagram of miR-99a site within the 3'UTR of Hs3st2 showing the complementary binding to miR-99a seed sequence, 8mer site highlighted in purple. d) Sequence alignment of the 3'UTR of Hs3st2 showing conservation of miR-99a binding site (highlighted in grey) across different vertebrates. **(b)** Dual luciferase assay of miR-99a predicted site in Hs3st2 3'UTR shows a decrease of 23.6% of control in the firefly/renilla luciferase activity ratio upon cotransfection of Hs3st2-site reporter along with miR-99a mimic (100nM) into the HEK293T cell line. On the other hand, miR-99a mimic had no significant effect on the firefly/renilla activity ratio when the Hs3st2-site was mutated, indicating that miR-99a regulates Hs3st2 by direct binding to its predicted site. Data expressed in percentage of mimic control and presented as mean±SEM, average of 3 independent experiments, each conducted in triplicate; one-way ANOVA with Dunnet's pos-hoc test, *$P<0.05$, n.s.: non-significant.

4.2.4 Expression profile of HS3ST2 in cortical cultures over development

Despite being enriched in the brain and known to be expressed in developmental models of C.elegans and in the zebrafish and mouse brain (Bülow and Hobert 2004; Cadwallader and Yost 2006; Lawrence et al. 2007), the function of HS3ST2 in the nervous system is largely unknown. Expression of *Hs3st2* in the cortical plates of mouse embryo hints at a possible function in cortical development (Yabe et al. 2005), however little is known about the role of *Hs3st2* in the different developmental stages, including axonal outgrowth.

To begin to elucidate the potential functions of HS3ST2 in cortical neuronal development, the expression of HS3ST2 was examined in cortical neurons growing *in vitro,* both at the transcript and at the protein levels. Firstly, the same total RNA samples extracted from primary cortical cultures at five different timepoints to profile miR-99a levels, were again used to investigate *Hs3st2* expression patterns in young neurons at DIV1, DIV2, DIV5, DIV9 and DIV12 in culture. Relative quantification by RT-qPCR revealed that *Hs3st2* is expressed in developing cortical neurons *in vitro* across all the timepoints analysed (average Ct of 26.18 from all samples tested) at high enough levels that allow for a potential miR-99a regulation axis (Baek et al. 2008). Moreover, these data indicates that *Hs3st2* is upregulated over cortical development, as shown in figure 4.6.a). *Hs3st2* is expressed as early as DIV1 (4h after plating) and DIV2 (24h after plating), after then, at DIV5, *Hs3st2* levels show a marked increase of 4.7 fold relative to DIV1 levels. This increasing trend was gradually maintained at DIV9 and DIV12, when HS3ST2 expression increased 5.3 fold of the initial DIV1 levels.

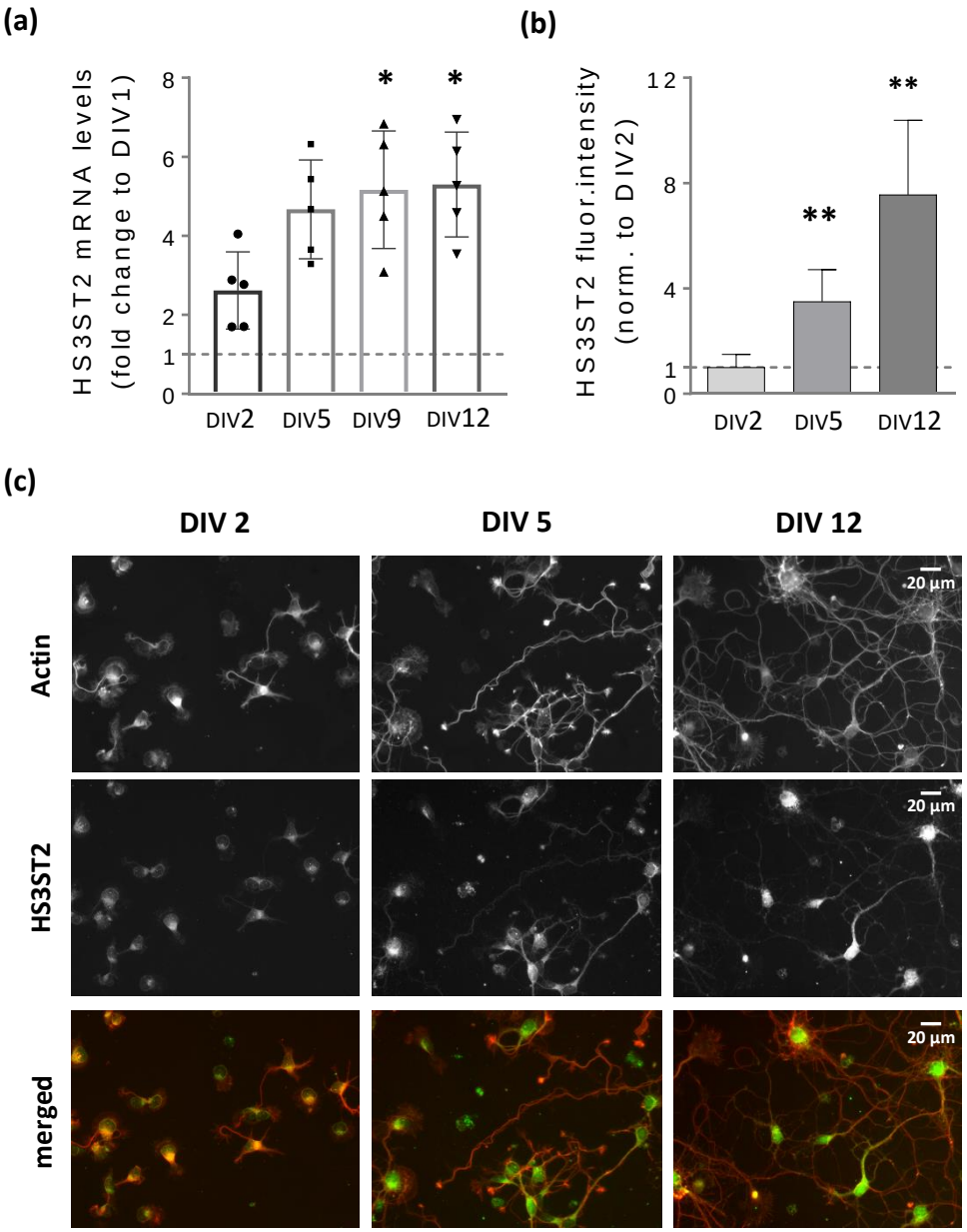


Figure 4.6. Endogenous HS3ST2 expression is upregulated over development of primary cortical cultures. (a) *Hs3st2* transcript was quantified by RT-qPCR in cortical cultures at DIV1, DIV2, DIV5, DIV9 and DIV12. The graph represents *Hs3st2* expression levels relative to DIV1, showing a marked increase over development. UBE2 and GAPDH were used as reference genes and for normalisation using the ΔΔCt method to DIV1 (see Methods). Data expressed as fold change to DIV1, mean±SEM of 5 independent experiments, each read in duplicate; One-way ANOVA with Dunnet's pos-hoc test *$p<0.05$. **(b)** Quantification of HS3ST2 immunofluorescence signal shows an accentuated increase of the protein levels over development of cortical neuronal cultures. In each experiment data were normalised to the average fluorescence at DIV2; mean±SEM from three independent experiments, in each at least 60 neurons were quantified per condition; Student's t-test **$p<0.01$. **(c)** Representative images of cortical cultures at DIV2, DIV5 and DIV12 following actin (phalloidin) and HS3ST2 staining (immunofluorescence). The increase of HS3ST2 protein levels is well visible between developmental stages, particularly at DIV12. In the merged panel, actin staining is represented in red and HS3ST2 in green.

In addition, HS3ST2 expression patterns in developing cortical cultures were investigated at the protein level. Toward this end, primary cortical cultures at three different stages of neuronal maturation, DIV2, DIV5 and DIV12 were immunostained for HS3ST2 to examine the protein endogenous levels. Phaloidin staining of actin filaments was used for better visualisation of neuronal morphology (figure 4.6.c). Protein expression levels of HS3ST2 were measured by quantification of fluorescence intensity and normalised as relative to DIV2 levels. Unsurprisingly, HS3ST2 protein expression recapitulated the profile of its transcript, showing a clear upregulation over time, particularly in the later timepoint, DIV12, when fluorescence intensity was 7.5 fold of DIV2 (Figure 4.6.b).

Collectively, these findings suggest that HS3ST2 is abundantly and dynamically expressed during the development or cortical neurons in culture. Notably, the profile of HS3ST2 over development in culture display the inverse expression patterns of miR-99a at the same timepoints, implying that they are inversely regulated as expected for a microRNA and its target transcript. This is in accordance with several reports where inverse expression profiles between a microRNA and their targets, including brain-enriched microRNAs (Manakov et al. 2009; Nielsen et al. 2009; Sood et al. 2006).

4.2.5 Role of HS3ST2 in axon development

4.2.5.1 HS3ST2 overexpression results in shorter axons

The role of HS3ST2 in the nervous system is largely unknown. Nevertheless, its expression has been shown in the developing zebrafish nervous system and the mouse brain (Cadwallader and Yost 2006; Yabe et al. 2005). Regarding function, HS3ST2 activity has been shown to be necessary for the abnormal phosphorylation of tau in cellular models and in zebrafish models of tauopathy, in which inhibition of HS3ST2 expression further inhibited the accumulation of abnormally phosphorylated tau epitopes in the fish brain and spinal cord. Importantly, HS3ST2 inhibition rescued the tau-induced functional defects in motor neuronal axons and let to the recovery of the animal motor

response to touch stimuli (Sepulveda-Diaz et al. 2015). These findings further encouraged the investigation of roles of HS3ST2 in axonal development.

It was hypothesised that if miR-99a modulates axonal outgrowth through regulation of its, now validated, target, then HS3ST2 must have a functional role in the cortical axon. With the goal to uncover a potential role for HS3ST2 in axonal development in mind, the first approach was to conduct gain and loss-of-function experiments in primary cortical neurons to examine the impact of this protein in axonal outgrowth. These experiments were performed at the same developmental stage selected for miR-99a functional assays, DIV2-DIV5, correspondent to a period, just after axonal specification, with a high rate of axonal outgrowth and a time frame when miR-99a-dependant regulation was shown to occur (section 4.2.1).

Mouse HS3ST2 coding sequence was subcloned into the pcDNA 3.1(+) vector (pc-HS3ST2) and cotransfected with a GFP plasmid into primary cortical neurons at DIV2 (24h after plating), cotransfection with pcDNA 3.1(+) vector was used as control (pcDNA control). At DIV5, GFP positive neurons were imaged and their axons measured following the same methodology as for previous miR-99a functional experiments.

As depicted in Figure 4.7.b), overexpression of HS3ST2 induced a decrease of 20.5% in axon length as compared to control. Figure 4.7.a) shows representative images of neurons in both conditions and illustrates the validation of HS3ST2 overexpression conducted by immunostaining of the protein, which confirmed HS3ST2 overexpression by a striking increase in HS3ST2 fluorescence intensity. Interestingly, the extent of the decrease in axon length caused by HS3ST2 is similar to the effect observed by inhibiting miR-99a, an approximately 20% reduction in relation to control. More importantly, a potential miR-99a-dependant regulation of HS3ST2 predicts that HS3ST2 overexpression recapitulates the effects of miR-99a inhibition, as supressing the microRNA constraint on the protein levels could prompt an expression boost. Indeed, both miR-99a inhibition and HS3ST2 overexpression resulted in a decrease in the outgrowth of developing cortical axons.

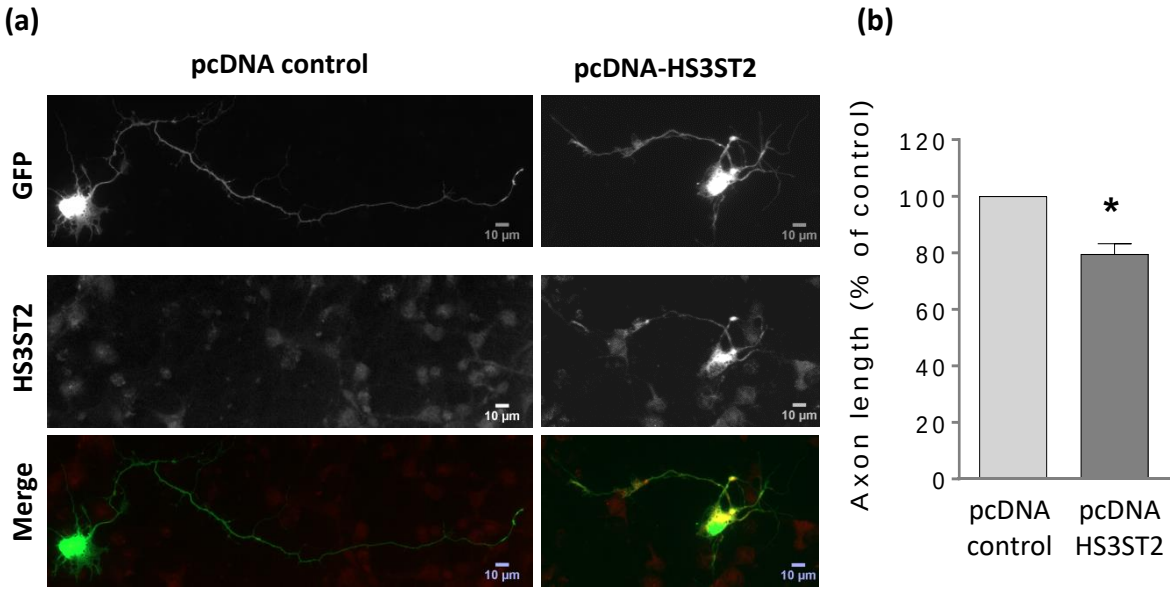


Figure 4.7 Overexpression of Hs3st2 in cortical neurons represses axonal outgrowth. **(a)** Representative images of control and Hs3st2 transfected neurons showing GFP signal and immunofluorescence detection of Hs3st2 overexpression in the pcDNA-Hs3st2 condition. Increased immunofluorescence signal of Hs3st2 in pcDNA-Hs3st2 transfected neurons in comparison to control verifies Hs3st2 overexpression. **(b)** Ectopic expression of Hs3st2 (pcDNA-Hs3st2) at DIV2-5 led to axons on average 20.9% shorter than control axons transfected with an empty vector (pcDNA control). GFP was cotransfected to identify and visualise transfected neurons. Data are expressed as percentage of the average length of control axons and presented as mean±SEM from four independent experiments (>200 axons measured for each condition); Student's t-test, ***p<0.01*.

4.2.5.2 HS3ST2 knockdown leads to an increase in axonal outgrowth

Loss-of-function experiments took advantage of transient transfection of small interfering RNA for HS3ST2 expression knockdown in order to evaluate the effects of its silencing in neuronal axon outgrowth. Following the experimental design described for the gain-of-function experiments discussed above, primary cortical cultures at DIV2 were cotransfected with GFP and siHs3st2 or siRNA control at 50nM and axon length was analysed at DIV5. The axons of neurons where HS3ST2 was silenced were on average 39.0% longer than control axons (figure 4.8.a) and b).

To confirm the efficacy of HS3ST2 knockdown, the mRNA levels of *Hs3st2* in primary cortical neurons were quantified 72h after transfection with siHs3st2 or siRNA control (50nM). RT-qPCR quantification showed a repression of 0.58 fold of control levels, a relatively mild silencing efficacy that was attributed to the low transfection efficiency in primary neurons, which hindered the

detection of the siHs3st2 mediated knockdown in the whole culture (figure 4.8.c). In fact, by replicating this experiment in Neuro2A, a mouse neuroblastoma cell line used in a great wealth of neuronal studies, it was possible to demonstrate that, in an easy-to-transfect cell line (see Methods), siHs3st2 efficiently repressed *Hs3st2* transcript levels as measured by RT-qPCR (0.08 fold of control levels, data not shown).

In accordance to the previously observed functional correlation in gain-of-function experiments, HS3ST2 silencing produced a similar effect in axonal outgrowth as mimicking miR-99a activity, being a significant increase in the length of developing axons. These observations are consistent with a scenario where miR-99a modulation of axonal outgrowth in primary cortical neurons occurs through repression of HS3ST2. Importantly, these findings suggest that HS3ST2 acts as a growth supressing gene in developing primary cortical neurons *in vitro*.

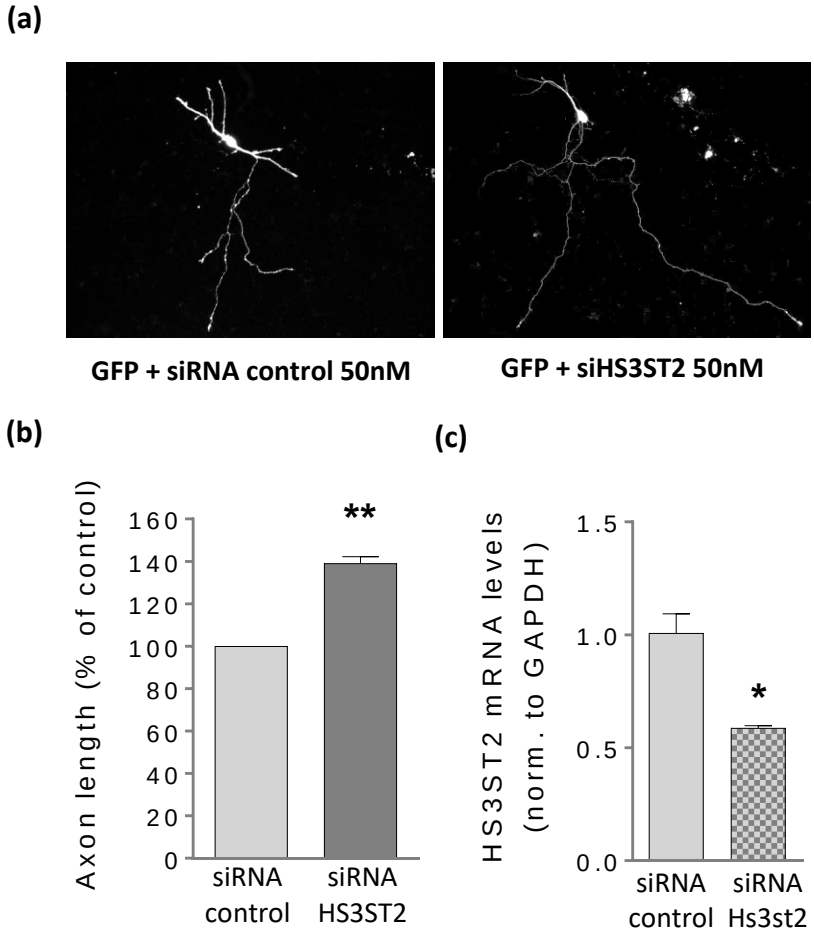


Figure 4.8. Silencing of Hs3st2 promotes axon extension in cortical neurons (a) Developing cortical neurons were transfected with 50nM siHs3st2 or siRNA control at DIV2 and GFP-positive neurons were imaged and analysed 72h after transfection (DIV5). Images depict representative neurons of both conditions. **(b)** Axons of neurons where HS3ST2 was silenced were on average 39.0% longer than control axons. Data are expressed as percentage of the average length of control axons and presented as mean±SEM from four independent experiments (>200 axons measured for each condition). **(c)** Verification of HS3ST2 knockdown in cortical cultures by RT-qPCR. In cortical cultures transfected with siHs3st2 at DIV2, *Hs3st2* mRNA levels decreased 0.59 fold of cultures transfected with siRNA control. Data analysed using ΔΔCt method and *Gapdh* as reference gene for normalisation. Data expressed as fold change to control, mean±SEM of 3 independent experiments, each read in duplicate; Student's t-test *$p<0.05$ **$p<0.01$.

HS3ST2 expression peak at DIV12 correspond to a developmental period when the rate of axonal outgrowth has declined (Dotti et al. 1988) and network activity, as measured by MEAs of neuronal networks, is on the rise to its peak at 2 weeks in vitro (Chiappalone et al. 2006; Wagenaar et al. 2006). Moreover, various studies on primary cortical and hippocampal cultures point towards an important role of cell plating density in neuronal development *in vitro*. Data from different groups exploring different techniques and outputs

(MEAs, calcium imaging and density of synaptic markers) showed that high density primary cultures, such as the ones used in the present work, exhibit an accelerated development as compared to lower density cultures, showing with increased growth rate at earlier timepoints *in vitro* and place the initial events of synaptic electrical activity as early as DIV5.

4.2.6 miR-99a modulates HS3ST2 in cortical neurons

The next obvious question is whether miR-99a can in fact modulate endogenous HS3ST2 to regulate its actions in the developing axon of cortical neurons. Toward this end, the mRNA and protein levels of HS3ST2 were analysed after transfection of miR-99a mimic.

As the notoriously difficult-to-transfect primary cortical neurons proved to be an inadequate model to detect repression of mRNA levels by RT-qPCR, even when a specific siHs3st2 was used (section above), Neuro2A cells were chosen for this experiment due to their high transfection efficiency as compared to other neuronal cell lines and abundant endogenous expression of HS3ST2 (see methods). Curiously, HS3ST2 was nearly undetectable by RT-qPCR in the non-neuronal HEK293T cell line, an observation in agreement with the brain-enrichment profile described for this gene in zebrafish and mouse models (Cadwallader and Yost 2006; Lawrence et al. 2007).

Hence, miR-99a mimic or mimic negative control were transfected into Neuro2A cells 24h after plating and *Hs3st2* mRNA levels were measured 72h thereafter, by RT-qPCR (*Gapdh* used as reference gene, data analysed using ΔΔCt method). *Hs3st2* did not show a significant change at the mRNA level, upon ectopic expression of miR-99a (figure 4.9.a.), suggesting that miR-99a does not regulate HS3ST2 expression through an mRNA degradation mechanism. This result is perhaps not completely unexpected. As discussed in the chapter 1, a microRNA can act on the target transcript to reduce protein synthesis by means of transcript degradation or inhibition of translation. Although several studies show that mRNA degradation accounts for the majority of microRNA-mRNA interactions in animals (Guo et al. 2010), evidence from microRNA regulatory effects on neuronal transcripts in the

nervous system suggests that microRNA-dependant regulation of neuronal mRNAs could be preferentially mediated by translational repression mechanisms (Schratt 2009a; Zhang et al. 2013). Furthermore, these findings challenge the general assumption in the field that postulate that microRNAs with high complementarity to the target binding site signal for transcript degradation. Here we describe *Hs3st2* bearing a 8mer binding site where the protein, but not transcript levels are downregulated by miR-99a.

Thus, further experiments were designed to assess whether miR-99a can regulate the endogenous expression of HS3ST2 at the protein level, independently of its transcript. If the above is true, mimicking miR-99a activity in cortical neurons should lead to a decrease in HS3ST2 levels. This reduction in protein levels could be investigated by western blot, however, in our hands, none of the anti-HS3ST2 antibodies tried were able to confidently detect HS3ST2 in a western blot experiment. Thus, quantitative fluorescent immunostaining of HS3ST2 was the technique selected to determine endogenous protein levels in cortical neurons after transfection with either miR-99a mimic or mimic negative control, in order to investigate a potential miR-99a dependant regulation. Cotransfection of GFP allowed for selection of transfected cells, which permitted the use of primary cortical neurons for this experiment. As shown in figure 4.8.b and c, miR-99a mimic caused a pronounced reduction in HS3ST2 expression as measured by fluorescence intensity, resulting in a significant 77.0% decrease in HS3ST2 levels as compared to control (Figure 4.9.b). Representative images of HS3ST2 immunostaining in both conditions are depicted in figure 4.9.c., demonstrating a clear reduction of HS3ST2 fluorescence intensity in the soma of a cortical neuron transfected with the mimic.

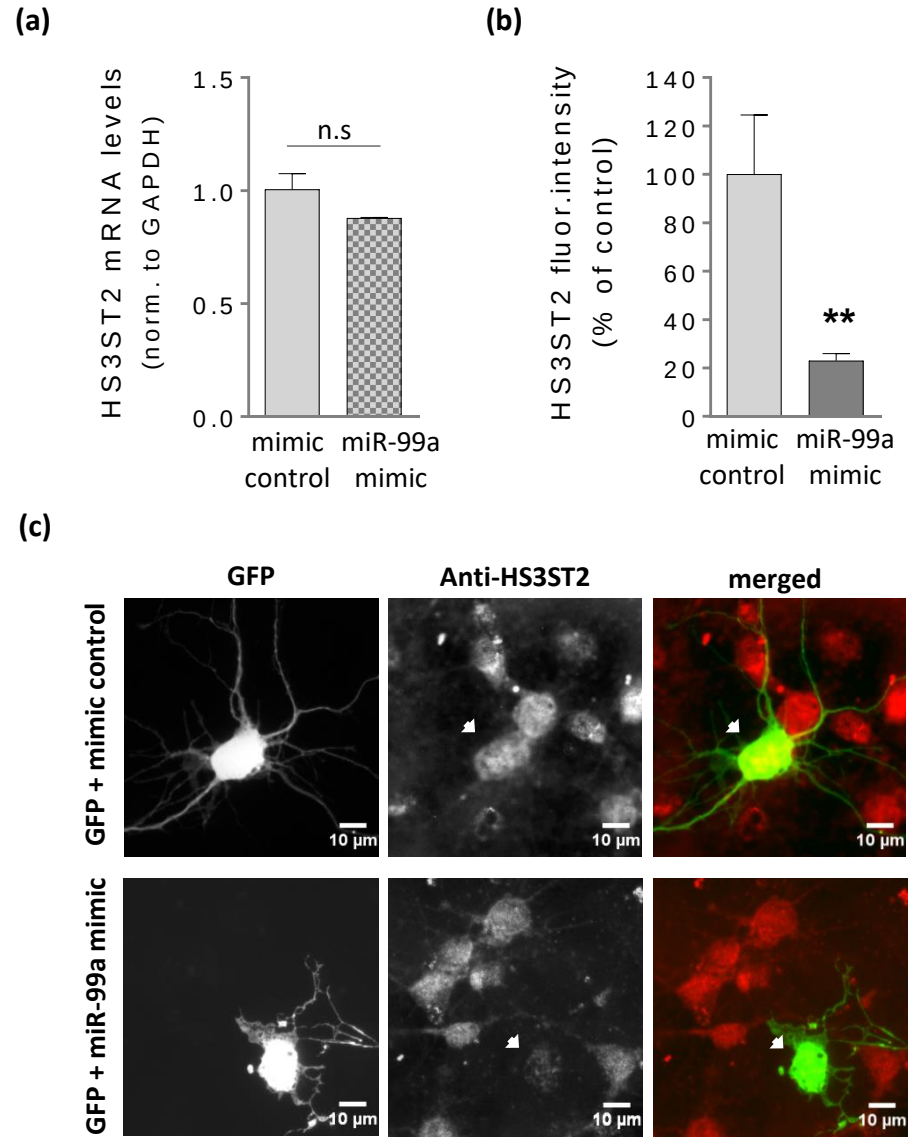


Figure 4.9. miR-99a regulates HS3ST2 protein levels in primary cortical neurons. **(a)** RT-qPCR quantification of *Hs3st2* transcript levels in Neuro2A cells 72h after transfection with either miR-99a mimic or mimic negative control (50nM). Ectopic expression of miR-99a failed to induce a significant decrease in the mRNA levels of *Hs3st2* (average of 0.88 fold change to mimic negative control) in Neuro2A cells. Data expressed as fold change to control, mean±SEM of 3 independent experiments, each read in duplicate; Student's t-test, n.s.: non-significant. **(b)** Quantification of HS3ST2 fluorescence intensity in primary cortical neurons transfected with miR-99a mimic or mimic negative control (50nM) show a decrease of 77.9% of control in HS3ST2 fluorescence intensity. Data are expressed as percentage of the average of control fluorescence; mean±SEM from four independent experiments, in each at least 50 neurons were quantified per condition; Student's t-test, $**p<0.01$. **(c)** Ectopic expression of miR-99a in cortical neurons led to a marked decrease in the endogenous HS3ST2 protein levels of transfected neurons (bottom panel, white arrow) in comparison to neurons transfected with mimic negative control (top panel, white arrow). HS3ST2 levels were detected in both conditions by immunofluorescence (red). GFP was cotransfected to identify and visualise transfected neurons.

Overall, these data indicate that endogenous expression of HS3ST2 in primary cortical neurons is under the regulatory actions of miR-99a and that this regulation appears to be mediated by direct microRNA-dependant translational repression of HS3ST2 transcript. Further experiments using *in situ* hybridisation (FISH) could help better understand miR-99a mechanism of action at the transcript level. FISH detection of miR-99a effect on HS3ST2 mRNA levels in cortical neurons could help validate the results obtained by RT-qPCR in Neuro2A, however not only is RT-qPCR a more sensitive technique, a FISH experiment would be equally limited by transfection efficiency constraints.

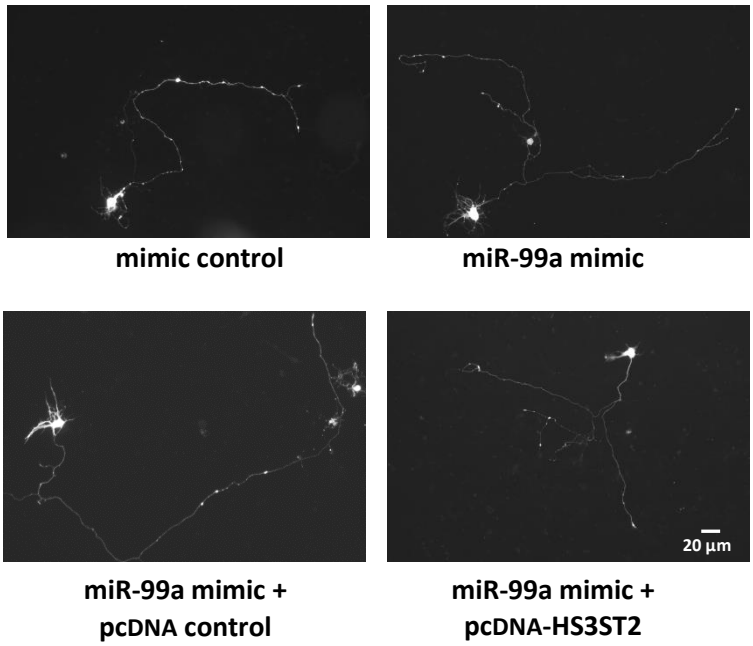
Nevertheless, these findings, together with miR-99a and HS3ST2 expression profiles in cortical cultures and, importantly, their functional actions in cortical axons point strongly towards a miR-99a-HS3ST2 regulatory axis that modulates axonal outgrowth in developing cortical neurons. This made the rational for the next step in the project, to devise rescue experiments of miR-99a function in order to probe this hypothesis.

4.2.7 miR-99a modulates axonal outgrowth through HS3ST2 regulation

4.2.7.1 HS3ST2 overexpression counteracts the effect of miR-99a mimics in axon growth

A gold standard experimental setup for validation of the specificity of RNAi activity of siRNA are phenotype rescue experiments through the expression of a siRNA-resistant sequence of the target gene (Cullen 2006). This same principle can also be applied to microRNA activity and its target, thus a similar approach was employed to determine whether targeting of HS3ST2 is necessary for miR-99a effects in axonal outgrowth, by performing rescue experiments wherein a miR-99a mimic is expressed in parallel with the overexpression of a HS3ST2 sequence deprived of its 3'UTR. Therefore, the lack of a miR-99a site should prevent microRNA binding and consequent downregulation of HS3ST2 levels by the mimic (Karbiener, Glantschnig, and Scheideler 2014). Hence, miR-99a mimic (25nM) was cotransfected together

with pc-HS3ST2 or empty vector (pcDNA control) in cortical neurons at DIV2 and axon length was measured 72h later. As in previous experiments, axon length of neurons transfected with a non-targeting LNA-oligonucleotide was used as control (mimic negative control) and GFP was used as a transfection indicator. In accordance to earlier observations, ectopic expression of miR-99a mimic alone caused an increase in axon length (section 4.2.2). However, overexpression of HS3ST2, together with miR-99a mimic, rescued axonal length back to levels of the control, while the empty vector failed to affect the growth-promoting actions of miR-99a mimic (Figure 4.10). Thus, this observation suggests that miR-99a effects in the outgrowth of developing axons is mediated by its direct target, HS3ST2.



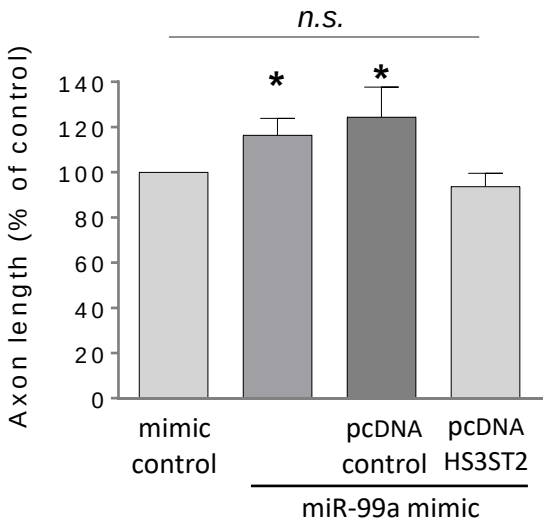
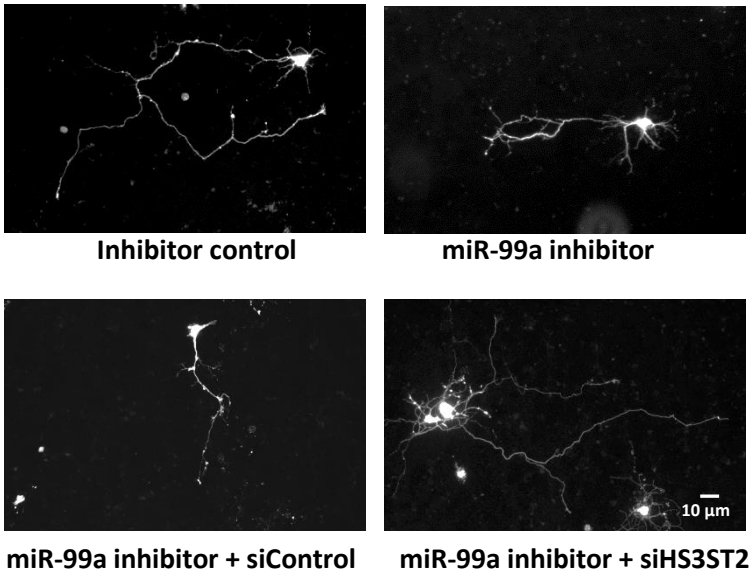


Figure 4.10. HS3ST2 overexpression abolishes the growth-promoting actions of miR-99a mimic in cortical axons. Axon length of primary cortical neurons was measured after cotransfection of miR-99a mimic (25nM) alone and miR-99a mimic (25nM) and the pcDNA-HS3ST2 construct or empty vector (pcDNA control) and compared to the length of axons of neurons transfected with mimic negative control alone. miR-99a mimic alone led to an increase of 16.4% in axon length relative to control, similar to the effect described in section 4.2.2. HS3ST2 overexpression, but not the empty vector (24.5% increase of control), restored axon length back to control levels in neurons expressing miR-99a mimic (93.85% of control). GPF was used as a transfection reporter and for visualisation of neuronal morphology. Data are expressed as percentage of the average length of control axons and presented as mean±SEM from four independent experiments (>200 axons measured for each condition); one-way ANOVA with Dunnet's pos-hoc test, *$p<0.01$, n.s.: non-significant.

4.2.7.2 HS3ST2 Knockdown rescues the phenotype of miR-99a inhibition in cortical axons

The question that immediately followed was whether the opposite experiment, where miR-99a and its target are inhibited in parallel, would demonstrate yet again a role for HS3ST2 in mediating miR-99a actions in growing axons. In this experiment, mir-99a function was inhibited using a specific miR-99a inhibitor, while simultaneously knocking down HS3ST2 to check whether this leads to a loss of the effects of miR-99a inhibition. For this, cortical neurons at DIV2 were transfected with a miR-99a inhibitor or inhibitor negative control (25nM) alone and miR-99a inhibitor plus siHS3ST2 or siRNA control (50nM). At DIV5, the length of GFP-positive axons was measured and analysed as relative to axon length of control neurons. Inhibition of miR-99a alone induced a reduction in axon length of approximately 20% of control, whereas silencing HS3ST2 in neurons where miR-99a was inhibited resulted in normal axon length, not significantly different from control axons (figure 4.11). This implies that the effects of miR-99a inhibition are due to derepression of its direct target, HS3ST2, and when HS3ST2 is knocked down in parallel, miR-99a inhibition has no observable effect on the extension of cortical axons.

Together, these two rescue experiments provide compelling support of our hypothesis that miR-99a modulates axon growth in developing cortical neurons by directly regulating HS3ST2.



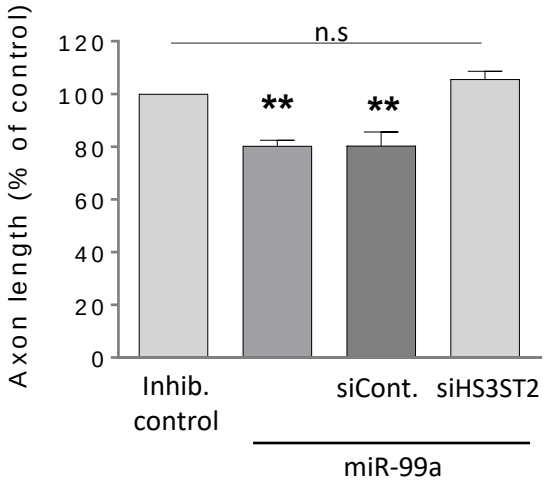


Figure 4.11 Silencing HS3ST2 rescues axon length decrease induced by miR-99a inhibition. a) Inhibition of endogenous miR-99a in cortical axons resulted in a decrease of 20.9% in the length of their axons (25nM) relative to inhibitor negative control, comparable to the effect observed in previous experiments (section 4.2.2). However, in neurons where HS3ST2 was silenced by siHS3ST2-mediated knockdown (35nM), inhibition of miR-99a (25nM) failed to induce a decrease in the outgrowth of cortical axons (105.6% of control). Cotransfection of miR-99a inhibitor and siRNA (35nM) control showed the same effect in axon length as miR-99a alone, leading to axons 20.7% shorter in comparison to inhibitor negative control. Right panel shows representative images of neurons from each condition. GPF was used as a transfection reporter and for visualisation of neuronal morphology. Data are expressed as percentage of the average length of control axons and presented as mean±SEM from four independent experiments (>200 axons measured for each condition); one-way ANOVA with Dunnet's pos-hoc test, . ***p<0.01,* n.s.: non-significant.

4.2.8 miR-99a regulates cortical axonal outgrowth locally in a microfluidic compartmentalised culture model

4.2.8.1 miR-99a and its target, HS3ST2, are enriched in cortical axons

As discussed in various sections across this dissertation, a deep sequencing screening identified a subset of axon-enriched microRNAs from pure axonal RNA fractions, obtained from compartmentalised cortical cultures (see Introduction, Taylor et al. 2009). This approach aimed at increasing our understanding of the roles that microRNAs residing in cortical axons play in axon development processes. In these experiments, miR-99a ranked top 5 amongst the selected top 25 axon-enriched microRNAs determined by axon/cell body enrichment analysis of miRNA-seq data obtained from cortical axon vs cell body fractions (see Chapter 1).

Subsequently, a RT-qPCR study of pure axonal RNA fractions was conducted to validate the relative abundance of the top 25 axon-enriched microRNAs in cortical axons. The Ct values for most axonal microRNAs were well within the range of detection for mature microRNAs, Ct value << 35 (Schmittgen et al. 2008). Moreover, Ct values were comparable to the ones obtained by other for microRNAs quantified in axons of cortical and DRG neurons (Natera-Naranjo et al. 2010; Zhang et al. 2013). After global normalisation (see methods), the 25 microRNAs were plotted according to their abundance and expressed as relative to the global mean. Amongst these, miR-99a was found to be the third most expressed axonal microRNA (Figure 4.11.a).

Thus, it was logical to hypothesise that the newly uncovered effects of miR-99a in axonal outgrowth could be achieved by the population of miR-99a mature sequences resident in cortical axons. This idea is supported by two important findings in the axon development field over the past 15 years: 1) local protein synthesis in the axon is necessary for normal axon growth and correct growth cone guidance over the course of development, both *in vivo* and *in vitro* (Campbell and Holt 2001; Hengst et al. 2009; Shigeoka et al. 2016; Wong et al. 2017); 2) our group and others, showed that the local axonal population of a microRNA has the capacity to regulate translation of its

target protein locally in the developing axon (Bellon et al. 2017; Dajas-Bailador et al. 2012; Hancock et al. 2014; Y. Zhang et al. 2015; Zhang et al. 2013).

In our model, miR-99a-mediated control of axonal outgrowth is achieved through the regulation of HS3ST2 translation, thus modulating its effects in the developing axon. Hence, the next step was to look for evidence of the presence of *Hs3st2* mRNA in cortical axons.

By taking advantage of compartmentalised cortical cultures once again, *Hs3st2* was measured in total RNA isolated from axon and cell body fractions, by RT-qPCR. Not only *Hs3st2* mRNA was detected in axonal RNA (average Ct value of axonal samples: 26.6), RT-qPCR data showed that *Hs3st2* is actually higher in axonal fractions when compared to the reference gene, *Gapdh*, in both cell body and axon fractions (Figure 4.11.b). This analysis is based on the assumption that *Gapdh* is equally distributed in the neuronal soma and axonal compartments. *Gapdh* has been used as internal control in a similar mRNA enrichment approach in primary motor neurons (Briese et al. 2016). Moreover, immunostaining of HS3ST2 in cortical neurons grown in these microfluidic devices showed the protein is well detectable in developing axons (Figure 4.11.c).

In line with our results, a recent study also places *HS3ST2* transcript in the axon, this time in distal projections of differentiated human embryonic stem cell-derived glutamatergic neurons (hESC neurons) grown in microfluidic devices and detected by microarray methodology (Bigler et al. 2017). This suggests a possible conserved function for HS3ST2 in human cortical axons.

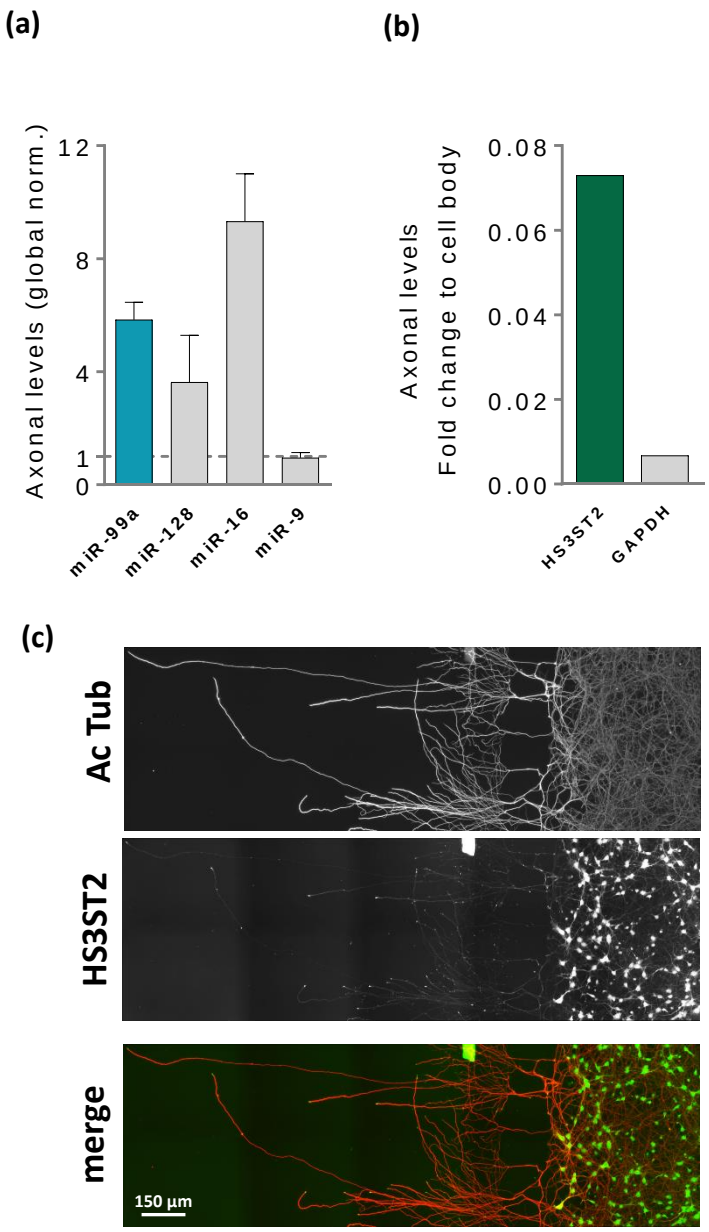


Figure 4.11 Expression of miR-99a and HS3ST2 in the axons of cortical neurons. **(a)** RT-qPCR quantification of the endogenous levels of axon-enriched miRNAs in purely axonal fractions obtained from compartmentalised cortical cultures grown in microfluidic devices. Individual miRNA levels were normalised to the global mean of the top 25 axon-enriched miRNAs and are expressed as fold change to global mean (global normalisation using ΔCt to global mean; n=2 purely axonal preparations, each read in duplicate). Data shows miR-99a was well detectable in cortical axons and one of the most abundant miRNA in cortical axons, 5.84 fold as com in a subset that includes miRNAs with well described roles in axonal outgrowth such as miR-9 and miR-16. **(b)** Pure axonal fractions obtained from compartmentalised cortical cultures in microfluidic devices were also used to quantify endogenous axonal *Hs3st2* levels by RT-qPCR. *Hs3st2* was quantified both in the soma and axonal fractions and axonal levels are presented as a ratio of the soma levels. **(c)** Immunofluorescence of HS3ST2 in cortical neurons cultured on compartmentalised devices at DIV6. HS3ST2 (green) can be detected in the somato-dendritic compartment (soma side) of cortical neurons, but also in cortical axons (axonal side). Acetylated tubulin was used as an axonal marker (red). Scale bar: 150µm; 10x images stitched using Fiji software.

4.2.8.2 miR-99a acts locally in the cortical axon to regulate axon growth

With both players present in cortical axons, it was logic to enquire whether axonal miR-99a is responsible for the miR-99a-dependant effects observed in axon outgrowth. Thus, further experiments used functional assays in microfluidic compartmentalised cortical cultures to determine the role of intra-axonal miR-99a in axon growth.

The microfluidic compartmentalised culture model, is used by us and other research groups (Bigler et al. 2017; Dajas-Bailador et al. 2012, 2014; Hengst et al. 2009; Kim and Jung 2015; Taylor et al. 2009) to study axonal processes that occur locally in the axon. Its greatest advantage compared to other compartmentalised culture models is the ability to fluidic isolate the axonal (axon side) from the somato-dendritic compartment (soma side) of cultured neurons by employing differential hydrostatic pressure. This allows for the application of treatments selectively in the axons, without affecting the cell bodies of neurons (Park et al. 2006; Taylor et al. 2005)

Accordingly, cortical neurons were grown in microfluidic devices and when their axons crossed the microgrooves toward the axonal compartment by DIV5, they were selectively perfused by either a cell-permeable miR-99a inhibitor or non-targeting control (T0). These inhibitors of miR-99a function are oligonucleotides modified to allow for incorporation by mammalian cells without the need for transfection regents and inhibit endogenous miR-99a activity by binding to its mature sequence (see methods). The spatial restriction of oligonucleotides applied to the axonal compartment of microfluidic neuronal cultures has been tested by Hengst et al., whereby application of FAM-labelled siRNAs to axons of peripheral neurons cultured in these devices showed no lateral diffusion to the soma compartment (Hengst et al. 2009).

To determine whether the application of specific miR-99a inhibitor exclusively to the axonal compartment has an effect in axon growth, developing axons were imaged live using phase contrast at 24h and 48h after treatment with either cell-permeable miR-99a inhibitor or inhibitor control (100nM) in the axonal side. A minimum of 50 axons in the axonal compartment were measured immediately before the treatment, T0, and at 24h and 48h.

Measurements obtained at different timepoints for each microfluidic culture were normalised to axon length at T0 and represented as % of T0 (see methods). Selective axonal inhibition of miR-99a activity led to no observable difference in length between treated and control axons 24h after treatment. However, after 48h of miR-99a inhibition, cortical axons showed a significant decrease in outgrowth when compared to control axons (Figure 4.12.a). The observation of a local effect 48h after microRNA inhibition is consistent with effects found for other microRNAs with local actions, using both cell-permeable or transfection approaches (Dajas-Bailador et al. 2012; Zhang et al. 2013).

Importantly, when the cell-permeable miR-99a inhibitor was applied exclusively to the soma compartment, replicating this way the previous experiment in the opposite compartment, the length of cortical axons growing in the axonal side remained unaltered in comparison to control soma-treated axons (Figure 4.12.b). This lack of effect is consistent with a model where miR-99a residing in the soma is not responsible for, at least the majority, of miR-99a actions in axonal outgrowth during cortical development.

Together, experiments in microfluidic compartmentalised cortical cultures suggest that miR-99a actions in the growth of cortical axons are mediated by the axonal population of miR-99a. The presence of HS3ST2 in cortical axons suggests that the local effect of miR-99a could occur through regulation of *Hs3st2* mRNA localised to the developing axon.

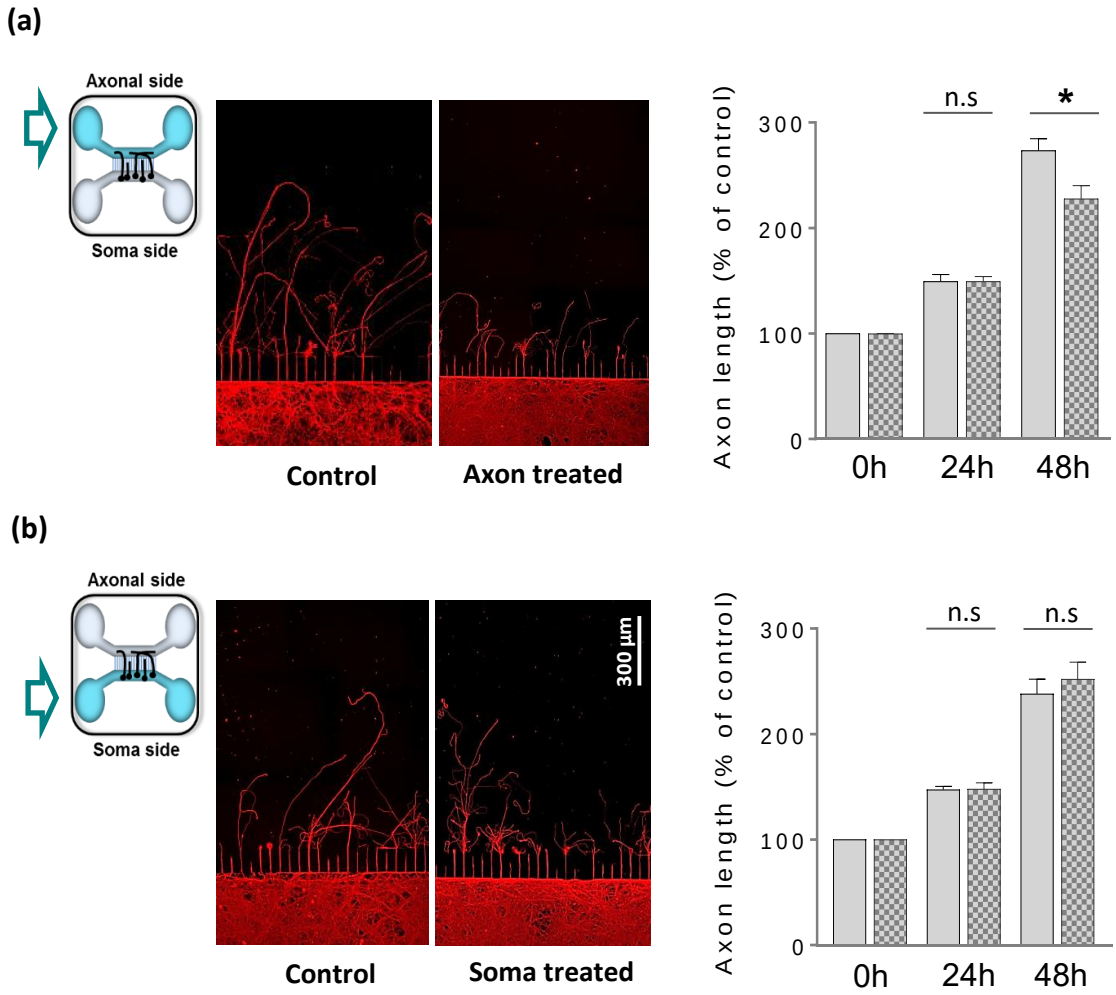


Figure 4.12 miR-99a acts locally in the axon to decrease axon outgrowth. Compartmentalised cortical cultures in microfluidic devices were used to investigate the effects of axonal miR-99a in axon extension over a 48h timecourse. This system allows not only for compartmentalisation of cortical axons from their soma but also for fluidic isolation between both compartments, the axonal and soma sides. Cell-permeable miR-99a inhibitor or inhibitor negative control was applied to compartmentalised cultures at DIV5 and axons growing in the axonal side were measured at 0h, 24h and 48h after treatment. **(a)** Inhibition of endogenous axonal miR-99a by application of a cell-permeable miR-99a inhibitor to the axonal compartment induced a decrease in axon length (227.8% of t_0) in comparison to a cell-permeable inhibitor negative control (273.4% of t_0), 48h after treatment. **(b)** When the cell-permeable miR-99a inhibitor or inhibitor negative control were applied to the soma compartment, no significant effect was observed in the length of axons growing in the axonal side, suggesting that miR-99a actions in axon outgrowth are attributed to local miR-99a residing in cortical axons. Data normalised to axon length at T=0h (t_0) and presented as percentage of t_0; mean±SEM from 5 independent experiments (>50 axons measured per timepoint in each compartmentalised culture); one-way ANOVA with Dunnet's pos-hoc test, *$p<0.01$, n.s.: non-significant.

4.2.9 miR-99a modulates the development of network connectivity

The wiring of neuronal networks within the nervous system depends on the precise and accurate growth of axons towards post-synaptic targets with which to form functional connections (Polleux and Snider 2010). Thus, factors controlling axonal outgrowth are expected to impact on the formation of functional neuronal networks. The experiments presented here have defined miR-99a as an important modulator of axonal outgrowth in developing cortical neurons, thus raising the question of whether miR-99a can influence the development and overall function of neuronal connectivity at the network level.

4.2.9.1. Spontaneous calcium transients in cultured cortical networks during development

Spontaneous activity is a fundamental feature of all known developing neuronal networks and has been well documented in such various systems as cerebral cortex, hippocampus, retina and spinal cord, both in vitro and in vivo (Blankenship and Feller 2010; Kirkby et al. 2013; Luhmann et al. 2016). In dissociated primary cortical cultures, as with other neuronal networks, the development of spontaneous activity undergoes a global increase over time with neurons exhibiting network-wide activity in characteristic spatiotemporal patterns (Kamioka et al. 1996; Maeda, Robinson, and Kawana 1995; Wagenaar et al. 2006). Indeed, a prominent feature of network maturation is the development of spontaneous synchronised bursts of activity across the network, which strongly correlate with the number of synaptic connections (Muramoto, Ichikawa, Kawahara, Kobayash, et al. 1993; Opitz 2002). Due to the well described close relationship between intracellular calcium oscillations and the developmental changes of spontaneous electrical activity in cortical networks (Jimbo, Robinson, and Kawana 1993; Robinson et al. 1993; Smetters et al. 1999; Takayama et al. 2009a), imaging of intracellular calcium transients was used to study the role of miR-99a in cortical network development.

In order to define the patterns of spontaneous activity over the development of primary cortical cultures, the calcium indicator dye Fluo-5 was used to detect intracellular calcium transients at different times. As shown in Fig 4.13, cortical cultures begin developing detectable activity during the first week *in vitro*. This correlates with the typical morphological development of dissociated cortical networks (figure 4.13.a), with significant axon and dendritic growth.

Raster plots depicting calcium events are used to represent the activity of each recorded neuron over a 900s period. Calcium events were defined as an increase of >15% above baseline fluorescence. At DIV6, the population of recorded neurons in culture demonstrate sparse calcium oscillations that coincide with the early signs of electric activity, as illustrated by figure 4.13.b (Takayama et al. 2009a). Just 72h later, at DIV9, the raster plot reveals a rich repertoire of spontaneous activity, with a striking increase in the number/frequency of calcium events (figure 4.13.b). Importantly, the appearance of synchronised network-wide events, defined as bursts of activity in which the majority of neurons are simultaneously co-active (4.13.c), are thought to correlate with the development of connectivity of the network. These observations are in accordance to the work of Verstraelen et al. which shows that the development of synchronised activity of primary hippocampal networks *in vitro* occurs within a well-defined time window. Moreover, the same report corroborates previous findings that network synchronisation of calcium transients coincides with network wiring and the increase in synaptic density characteristic of this time in cortical culture development (Cornelissen et al. 2013b; Muramoto, Ichikawa, Kawahara, Kobayash, et al. 1993; Verstraelen et al. 2014).

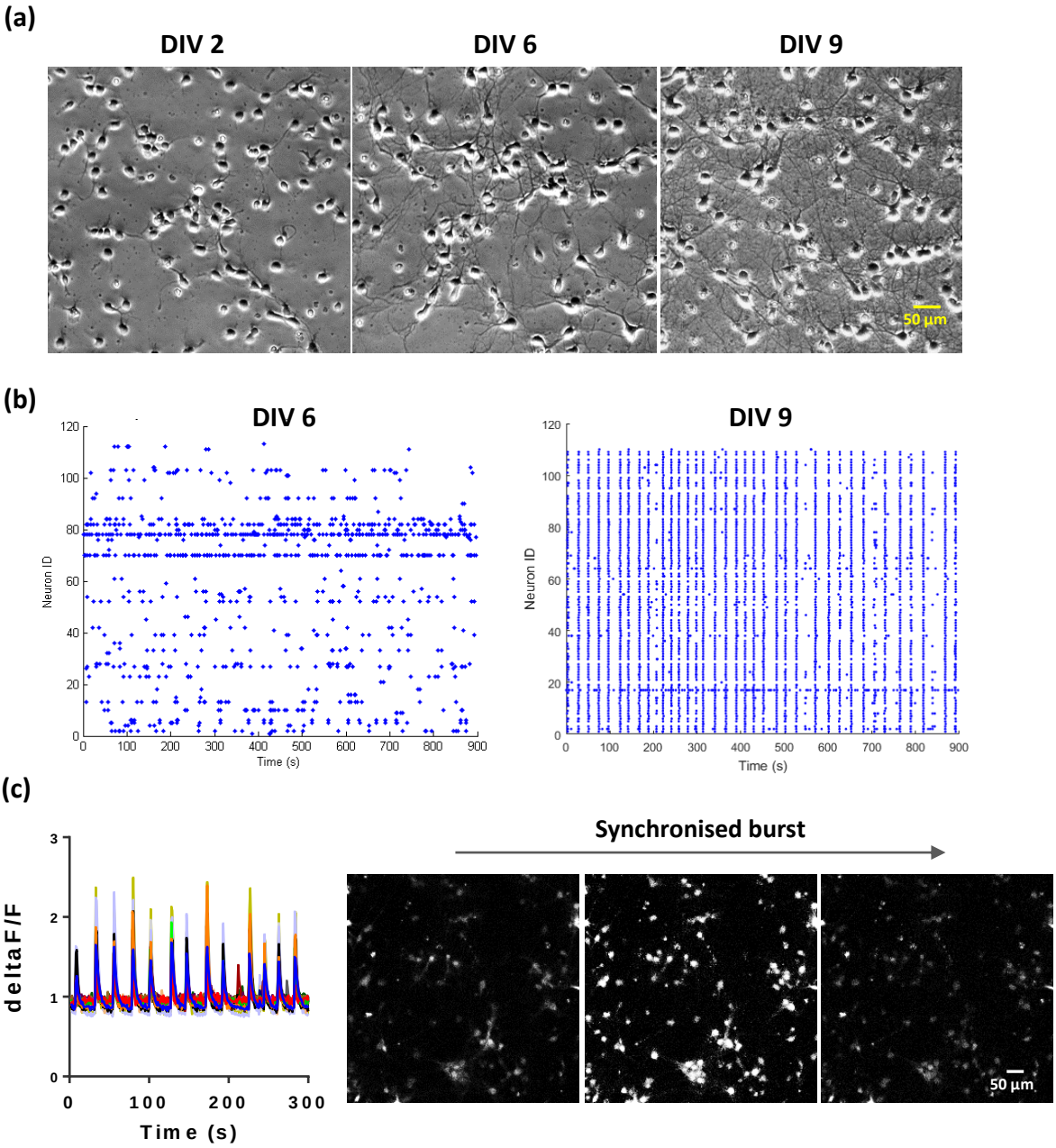


Figure 4.13. Development of spontaneous activity patterns in cortical cultures. (a) Representative images of cortical cultures at DIV2, 6 and 9 showing an increase in anatomical network connectivity over time, phase contrast 10x magnification. **(b)** Raster plots of calcium transients recorded in cortical cultures at DIV 6 and DIV9 shows the developmental changes in network activity, with activity patterns evolving from sparse and random at DIV6 to synchronised bursts at DIV9. Data shows detected calcium events (each blue dot represents a calcium event) of each recorded neuron over a 900s (15min) period. Images were acquired at a rate of 1 frame per second and calcium events defined as a fluorescence increase of 15% above the average baseline fluorescence (see methods). **(c)** Calcium traces of corresponding the calcium oscillations of neurons within a network over a period of 300s are represented in different colours. Calcium traces show the rhythmic synchronised events of a large proportion of neurons, characteristic of mature cultures. On the right, representative frames depict a synchronous network-wide event, showing the occurrence of simultaneous calcium events (measured by increase in fluo-5 fluorescence) in nearly all of the cells within the field of view. 10x magnification.

4.2.8.2 miR-99a inhibition alters the patterns of spontaneous calcium oscillations in developing cortical networks

To address the role that miR-99a might have in the development of these neuronal network processes, the activity of miR-99a was inhibited at DIV6, just before the development of synchronicity patterns. For this, we added to the cultures the same cell-permeable inhibitor and cell-permeable negative control used in the previous section. By recording 900s of spontaneous calcium transients from control cortical cultures and cultures where miR-99a was inhibited (72h after cell loading), it was possible to investigate the impact of miR-99a inhibition in the development of cortical network activity at DIV9.

The measurement of changes in frequency and amplitude of calcium fluxes and network-wide synchronous events allows calcium transients data to be converted into a metric for neuronal network activity and synchronicity. In figure 4.14.a, representative raster plots of calcium events across the culture illustrate the effects of miR-99a inhibition on the overall activity of the neuronal network as compared to negative control. These suggest that inhibition of miR-99a function altered the spontaneous activity of cortical networks. Indeed, although miR-99a inhibition did not abolish the occurrence of intracellular calcium oscillations or network-wide synchronous events, their spatiotemporal patterns across the network appeared to be disrupted.

When looking at the single cell kinetics of cultures from the two conditions, the analysis showed a decrease in the average total number of calcium events detected per neuron over the 15min recording period in cultures where miR-99a was blocked as compared to control cultures. This was accompanied by an increase in the mean interspike interval (ISI) between two subsequent calcium events from 32.3s in control cultures to 44.9s following miR-99a inhibition, which indicates a decrease in the frequency of calcium events. These parameters provide a metric for the overall neuronal activity of the network, with less calcium events corresponding to lower activity (Kamioka et al. 1996; Verstraelen et al. 2014).

Hence, the data presented suggests that inhibition of miR-99a during neuron development leads to a less active neuronal network. At the same time, the mean amplitude per neuron did not present significant changes between

conditions (figure 4.14.b), suggesting that the levels of calcium entering the cells remained unaffected. This is an important observation, and suggests that inhibition of miR-99a does not likely interferes with specific calcium channels and/or intracellular stores mediating intracellular calcium increases.

The synchronisation of the network, given by the levels of synchronous and asynchronous events across time and space, provides a readout of communication and connectivity at the network level (Kamioka et al. 1996; Opitz 2002). Upon inhibition of miR-99a, the number of network-wide synchronous events detected in DIV9 cortical networks showed a significant decrease (average of 21.2 network bursts over 15min) in comparison to control cultures (average of 28.2 bursts over 15min). The next question was whether the asynchronous activity, given by the number of calcium events that fall out of networks bursts, followed the same trend. On the contrary, the number of asynchronous events per neuron increased when miR-99a was inhibited. Together, these observations suggest that miR-99a is involved in neuronal network formation in developing cultures and, when its activity is inhibited, the neuronal network demonstrates altered patterns of activity altered. Rhythmic network-wide synchronous events, considered a hallmark of neuronal connectivity maturation (Maeda et al. 1995; Muramoto et al. 1993; Opitz 2002; Takayama et al. 2009; Wagenaar et al. 2006), are attenuated and asynchronous activity becomes more frequent across the network, therefore suggesting a decrease in network connectivity.

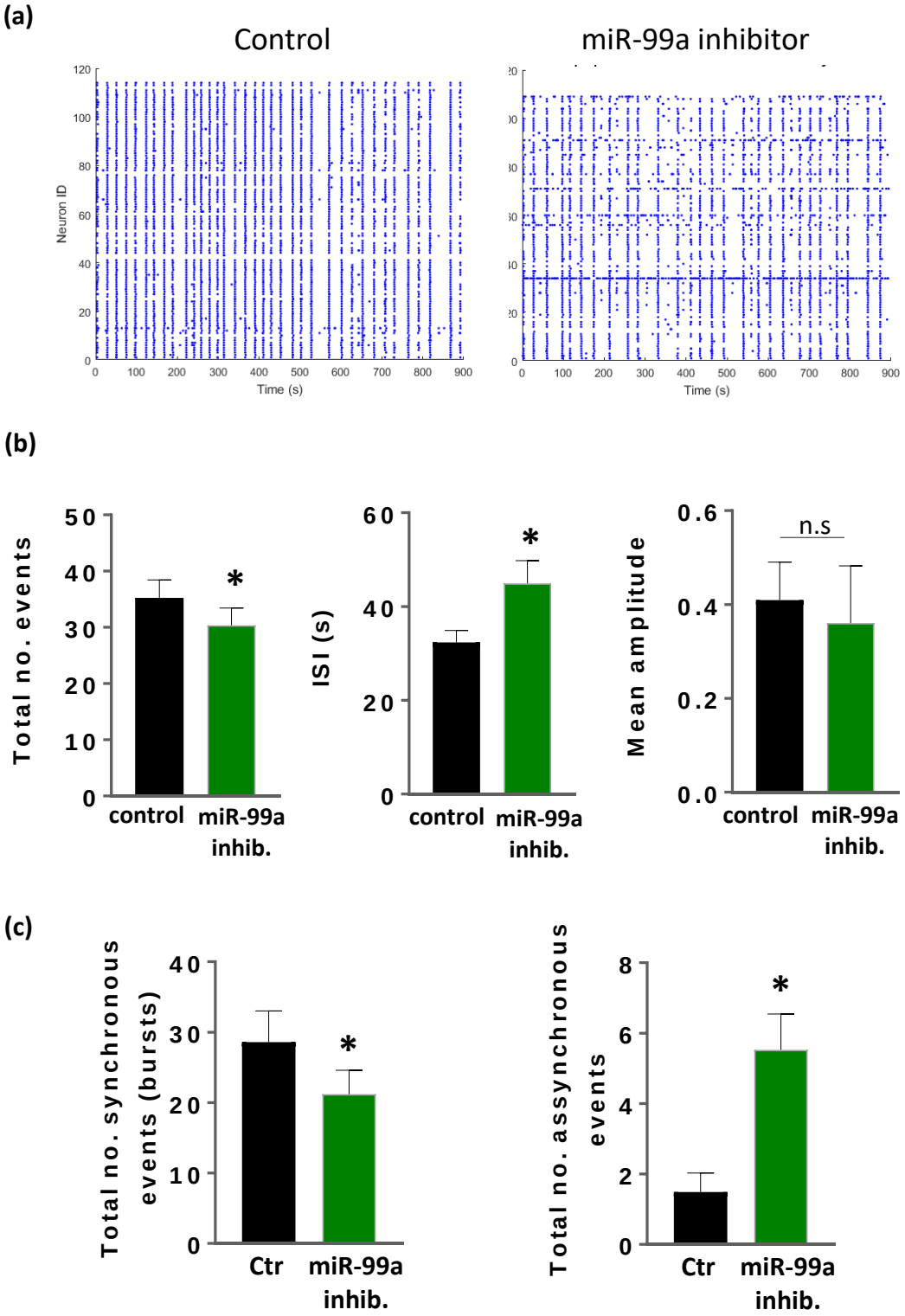

(a)
Control
miR-99a inhibitor
Neuron ID
Time (s)
Time (s)
(b)
Total no. events
control
miR-99a inhib.
ISI (s)
control
miR-99a inhib.
Mean amplitude
n.s
control
miR-99a inhib.
(c)
Total no. synchronous events (bursts)
Ctr
miR-99a inhib.
Total no. assynchronous events
Ctr
miR-99a inhib.

Figure 4.14 Inhibition of miR-99a function alters the patterns of spontaneous calcium oscillations. (a) Raster plots of spontaneous calcium events detected in cortical networks (DIV9) treated with cell-permeable miR-99a inhibitor or respective negative control at DIV6 show the impact on the spontaneous activity at the network level (>100 neurons recorded per condition over 900s, 1 frame per second; each blue dot corresponds to one calcium event). **(b)** Graphs representing distinct analysis parameters upon miR-99a inhibition in comparison to negative inhibitor control. Data from the upper graphs were obtained from individual neurons, while the lower graphs represent parameters which are measured at the network level. Total number of events and mean interspike interval (ISI) suggest that miR-99a inhibition leads to a decrease in overall neuronal activity although no effect was observed in the average event amplitude, per neuron (upper graphs). **(c)** Analysis of network synchronicity showed a decrease in the total number of network-wide synchronous events accompanied by an increase in number of asynchronous events recorded per cell (lower graphs). Data of >100 neurons per condition, from five independent experiments and expressed as mean±SEM; * $p < 0.05$, Student's t-test.

The existence of a close relationship between anatomical and functional connectivity in neuronal networks has been studied over development (Chen and Kriegstein 2015; Li et al. 2007) and is even more apparent in neurodevelopmental disorders as autism spectrum disorder and schizophrenia, where abnormal axon growth and guidance in human embryonic development is thought to underlie a substantial part of the observed defects in brain functional connectivity (Korecka et al. 2016; McFadden and Minshew 2013). Indeed, in a schizophrenia mouse model bearing a disease-causing deletion, axons showed impaired terminal arborisation causative of decreased synaptic strength and altered functional connectivity (Mukai et al. 2015). Although the available calcium imaging data has not been sufficient to pinpoint the mechanisms mediating miR-99a effects in network activity development, evidence presented throughout this chapter showed the functional consequences of miR-99a in axonal outgrowth during development. Notably, functional assays in cultured cortical neurons showed that miR-99a activity had no observable effects in dendrite outgrowth upon transfection of miR-99a mimic into cortical neurons. Hence, it is possible that the defects in axonal development provoked by miR-99a inhibition could be in the origin of the alterations observed in spontaneous activity patterns at the network level.

4.3 Concluding remarks and future implications

4.3.1 Axon-enriched miR-99a regulates axonal development

The work presented in this chapter applied bioinformatics, microRNA functional analysis and calcium imaging approaches in mouse primary cortical cultures to examine the role of miR-99a, a microRNA previously found to be enriched in developing cortical axons (Chapter 1), in axonal development and network connectivity. The data showed that miR-99a is developmentally regulated in cultured cortical neurons and identified mir-99a as a growth-promoting factor in axonal development. Moreover, this work adds to the current knowledge on the roles of microRNAs residing in axons, such as the previously described miR-9, miR-132, miR-72a and miR-29c and the recently found by us, miR-26a (unpublished data), that bear intra-axonal functions (Dajas-Bailador et al. 2012; Hancock et al. 2014; Y. Zhang et al. 2015; Zhang et al. 2013). Indeed, experiments in microfluidic compartmentalised cultures showed that miR-99a localised to developing cortical axons has the capacity to regulate axonal outgrowth locally, presumably through modulation of its target, HS3ST2.

Importantly, this work demonstrated how heparin sulfate 3-O-sulfotransferase 2, HS3ST2, acts as a functional target gene of miR-99a by luciferase reporter binding assays and regulation of its endogenous levels upon transfection with a miR-99a mimic. Functional rescue experiments placed HS3ST2 at the centre of miR-99a-mediated actions in the outgrowth of developing cortical axons, with HS3ST2 knockdown or overexpression leading to the phenotypic rescue of the axonal growth defects caused by inhibiting or mimicking miR-99a activity.

4.3.2 HS3ST2: a potential modulator of axon-ECM interactions over development

Components of the extracellular matrix (ECM) play important roles in the development of the nervous system, crucially interacting with developing axons to secure the correct formation of neuronal circuits (Barros et al. 2011;

Myers et al. 2011). Heparan sulfate proteoglycans (HSPG) are a diverse group of cell-surface and extracellular proteins bearing heparin sulfate (HS) glycan chains that compose and interact with the ECM, and are thought to play crucial roles in several developmental processes such as axon outgrowth, branching, pathfinding and synaptogenesis (Minge et al. 2017; Poulain 2015; Van Vactor et al. 2006). An important feature of HSPGs is the diversity of their HS-modified sugar chains which form distinct HS domains that serve as ligands and receptors (Xu and Esko 2014). This allows HSPGs to interact with many different factors with high specificity and, thus, coordinate several pathways essential for neuronal wiring (Bülow and Hobert 2004; Lee and Chien 2004).

HS chains of HSPGs are linear glycosaminoglycan polysaccharides of variable length composed of hexuronic acid and glucosamine repeat units that are decorated by HS motifs through extensive enzymatic modification during HSPGs biosynthesis. HS3ST2 is part of a family of proteins, heparin sulfate 3-O-sulfotransferases, (HS3STs or 3-OSTs) responsible for 3-O-sufation in the terminal step of HSPGs biosynthesis (Thacker et al. 2014). 3-O-sulfation is widely conserved in animals and 3-O-sulfotransferase orthologs can be found in the worm, fly, fish and across mammals to human, which supports the functional relevance of this HS modification (Cadwallader and Yost 2006; Kamimura et al. 2004; Lázaro-Peña et al. 2018; Sepulveda-Diaz et al. 2015; Yabe et al. 2005). Despite this, 3-O-sulfation is relatively rare, found in only ~0.5% of heparan sulfates (Colliec-Jouault et al. 1994). Conversely, HS3STs is the largest family of sulfotransferases composed of 6 isoforms in mammals, each showing high tissue specificity and developmentally regulated patterns of expression (Cadwallader and Yost 2006; Yabe et al. 2005). It is thought that these characteristics place HS3STs in a privileged position to regulate the specificity of binding to HS and to fine-tune biological functions of HSPGs (Thacker et al. 2014).

Accumulating evidence from genetic mutant models in the past decade has shed light on the functional roles of several HS modifying enzymes in neuronal development, building on the proposed theory for the existence of a *sugar code*, in which specific HS modifications of HSPGs might direct developmental decisions (Dani et al. 2012; Lee and Chien 2004; Poulain and Yost 2015). For example, conditional inactivation of Ext1 in mice postnatal neurons, an

essential enzyme for chain elongation in HSPG biosynthesis, recapitulates almost the full range of autistic symptoms (Irie, Badie-Mahdavi, and Yamaguchi 2012). Nevertheless, the role of 3-O-sulfation in the nervous system and, in particular, the functional role of HS3ST2, are largely unknown. A few pieces of evidence support a relevant role for HS3ST2 in neuronal function. Amongst HS3STs isoforms, HS3ST2 was shown to be mostly enriched in the brain and nervous system of zebrafish, mouse and human, where it was found to be regulated across developmental stages (Cadwallader and Yost 2006; Lawrence, Yabe, HajMohammadi, et al. 2007; Sepulveda-Diaz et al. 2015). HS3ST2 was found to be a marker of a type of mechanosensory endings of dorsal root ganglia (DRG) and trigeminal ganglia neurons in knock-in HS3ST2-hPLAP mice (Hasegawa and Wang 2008). Moreover, HS3ST2 was anticipated to modulate neuronal processes as the Drosophila 3-OST isoform is essential for a conserved neurogenic signalling pathway regulated by Notch in the fly (Kamimura et al. 2004).

As HS3ST2 was identified as a functional target of miR-99a, our study sought to investigate the role of HS3ST2 in axon development of mice cortical neurons. Interestingly, HS3ST2 function in growth related pathways had been focus of attention in cancer biology, where accumulating observations documented growth and proliferation-promoting effects when the HS3ST2 gene was found methylated (Hellec et al. 2018; Vijaya et al. 2014). In work presented in this chapter, HS3ST2 was found to be expressed in mouse cortical neurons with its levels markedly increasing over development (DIV1 to 12). Furthermore, our data implicates HS3ST2 in neuronal development and identified a novel function for HS3ST2 in axonal outgrowth of developing neurons. Indeed, silencing of HS3ST2 promoted the growth of cortical axons whereas HS3ST2 overexpression led to the opposite action. This is consistent with a previous observation in zebrafish where a morpholino of the HS3ST2 ortholog induced the recovery of the fish spinal cord in a model of tauopathy (Sepulveda-Diaz et al. 2015).

To date, very few binding partners have been found for heparan sulfates bearing 3-O-sulfation modifications and even fewer for 3-O-sulfation mediated specifically by HS3ST2. The best described function of HS3T2 links it to the formation of a specific 3-O-sulfated epitope in the cell surface that allows

herpes simplex virus entry (Shukla et al. 1999). Recently, Thacker et al. set up an affinity chromatography approach to reveal 3-O-sulfated HS binding partners, identifying several proteins involved in ECM processes, including neuropilin, a co-receptor for semaphorins involved in signalling pathways of growth cone turning and guidance. The same work showed that neuropilin 1 binds to 3-O-sulfated HS to modulate DRG growth cone response to Sema 3A and that this 3-O-sulfation modification is specific to HS3ST2 activity (Thacker et al. 2016). In the context of cortical axon development, it will be interesting to determine the specific HSPGs binding partners whose interactions are regulated by HS3ST2 3-O-sulfation to cause the observed functional effects in axonal outgrowth. Given the roles of HSPGs in neuronal development and axon biology, HS3ST2 effects are expected to impact on axon-ECM interactions during their journey to form neural circuits.

4.3.3 Impact in the development of spontaneous network activity

Several microRNAs have previously been shown to regulate various aspects of neuronal development and morphology including synapse formation and maturation (Rajman and Schratt 2017). However the present work represents one of the few examples of a microRNA with impact in the development of spontaneous activity patterns in developing cortical networks. Unlike previously reported for microRNA actions in spontaneous network activity, such as those of miR-128 and miR-101 whose inhibition promote neuronal excitability (Lippi et al. 2016; McSweeney et al. 2016; Tan et al. 2013), blockade of miR-99a function attenuates overall network activity, with a lower number of more sparse spontaneous calcium events. Moreover, miR-99a inhibition in developing cortical networks led to an increase of asynchronous activity while the number of network-wide events declined.

It is known that errors in the development of neuronal circuitry can have long-term consequences for network function (Cancedda et al. 2007; Korecka et al. 2016; McFadden and Minshew 2013). Thus, it remains to be assessed whether the changes in network activity provoked by transient disruption of miR-99a function during early network development can have long-lasting effects in well mature cortical networks, even after miR-99a function has been restored. Luppi et al. were the first to document this effect for a microRNA in the mouse

brain, whereby inhibition of miR-101 restricted to the first week of postnatal life resulted in alterations to network excitability and behaviour that were still observed in adulthood. Future experiments will analyse neuronal network activity of mature cortical networks, after three weeks *in vitro* when synaptic pruning and consolidation have occurred (Chiappalone et al. 2006; Wagenaar et al. 2006), upon blockade of miR-99a function during the first week of development. Thus, calcium imaging of cortical networks could be used to determine sustained effects of miR-99a actions during network formation. Although miR-99a expression in cortical cultures follows a decreasing trend over development, its relative levels remain comparable to other functional neuronal microRNAs such as miR-26a at later timepoints (DIV12; Jiang et al. 2015 and in house data), therefore a possible role of miR-99a in mature neurons and neuronal activity cannot be ruled out. Though out of the scope of this work, calcium imaging and/or microelectrode array models (discussed in previous chapters) could be used to assess miR-99a effects in spontaneous activity of mature cortical networks.

Further studies will be necessary to determine which target pathways are responsible for miR-99a function in developing spontaneous network activity. An obvious candidate is HS3ST2. In addition to the discussed effects in axonal outgrowth, could HS3ST2 be mediating miR-99a regulatory actions in network activity development? Of note, HS3ST2 could be involved in the formation of synaptic connections. A recent study using *C.elegans* mutants documents that loss of 3-O sulfation in the postsynaptic cell resulted in accumulation of a presynaptic vesicle marker in the presynaptic cell of the worm mating circuit, thus disrupting synapse formation and likely leading to behavioural mating defects (Lázaro-Peña et al. 2018). Nevertheless, such findings in synaptogenesis remain to be observed in vertebrates.

Taking into account the role of the miR-99a-HS3ST2 axis in developing axons, it is possible that miR-99a actions in spontaneous network activity depend on HS3ST2 regulation of axonal outgrowth. Future work will knockdown HS3ST2 in developing cortical cultures to investigate its relevance to network activity and the possible link to miR-99a actions in functional connectivity, using calcium imaging techniques.

Collectively, our findings reveal a new microRNA-mediated regulatory mechanism for a HS-modifying enzyme, HS3ST2, involved in the modulation of the biological functions of HSPGs. Indeed, our data show that miR-99a regulation of HS3ST2 and, therefore, HSPG biosynthesis, is necessary for normal axonal outgrowth in cortical neurons. Crucially, this works describes a novel role for HS3ST2 in neuronal development, which is one of the first functions described for HS3ST2 in neurons. Finally, analysis of calcium transients in growing cortical cultures implicates miR-99a regulatory functions in the development of spontaneous network activity and functional network connectivity.

5. General discussion

5.1 microRNA function in neuronal wiring

The development of the cerebral cortex is a very dynamic process that involves a series of complex morphogenic events, from cell fate determination and neuronal differentiation to migration toward the cortical plate where neurons establish functional circuits (Lewis et al. 2013). For correct development to occur, such complex phenomena require the coordinated action of extracellular signals, receptors and multiple cell signalling pathways, in a process made possible by the tight control from gene regulatory networks. microRNAs have emerged as attractive candidates to regulate these pathways due to their developmental and tissue-specific expression patterns (Lagos-Quintana et al. 2002; Yao et al. 2012). Indeed, these post-translational regulators are now recognised to be crucial modulators of virtually all aspects of neuronal development, with convergent microRNA actions orchestrating neuron developmental programs (Barca-Mayo and De Pietri Tonelli 2014; Rajman and Schratt 2017).

Accumulating studies have implicated microRNAs in all phases of cortical development (Chiu et al. 2014; Follert et al. 2014; Ryan et al. 2015; Volvert et al. 2012; Wang and Bao 2017). The relevance of microRNA regulatory networks in early neuronal differentiation has been the focus of special interest due to the ability of some microRNAs to act as pluripotency and neuronal-fate switches (Peng et al. 2012; Stappert et. al 2015; Tay et al. 2008). This work explores microRNA function in differentiated neurons at the period of neuronal wiring, when axons extend towards specific post-synaptic partners to form functional synaptic circuits (Polleux and Snider 2010). Indeed, how axons manage to follow such precise paths to reach their partners so accurately is one of the big questions in the axon development field, and the layers of regulation provided by converging microRNA regulatory networks might be part of the answer. As neuronal polarisation and the development of neuron connectivity involves a temporally regulated series of cellular processes that include axon specificiation and outgrowth, pathfinding and the formation of pre-synaptic boutons, it has now become clear that such tightly regulated events need the coordinated expression of microRNAs and their target genes.

However the current knowledge of the microRNAs regulating axonal function is still very limited.

Several studies profiled microRNA expression in rodent brains from early embryos into adults, providing a crucial first step in the identification of microRNAs with potential function in development (Lagos-Quintana et al. 2002; Nielsen et al. 2009b; Yao et al. 2012). However, as these studies sample the whole cortex, they fail to provide information on the intracellular localisation of microRNAs. This is most important in axon development studies, when neurons break cell asymmetry to become highly polarised cells with specific functions being attributed to the specific somato-dendritic and axonal compartments. Indeed, a few microRNAs have been found to regulate intrinsic axon growth programs as well as axonal growth stimulated by specific guidance cues (Dajas-Bailador et al. 2012; Wang and Bao 2017). More recent findings suggest that microRNAs are also involved in mediating the spatiotemporal effects of such guidance/ growth factors during axonal growth (Bellon et al. 2017; Y. Zhang et al. 2015). However, beyond specific examples, the localization, function, and regulatory mechanism of microRNAs in the axon remain largely unknown.

Our preliminary study used a microfluidic compartmentalised culture system as a platform to isolate pure axonal RNA, in order to identify microRNAs enriched in axons of developing cortical neurons by next generation sequencing techniques. The use of microfluidic cultures to obtain RNA specifically from the axon compartment had previously been conducted to identify axonally located mRNA transcripts relevant for axonal function in rodent hippocampal neurons and, very recently, in distal projections from human stem cell derived neurons, with great success (Bigler et al. 2017; Taylor et al. 2009). The work described in this thesis reveals the function of two axon-enriched microRNAs, miR-3470b and miR-99a, in axonal development and, thus, validates the used axon enrichment approach as a valuable tool for the identification of microRNAs regulating axonal processes.

A few studies before us took advantage of microfluidic and other compartmentalised culture methods to investigate the population of microRNAs localised to the axons of rodent sympathetic, primary sensory and cortical neurons by microarray and RT-qPCR approaches, generating some of

the first clues into the functional roles of axonal microRNAs (Hancock et al. 2014; Natera-Naranjo et al. 2010; Sasaki et al. 2014). However, this is the first study to use microRNA sequencing for this purpose, which allows for the detection of novel/recently discovered microRNAs that are not commonly assayed in microarray or RT-PCR array methodologies. Indeed, this work is a good example of the advantages of next-generation sequencing techniques as this approach allowed for the identification of miR-3470b, a relatively unknown microRNA that showed high axonal expression in our enrichment analysis and for which further functional studies showed relevant roles in neuronal development.

Moreover, further investigation into the genomic origins of miR-3470b showed that miR-3470b is a mouse-specific microRNA with relatively recent origins in the rodent genome and, despite this, has found a function in mouse cortical development *in vitro*. The observation that species-specific microRNAs can have relevant roles in cortical function and development could have interesting implications to the evolution of the human brain. Evidence from computational and microRNA profiling studies in primates (Salisbury 1946; Yuan et al. 2010) suggest that microRNAs are important motors of evolution, and some studies have since proposed that the appearance of primate and human-specific microRNAs and their regulatory target interactions in the brain might provide evolutionary advantages associated with the emergence of a highly complex brain (Hu et al. 2012; McCreight et al. 2017; SALISBURY 1946). With the improvement of cell differentiation methodologies to yield functional neurons, human induced pluripotent and embryonic stem cell-derived neurons are expected to be a promising experimental system to test, at the cellular level, the functional relevance of primate and human-specific microRNAs in neurodevelopmental processes and to investigate their spatiotemporal patterns of expression and action.

Importantly, as described for mRNA transcripts before them, the differential expression of specific microRNAs in axons is yet another strong evidence that the axonal microRNA population is not a mere sampling of the cytoplasm, but rather that microRNAs reach axons not simply by diffusion, but by active and selective transportation. Although the mechanisms by which microRNAs are transported to the axon remain largely unknown, likely due to technical

limitations related to their size and stability, recent studies by us and others started to explore the capacity of axonal microRNAs to participate in the local regulation of axonal transcripts and protein synthesis, modulating axonal function over development. The discovery that the axonal miR-99a has the capacity to control axonal outgrowth in cortical neurons builds on the current knowledge of microRNAs with intra-axonal regulatory actions relevant to development.

As neurons form neuronal circuits, the emergence of spontaneous neuronal activity is believed to drive and correlate with the refinement of the connections toward synaptic maturation (Blankenship and Feller 2010; Kamioka et al. 1996; Muramoto, Ichikawa, Kawahara, Kobayashi, et al. 1993). Due to the discussed involvement of microRNAs in neurodevelopmental processes, it is not surprising that microRNA regulatory networks are also likely to be in control of these events. Work described in this thesis constitutes one of the first reports exploring the role of microRNAs in the development of spontaneous neuronal activity at the network level. Indeed, we showed that miR-3470b and miR-99a functions are necessary for the normal development of spontaneous network activity in cortical cultures, supporting the functional relevance of microRNA regulation for the establishment of functional connectivity. Unlike the previously described miR-101 and miR-128, miR-3470b and miR-99a appear to be positive regulators of network activity (Lippi et al. 2016; McSweeney et al. 2016; Tan et al. 2013).

Both microelectrode arrays (MEAs) and imaging of calcium transients approaches were used in our studies. A few reports have compared these methodologies in the detection of spontaneous activity of neuronal networks, suggesting that, at least in the first stages of activity development and synchronised network-wide activity, intracellular calcium oscillations correlate with electrical firing patterns measured by MEAs recordings (Opitz 2002; Takayama et al. 2009b). Although the use of MEA cultures has proved to be very prolific in the study of neuronal networks, it bears a few disadvantages as the electrodes can only sample extracellular electric potentials of a small proportion of neurons in a given area within the network. Moreover, because more than one neuron can sit on one electrode, the recordings lack information about the particular cells responsible for the measured electrical

firing, making it difficult to interpret. On the other hand, MEAs allow non-invasive multiple recordings of the same culture over development, which is suitable to test specific treatments and makes this platform very attractive for drug screening studies. For the purpose of investigating spontaneous activity, optical recording of calcium oscillations is an alternative approach that allows for the simultaneous recording from many neurons. This permits the study of single cell kinetics as well as network activity patterns, with good temporal resolution, mostly dependant on the optic equipment used for detection. Overall, we have successfully used both approaches for the study of microRNA function in spontaneous activity development, however, given that the magnitude of microRNA effects in neuronal function are often mild, the single cell resolution of calcium imaging is likely to be advantageous.

5.2 microRNAs in axonal terminals and beyond: implications to cell-to-cell communication

It is known that local translation of mRNA transcripts localised to neuronal terminals/synapse is necessary for the formation of synaptic contacts and, in the mature neuron, the occurrence of activity-dependant plasticity (Kelleher, Govindarajan, and Tonegawa 2004; Sutton and Schuman 2006; Zhang and Poo 2002). As with other neuronal processes, is not surprising that microRNAs are part of the toolbox crucial for the regulation of these events. A paradigmatic example is miR-134, a microRNA localised to the dendrites of rodent hippocampal neurons that has been shown to regulate spine morphology by local inhibition of Limk1 mRNA, a cytoskeleton regulator (Schratt et al. 2006). microRNAs with action in the presynaptic terminal have also been documented. For instance, miR-137 gain of function was shown to lead to decreased mRNA translation of the presynaptic target proteins complexin-1, Nsf and synaptotagmin-1, causing impaired pre-synaptic vesicle release (Siegert et al. 2015).

Accordingly, increasing number of studies have shown that a considerable number of microRNAs and microRNA precursors are enriched in synaptic fractions compared to total homogenate levels (Li et al. 2015; Lugli et al.

2008b). Moreover, components of microRNA maturation machinery, such as dicer, FMRP and Ago2, are also found at synaptic fractions (Lugli et al. 2005, 2008b).

microRNAs located to the synapse have the potential to not only modulate local signalling effectors, such as pre-synaptic receptors and components of the postsynaptic density as has been documented in the literature , but also to be secreted in response to activity or to regulate signalling pathways involved in the formation of synaptic contacts (Ryan et al. 2015; Schratt 2009b; Wayman et al. 2008). Although the latter is still in the realm of possibility, some microRNAs have been found in fractions enriched in synaptic vesicles (Li et al. 2015) and in pre-synaptic terminals (Xu et al. 2013), where they were found to be associated to Ago2.

Interestingly, when exploring the possibility that excitable synaptic fractions might secret microRNAs under physiological stimulation, Xu et al. found that microRNAs can be functionally released, in a calcium-dependent manner, from pre-synaptic enriched fractions called synaptosomes. Similarly, another microRNA was shown to be uptaken by endocytosis (Xu et al. 2013).

Due to the intrinsic function of axons in neurotransmitter release, it is appealing to speculate that microRNAs enriched in the axon would be perfectly placed to be transported to the pre-synaptic terminal, incorporated into synaptic vesicles and later released to the synaptic space to exert local actions in the post-synaptic cell. In accordance to this theory, preliminary data from our lab found some of the top axon-enriched microRNAs to be highly expressed in synaptosome fractions of postnatal day 14 and 21 of mice brain (appendix X). One of these was miR-99a, intriguingly also one of the microRNAs shown to be functionally released by synaptosomes in the report by Xu et al. 2013.

Furthermore, findings from the extracellular vesicles field suggest that microRNAs are no strangers to cell-to-cell communication and their potential to modulate regulatory networks away from the cells of origin has been subject of great interest in the study of cancer metastases. microRNAs are known to be loaded into vesicles derived from multivesicular bodies within endosomes, named exosomes. microRNAs within exosomes were shown to be actively

released into the extracellular space and subsequently uptaken to exert regulatory actions in the recipient cells (Zhang et al. 2015). In the brain, various cell-types are known to secrete exosomes, including glia and cortical neurons (Sharma, Schiapparelli, and Cline 2013; Xu et al. 2017). In fact, accumulating evidence suggests that microRNAs can be secreted by glia cells via exosomes and are involved in glia-neuron communication in neurodevelopmental processes and even neuroregeneration (Frühbeis, Fröhlich, and Krämer-Albers 2012). Also, although neuronal exosomes express microRNAs, it is not well understood how exosomal microRNAs may be related to neuronal function, formation of synaptic contacts or synaptic transmission.

It is possible that microRNAs within neuronal exosomes could be uptaken non-synaptically by neighbouring neurons and glial cells. An interesting hypothesis developed by Smalheiser et al suggests that, as neuronal networks within the brain show highly correlated input and output firing patterns, activity-mediated exosome release of microRNAs (and other non-coding RNAs) by many neurons, in a coordinated manner, could provide a mean to synchronise their gene expression dynamics, which could aid in driving the establishment and/or re-enforcement of neuronal circuits (Smalheiser 2014).

The roles of exosomal microRNAs secreted by cortical neurons in neuro-to-neuron communication and the potential function of neuronal exosomal microRNAs in the establishment of neuronal networks over development are subject of current work in our lab. Interestingly, preliminary data suggest that miR-99a, an axonal microRNA highly expressed in pre-synaptic fractions from juvenile and adult mouse brain, is also enriched in neuronal exosomes from cortical cultures. These observations added to the discovered functions of miR-99a in axon development and network activity discussed here and in chapter 4, raise many more questions. It seems apparent that miR-99a can be secreted from neurons in vesicles, either synaptic or exosomal, but what could be miR-99a regulatory effects in the recipient cell? Could exosomal miR-99a be exerting regulatory actions in the outgrowth of axons of neighbouring neurons? If so, could miR-99a be uptaken by axons to produce local effects? And, importantly, could miR-99a modulation of cortical network activity over development be linked to cell-to-cell communication? From a more general

perspective, similar questions can be asked about the functions of the overall population of neuronal exosome-derived microRNAs in neuronal development.

5.3 Implications to disease

The activity of microRNAs, as well as dysregulated microRNA processing, have been directly implicated in the pathogenesis of both neurodevelopmental and neurodegenerative diseases (Wang, Kwon, and Tsai 2012).

Two of the better documented neurodevelopmental disorders for which microRNA dysfunction plays a relevant role are schizophrenia and autism spectrum disorders, extensively reviewed in Beveridge and Cairns, 2012 and Fregeac et al., 2016, respectively. One of the most studied microRNAs implicated in schizophrenia is miR-137. Since large-scale gene genome-wide association studies of schizophrenia patients revealed that single nucleotide polymorphisms (SNPs) located in the MIR137 gene were amongst the most significant SNPs associated with the disease, various reports have suggested that miR-137 function is necessary for correct synaptogenesis and synaptic physiology (Siegert et al. 2015; Thomas et al. 2017).

Also in neurodegenerative disorders microRNA dysfunction underlying disease etiology has been focus of interest and, importantly, the potential use of circulating microRNAs detected in biological fluids as early biomarkers of disease onset is being intensely researched.

Here, we sought to investigate a potential role for miR-99a in Alzheimer's disease (AD). Due to the newly discovered role of miR-99a in axonal circuitry formation and connectivity over development, it seemed appropriate to explore the possibility that miR-99a dysregulation could be involved in the disruption of connections that constitute one of the first hallmarks of this disorder, loss of neuronal connectivity. For this, miR-99a expression was profiled in the cortical forebrain of post mortem AD patients in comparison to age and gender-matched control individuals (Appendix X), however no significant differential expression could be observed for this microRNA in AD forebrains. One possible explanation is that this microRNA has no relevance

for mature circuits and its actions are restricted to development. Nevertheless, it is also possible that miR-99a is dysregulated early and affects the pathological process at initial stages, before the onset of the disease.

**

Collectively, the work presented and discussed in this thesis represents another step in our increased understanding of the functions of microRNAs in neuronal function and development. It has unravelled novel and exciting roles for axonal microRNAs in the development of axonal projections that wire the brain and ultimately establish brain connectivity.

6. Appendix I

1. miR-99a is highly expressed in synaptic fractions of the developing mouse brain

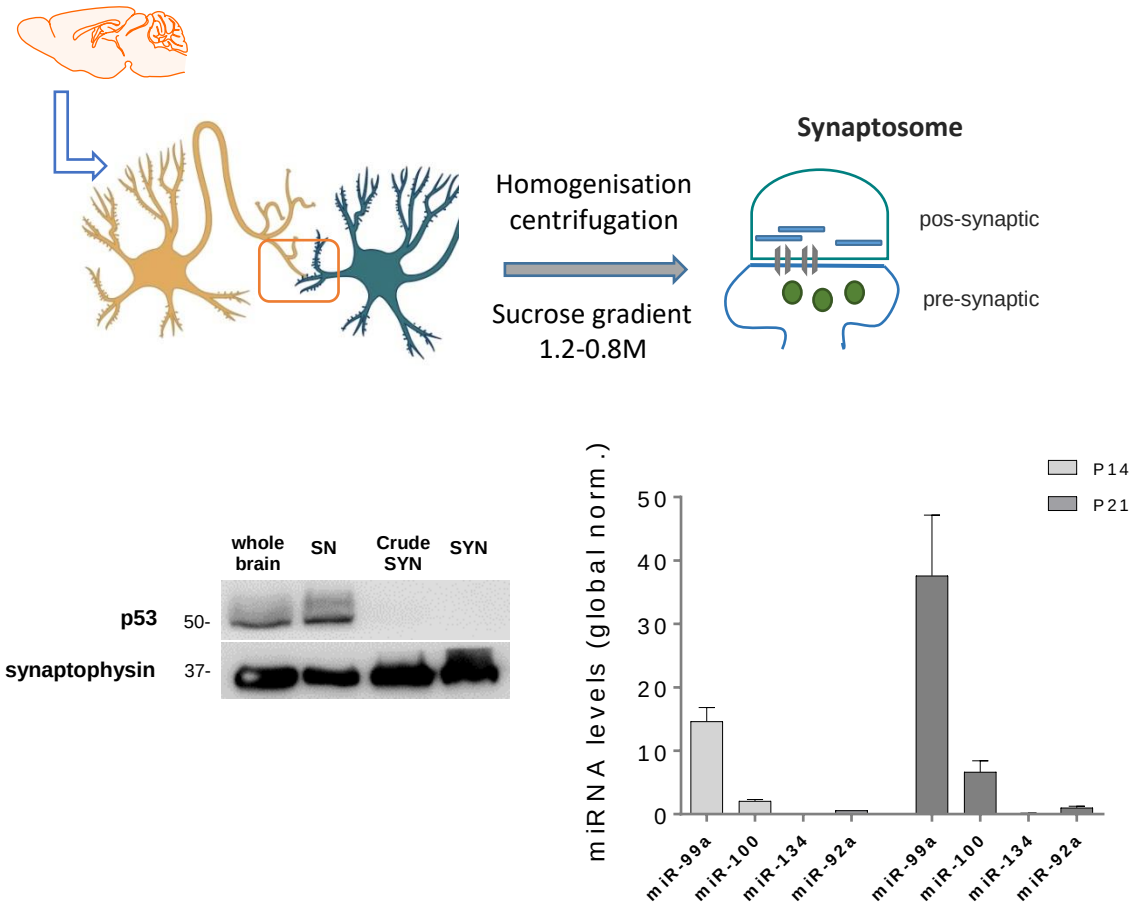


Figure S1. miR-99a quantification in synaptic fractions by RT-qPCR. Representation of the methods to obtain such fractions. Synaptosomes are biochemical preparations where subcellular fractionation, achieved by means of a glucose gradient, yields membrane fractions that retain part or the pre and pos-synaptic terminals (synaptic vesicles and postsynaptic density; upper pannel). Western blot analysis confirmed the success of the purification, with more pure synaptic fractions showing an increase in synaptophysin, whereas p53, mainly nuclear, disappears (SN: supernatant; Crude SYN: crude synaptosome fraction; SYN: purified synaptosome fraction). miR-99a is highly expressed in mouse synaptic fractions at postnatal day 14 and 21, when compared to other miRNAs assayed, inclusively the dendritic miR-134.

2. miR-99a is not altered in the forebrain of Alzheimer's Disease patients

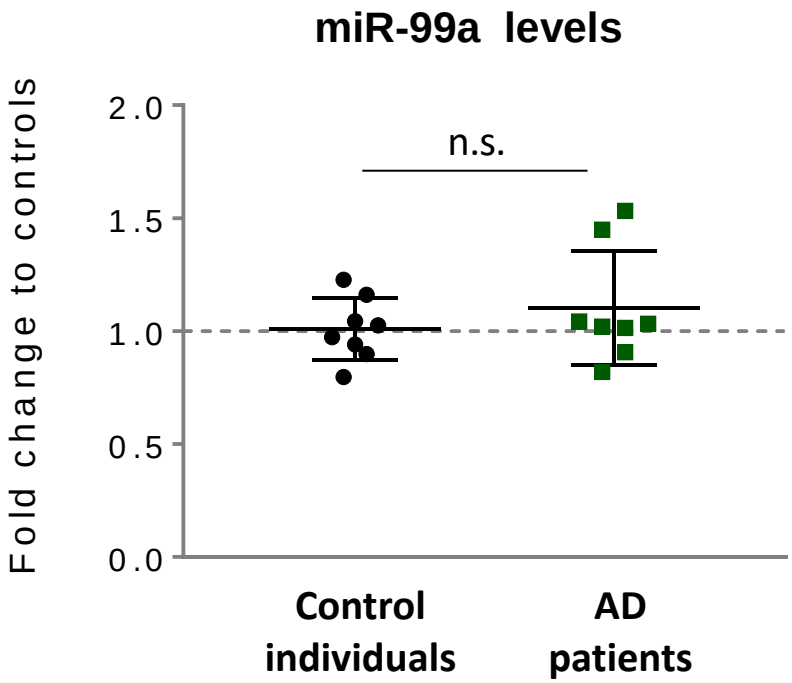


Figure S2. miR-99a expression levels in the forebrain of AD patients as compared to age and gender-matched control individuals. Cohort of 16 individuals, 8 from each category. Data indicates miR-99a appears to not be dysregulated in AD forebrains.

7. Abbreviations

3’UTR
3' untranslated region

AD
Alzheimer's disease

AKT
protein kinase B

ATP
adenosine triphosphate

BDNF
brain derived neurotrophic factor

BSA
bovine serum albumine

cDNA
complementary DNA

circRNAs
circular RNAs

Ct
cycle threshold

Ctdspl
CTD (carboxy-terminal domain, RNA polymerase II, polypeptide A) small phosphatase like 2

DGCR8
DiGeorge syndrome chromosomal region

DIV
day in vitro

DMEM
Dulbecco's modified Eagle's medium

DRG
dorsal root ganglia

eIF2B2
eukaryotic initiation factor-2B

F_0
baseline fluorescence

Fwd
forward

Fzd5
frizzled class receptor 5

Gapdh
glyceraldehyde 3-phosphate dehydrogenase

GFP
green fluorescent protein

Gramd1c
GRAM domain-containing 1C (also protein Aster-C)

GSK-3β
glycogen synthase kinase 3

HEK-293T
human embryonic kidney 293 cells

HPA
Human Protein Atlas

Hs3st2
heparan sulfate-glucosamine 3-O-sulfotransferase

Hs3st3b
heparan sulphate 3-O-sulfotransferase 3b

ISI
interspike interval

JIP1
C-Jun-amino-terminal kinase-interacting protein 1

KCl
potassium chloride

LINE2
long interspaced nuclear element 2

LKB1
liver kinase B1

LNA
locked nucleic acid

lncRNAs
long noncoding RNAs

LTR
Long terminal repeat

MAP1b
microtubule associated protein 1b

Map2
microtubule-associated protein 2

MEAs
microelectrode array devices

MicroRNA
micro ribonucleic acid, same as miRNA

miRISC complex
microRNA-induced silencing complex

mRNA
messenger RNA

mTOR
mammalian target of rapamycin

Neuro2A
mouse neuroblastoma cell line

NRP1
neuropilin 1

ORF
open reading frame

PAR
partitioning-defective protein pamily

PBS
Phosphate buffer saline

PCR
polymerase chain reaction

PLO
poly-L-ornithine

PNA
pedtide nucleic acid

pre-miRNA
miRNA precursor transcript

PTBP1/2
Polypyrimidine tract-binding protein 1/2

PTEN
phosphatase and tensin homolog

Rev
reverse

RGC
retinal ganglion cell

RhoA
Ras homolog gene family, member

RIN
RNA integrity number

RNA
Ribonucleic acid

ROI
region of interes

RT-qPCR
real-time quantitative PCR

S.D.
standard deviation

S.E.M.
standard error of mean

Sema3a
semaphorin 3a

SINEs
short interspersed nuclear elements

siRNA
small interfering RNA

Slit-2
Slit homolog 2 protein

Smad7
mothers against decapentaplegic homolog 7

snRNA
small nuclear RNA

TEs
transposable elements

TGF-β
transforming growth factor beta

TPM
transcripts per kilibase million

8. References

Agarwal, Vikram, George W. Bell, Jin-Wu Nam, and David P. Bartel. 2015. "Predicting Effective MicroRNA Target Sites in Mammalian MRNAs." *ELife* 4.

Aschrafi, A. et al. 2008. "MicroRNA-338 Regulates Local Cytochrome c Oxidase IV MRNA Levels and Oxidative Phosphorylation in the Axons of Sympathetic Neurons." *Journal of Neuroscience*.

Baek, Daehyun, Judit Villén, Chanseok Shin, Fernando D. Camargo, et al. 2008. "The Impact of MicroRNAs on Protein Output." *Nature* 455(7209):64–71.

Baek, Daehyun, Judit Villén, Chanseok Shin, Fernando D. Camargo, et al. 2008. "The Impact of MicroRNAs on Protein Output." *Nature* 455(7209):64–71.

Banker, Gary. 2018. "The Development of Neuronal Polarity: A Retrospective View." *The Journal of Neuroscience : The Official Journal of the Society for Neuroscience* 38(8):1867–73.

Barbash, Shahar, Sagiv Shifman, and Hermona Soreq. 2014. "Global Coevolution of Human MicroRNAs and Their Target Genes." *Molecular Biology and Evolution* 31(5):1237–47.

Barca-Mayo, Olga and Davide De Pietri Tonelli. 2014. "Convergent MicroRNA Actions Coordinate Neocortical Development." *Cellular and Molecular Life Sciences : CMLS* 71(16):2975–95.

Barros, Claudia S., Santos J. Franco, and Ulrich Müller. 2011. "Extracellular Matrix: Functions in the Nervous System." *Cold Spring Harbor Perspectives in Biology* 3(1):a005108.

Bartel, David P. 2009. "MicroRNAs: Target Recognition and Regulatory Functions." *Cell* 136(2):215–33.

Bartel, David P. 2009. "MicroRNAs: Target Recognition and Regulatory Functions." *Cell* 136:215–33.

Baudet, Marie-Laure et al. 2011. "MiR-124 Acts through CoREST to Control Onset of Sema3A Sensitivity in Navigating Retinal Growth Cones." *Nature Neuroscience* 15:29–38.

Baudet, Marie-Laure et al. 2012. "MiR-124 Acts through CoREST to Control Onset of Sema3A Sensitivity in Navigating Retinal Growth Cones." *Nature Neuroscience* 15(1):29–38.

Bellon, Anais et al. 2017. "MiR-182 Regulates Slit2-Mediated Axon Guidance by Modulating the Local Translation of a Specific MRNA Accession Numbers GSE86883." *CellReports* 18:1171–86.

Berezikov, Eugene. 2011. "Evolution of MicroRNA Diversity and Regulation in Animals." *Nature Reviews Genetics* 12(12):846–60.

Beveridge, Natalie J. and Murray J. Cairns. 2012. "MicroRNA Dysregulation in Schizophrenia." *Neurobiology of Disease* 46(2):263–71.

Bigler, Rebecca L., Joyce W. Kamande, Raluca Dumitru, Mark Niedringhaus, and Anne Marion Taylor. 2017. "Messenger RNAs Localized to Distal Projections

of Human Stem Cell Derived Neurons." *Scientific Reports* 7(1):611.

Blankenship, Aaron G. and Marla B. Feller. 2010. "Mechanisms Underlying Spontaneous Patterned Activity in Developing Neural Circuits." *Nature Reviews Neuroscience* 11(1):18–29.

Borchert, Glen M. et al. 2011. "Comprehensive Analysis of MicroRNA Genomic Loci Identifies Pervasive Repetitive-Element Origins." *Mobile Genetic Elements* 1(1):8–17.

Bramsen, Jesper B. et al. 2007. "Improved Silencing Properties Using Small Internally Segmented Interfering RNAs." *Nucleic Acids Research* 35(17):5886–97.

Briese, Michael et al. 2016. "Whole Transcriptome Profiling Reveals the RNA Content of Motor Axons." *Nucleic Acids Research* 44(4):e33.

Buckley, Peter T. et al. 2011. "Cytoplasmic Intron Sequence-Retaining Transcripts Can Be Dendritically Targeted via ID Element Retrotransposons." *Neuron* 69(5):877–84.

Bülow, Hannes E. and Oliver Hobert. 2004. "Differential Sulfations and Epimerization Define Heparan Sulfate Specificity in Nervous System Development." *Neuron* 41(5):723–36.

Bustin, S. A. et al. 2009. "The MIQE Guidelines: Minimum Information for Publication of Quantitative Real-Time PCR Experiments." *Clinical Chemistry* 55(4):611–22.

Cadwallader, Adam B. and H. Joseph Yost. 2006. "Combinatorial Expression Patterns of Heparan Sulfate Sulfotransferases in Zebrafish: I. The 3- *O* -Sulfotransferase Family." *Developmental Dynamics* 235(12):3423–31.

Campbell, Douglas S. and Christine E. Holt. 2001. "Chemotropic Responses of Retinal Growth Cones Mediated by Rapid Local Protein Synthesis and Degradation." *Neuron* 32(6):1013–26.

Cancedda, L., H. Fiumelli, K. Chen, and M. -m. Poo. 2007. "Excitatory GABA Action Is Essential for Morphological Maturation of Cortical Neurons In Vivo." *Journal of Neuroscience* 27(19):5224–35.

Cao, Fujiang, Tao Liu, Shiwei Sun, and Shiqing Feng. 2017. "The Role of the MiR-99b-5p/MTOR Signaling Pathway in Neuroregeneration in Mice Following Spinal Cord Injury." *Molecular Medicine Reports* 16(6):9355–60.

Cao, Zhengyu et al. 2013. "Enhanced Asynchronous Ca(2+) Oscillations Associated with Impaired Glutamate Transport in Cortical Astrocytes Expressing Fmr1 Gene Premutation Expansion." *The Journal of Biological Chemistry* 288(19):13831–41.

Cao, Zhengyu et al. 2017. "Influence of Tetramethylenedisulfotetramine on Synchronous Calcium Oscillations at Distinct Developmental Stages of Hippocampal Neuronal Cultures."

Cartault, F. et al. 2012. "Mutation in a Primate-Conserved Retrotransposon Reveals a Noncoding RNA as a Mediator of Infantile Encephalopathy." *Proceedings of the National Academy of Sciences* 109(13):4980–85.

Chakrabarti, Mrinmay et al. 2013. "Photofrin Based Photodynamic Therapy and MiR-99a Transfection Inhibited FGFR3 and PI3K/Akt Signaling Mechanisms to Control Growth of Human Glioblastoma In Vitro and In Vivo" edited by R. K. Srivastava. *PLoS ONE* 8(2):e55652.

Chen, Jiadong and Arnold R. Kriegstein. 2015. "A GABAergic Projection from the Zona Incerta to Cortex Promotes Cortical Neuron Development." *Science (New York, N.Y.)* 350(6260):554–58.

Chen, Ya-wen et al. 2014. "Resource Systematic Study of Drosophila MicroRNA Functions Using a Collection of Targeted Knockout Mutations." *Developmental Cell* 31(6):784–800.

Cheng, Li-Chun, Erika Pastrana, Masoud Tavazoie, and Fiona Doetsch. 2009. "MiR-124 Regulates Adult Neurogenesis in the Subventricular Zone Stem Cell Niche." *Nature Neuroscience* 12(4):399–408.

Chevalier, David and Glen M. Borchert. 2017. "Genome-Wide Analysis of MicroRNA-Regulated Transcripts." Pp. 93–107 in. Humana Press, New York, NY.

Chiappalone, M. et al. 2003. "Networks of Neurons Coupled to Microelectrode Arrays: A Neuronal Sensory System for Pharmacological Applications." *Biosensors & Bioelectronics* 18(5–6):627–34.

Chiappalone, Michela, Marco Bove, Alessandro Vato, Mariateresa Tedesco, and Sergio Martinoia. 2006. "Dissociated Cortical Networks Show Spontaneously Correlated Activity Patterns during in Vitro Development." *Brain Research* 1093(1):41–53.

Chiu, Hui, Amel Alqadah, and Chieh Chang. 2014. "The Role of MicroRNAs in Regulating Neuronal Connectivity." *Frontiers in Cellular Neuroscience* 7(January):283.

Chuong, Edward B., Nels C. Elde, and Cédric Feschotte. 2017. "Regulatory Activities of Transposable Elements: From Conflicts to Benefits." *Nature Reviews. Genetics* 18(2):71–86.

Cioni, Jean-Michel, Max Koppers, and Christine E. Holt. 2018. "Molecular Control of Local Translation in Axon Development and Maintenance." *Current Opinion in Neurobiology* 51:86–94.

Colliec-Jouault, S., N. W. Shworak, J. Liu, A. I. de Agostini, and R. D. Rosenberg. 1994. "Characterization of a Cell Mutant Specifically Defective in the Synthesis of Anticoagulantly Active Heparan Sulfate." *The Journal of Biological Chemistry* 269(40):24953–58.

Coolen, Marion, Shauna Katz, and Laure Bally-Cuif. 2013. "MiR-9: A Versatile Regulator of Neurogenesis." *Frontiers in Cellular Neuroscience* 7(November):220.

Cordaux, Richard and Mark A. Batzer. 2009. "The Impact of Retrotransposons on Human Genome Evolution." *Nature Reviews. Genetics* 10(10):691–703.

Cornelissen, Frans et al. 2013a. "Quantitation of Chronic and Acute Treatment Effects on Neuronal Network Activity Using Image and Signal Analysis." *Journal of Biomolecular Screening* 18(7):807–19.

Cornelissen, Frans et al. 2013b. "Quantitation of Chronic and Acute Treatment Effects on Neuronal Network Activity Using Image and Signal Analysis." *Journal of Biomolecular Screening*.

Coufal, Nicole G. et al. 2009. "L1 Retrotransposition in Human Neural Progenitor Cells." *Nature* 460(7259):1127–31.

Cullen, Bryan R. 2006. "Enhancing and Confirming the Specificity of RNAi Experiments." *Nature Methods* 3(9):677–81.

Dajas-Bailador, Federico et al. 2012. "MicroRNA-9 Regulates Axon Extension and Branching by Targeting Map1b in Mouse Cortical Neurons." *Nature Neuroscience* 15:697–99.

Dajas-Bailador, Federico, Ioannis Bantounas, Emma V Jones, and Alan J. Whitmarsh. 2014. "Regulation of Axon Growth by the JIP1-AKT Axis." *Journal of Cell Science* 127:230–39.

Dajas-Bailador, Federico, Emma V Jones, and Alan J. Whitmarsh. 2008. "The JIP1 Scaffold Protein Regulates Axonal Development in Cortical Neurons." *Current Biology : CB* 18(3):221–26.

Dani, Neil, Minyeop Nahm, Seungbok Lee, and Kendal Broadie. 2012. "A Targeted Glycan-Related Gene Screen Reveals Heparan Sulfate Proteoglycan Sulfation Regulates WNT and BMP Trans-Synaptic Signaling" edited by N. Perrimon. *PLoS Genetics* 8(11):e1003031.

Daskalova, Evelina, Vesselin Baev, Ventsislav Rusinov, and Ivan Minkov. 2007. "3'UTR-Located ALU Elements: Donors of Potential MiRNA Target Sites and Mediators of Network MiRNA-Based Regulatory Interactions." *Evolutionary Bioinformatics Online* 2:103–20.

Deininger, Prescott. 2011. "Alu Elements: Know the SINEs." *Genome Biology* 12(12):236.

Dorfman, Julia and Ian G. Macara. 2008. "STRADalpha Regulates LKB1 Localization by Blocking Access to Importin-Alpha, and by Association with Crm1 and Exportin-7." *Molecular Biology of the Cell* 19:1614–26.

Dotti, C. G., C. a Sullivan, and G. a Banker. 1988. "The Establishment of Polarity by Hippocampal Neurons in Culture." *The Journal of Neuroscience : The Official Journal of the Society for Neuroscience* 8(4):1454–68.

Dravid, Shashank M. and Thomas F. Murray. 2004. "Spontaneous Synchronized Calcium Oscillations in Neocortical Neurons in the Presence of Physiological [Mg2+]: Involvement of AMPA/Kainate and Metabotropic Glutamate Receptors." *Brain Research* 1006(1):8–17.

Dridi, Sami. 2012. "Alu Mobile Elements: From Junk DNA to Genomic Gems." *Scientifica* 2012:545328.

Dunker, William, Yang Zhao, Yu Song, and John Karijolich. 2017. "Recognizing the SINEs of Infection: Regulation of Retrotransposon Expression and Modulation of Host Cell Processes." *Viruses* 9(12).

Edelstein, Arthur, Nenad Amodaj, Karl Hoover, Ron Vale, and Nico Stuurman. 2010. "Computer Control of Microscopes Using Manager." *Current Protocols in Molecular Biology* (SUPPL. 92).

Eom, Taesun, Valerio Berardi, Jun Zhong, Gianfranco Risuleo, and Henri Tiedge. 2011. "Dual Nature of Translational Control by Regulatory BC RNAs." *Molecular and Cellular Biology* 31(22):4538–49.

Erwin, Jennifer A., Maria C. Marchetto, and Fred H. Gage. 2014. "Mobile DNA Elements in the Generation of Diversity and Complexity in the Brain." *Nature Reviews Neuroscience* 15(8):497–506.

Feng, Yougang et al. 2014. "MicroRNA-99a Acts as a Tumor Suppressor and Is down-Regulated in Bladder Cancer." *BMC Urology* 14:50.

Feschotte, Cédric. 2008. "Transposable Elements and the Evolution of Regulatory Networks." *Nature Reviews Genetics* 9(5):397–405.

Filshtein, Teresa J. et al. 2012. "OrbId: Origin-Based Identification of MicroRNA Targets." *Mobile Genetic Elements* 2(4):184–92.

Fiore, Roberto, Sharof Khudayberdiev, Reuben Saba, and Gerhard Schratt. 2011. "MicroRNA Function in the Nervous System." *Progress in Molecular Biology and Translational Science* 102:47–100.

Follert, Philipp, Harold Cremer, and Christophe Béclin. 2014. "MicroRNAs in Brain Development and Function: A Matter of Flexibility and Stability." *Frontiers in Molecular Neuroscience* 7(February):5.

Fort, Alexandre et al. 2014. "Deep Transcriptome Profiling of Mammalian Stem Cells Supports a Regulatory Role for Retrotransposons in Pluripotency Maintenance." *Nature Genetics* 46(6):558–66.

França, Gustavo S., Ludwig C. Hinske, Pedro A. F. Galante, and Maria D. Vibranovski. 2017. "Unveiling the Impact of the Genomic Architecture on the Evolution of Vertebrate MicroRNAs." *Frontiers in Genetics* 8:34.

Fregeac, Julien, Laurence Colleaux, and Lam Son Nguyen. 2016. "The Emerging Roles of MicroRNAs in Autism Spectrum Disorders." *Neuroscience and Biobehavioral Reviews* 71:729–38.

Frühbeis, Carsten, Dominik Fröhlich, and Eva-Maria Krämer-Albers. 2012. "Emerging Roles of Exosomes in Neuron–Glia Communication." *Frontiers in Physiology* 3:119.

Gangaraju, Vamsi K. and Haifan Lin. 2009. "MicroRNAs: Key Regulators of Stem Cells." *Nature Reviews. Molecular Cell Biology* 10(2):116–25.

Garcez, Patricia P., Francois Guillemot, and Federico Dajas-Bailador. 2017. "Study of MiRNA Function in the Developing Axons of Mouse Cortical Neurons: Use of Compartmentalized Microfluidic Chambers and in Utero Electroporation." Pp. 59–71 in *Neuromethods*. Vol. 128.

Garcia-Perez, Jose L., Thomas J. Widmann, and Ian R. Adams. 2016. "The Impact of Transposable Elements on Mammalian Development." *Development (Cambridge, England)* 143(22):4101–14.

Gee, H. E. et al. 2011. "The Small-Nucleolar RNAs Commonly Used for MicroRNA Normalisation Correlate with Tumour Pathology and Prognosis." *British Journal of Cancer* 104(7):1168–77.

Gim, Jeong-An, Hong-Seok Ha, Kung Ahn, Dae-Soo Kim, and Heui-Soo Kim.

2014. "Genome-Wide Identification and Classification of MicroRNAs Derived from Repetitive Elements." *Genomics & Informatics* 12(4):261–67.

Giraldez, Antonio J. et al. 2005. "MicroRNAs Regulate Brain Morphogenesis in Zebrafish." *Science (New York, N.Y.)* 308:833–38.

Giuditta, A., W. D. Dettbarn, and M. Brzin. 1968. "Protein Synthesis in the Isolated Giant Axon of the Squid." *Proceedings of the National Academy of Sciences of the United States of America* 59(4):1284–87.

Giuditta, Antonio, Barry B. Kaplan, Jaime Alvarez, and Edward Koenig. 2002. "Axonal and Presynaptic Protein Synthesis: New Insights into the Biology of the Neuron." *Trends in Neurosciences* 25(8):400–404.

Göke, Jonathan and Huck Hui Ng. 2016. "CTRL+INSERT: Retrotransposons and Their Contribution to Regulation and Innovation of the Transcriptome." *EMBO Reports* 17(8):1131–44.

Goldberg, Jeffrey L. 2003. "How Does an Axon Grow?" *Genes & Development* 17(8):941–58.

Gong, Jing et al. 2014. "Comprehensive Analysis of Human Small RNA Sequencing Data Provides Insights into Expression Profiles and MiRNA Editing." *RNA Biology* 11(11):1375–85.

Gonzalez-Lozano, Miguel A. et al. 2016. "Dynamics of the Mouse Brain Cortical Synaptic Proteome during Postnatal Brain Development." *Scientific Reports* 6(1):35456.

Gracias, N. G., N. J. Shirkey-Son, and U. Hengst. 2014. "Local Translation of TC10 Is Required for Membrane Expansion during Axon Outgrowth." *Nat Commun* 5:3506.

Grienberger, Christine and Arthur Konnerth. 2012. "Imaging Calcium in Neurons." *Neuron* 73(5):862–85.

Griffiths-Jones, Sam, Jerome H. L. Hui, Antonio Marco, and Matthew Ronshaugen. 2011. "MicroRNA Evolution by Arm Switching." *EMBO Reports* 12(2):172–77.

Grimson, Andrew et al. 2008. "Early Origins and Evolution of MicroRNAs and Piwi-Interacting RNAs in Animals." *Nature* 455(7217):1193–97.

Guo, Huili, Nicholas T. Ingolia, Jonathan S. Weissman, and David P. Bartel. 2010. "Mammalian MicroRNAs Predominantly Act to Decrease Target MRNA Levels." *Nature* 466(7308):835–40.

Hadjiargyrou, Michael and Nicholas Delihas. 2013. "The Intertwining of Transposable Elements and Non-Coding RNAs." *International Journal of Molecular Sciences* 14(7):13307–28.

Hales, Chadwick M. et al. 2012. "Stimulus-Evoked High Frequency Oscillations Are Present in Neuronal Networks on Microelectrode Arrays." *Frontiers in Neural Circuits* 6:29.

Han, Xinwei et al. 2009. "Transcriptome of Embryonic and Neonatal Mouse Cortex by High-Throughput RNA Sequencing." *Proceedings of the National Academy of Sciences of the United States of America* 106(31):12741–46.

Hancock, Melissa L., Nicolas Preitner, Jie Quan, and John G. Flanagan. 2014. "MicroRNA-132 Is Enriched in Developing Axons, Locally Regulates Rasa1 MRNA, and Promotes Axon Extension." *The Journal of Neuroscience : The Official Journal of the Society for Neuroscience* 34:66–78.

Hartl, Daniela et al. 2008. "Transcriptome and Proteome Analysis of Early Embryonic Mouse Brain Development." *PROTEOMICS* 8(6):1257–65.

Hasegawa, Hiroshi and Fan Wang. 2008. "Visualizing Mechanosensory Endings of TrkC-Expressing Neurons in HS3ST-2-HPLAP Mice." *Journal of Comparative Neurology* 511(4):543–56.

Häsler, Julien and Katharina Strub. 2006. "Alu Elements as Regulators of Gene Expression." *Nucleic Acids Research* 34(19):5491–97.

Heimberg, Alysha M., Lorenzo F. Sempere, Vanessa N. Moy, Philip C. J. Donoghue, and Kevin J. Peterson. 2008. "MicroRNAs and the Advent of Vertebrate Morphological Complexity." *Proceedings of the National Academy of Sciences of the United States of America* 105(8):2946–50.

Hellec, Charles, Maxime Delos, Mathieu Carpentier, Agnès Denys, and Fabrice Allain. 2018. "The Heparan Sulfate 3-O-Sulfotransferases (HS3ST) 2, 3B and 4 Enhance Proliferation and Survival in Breast Cancer MDA-MB-231 Cells." *PloS One* 13(3):e0194676.

Hengst, Ulrich, Alessia Deglincerti, Hyung Joon Kim, Noo Li Jeon, and Samie R. Jaffrey. 2009. "Axonal Elongation Triggered by Stimulus-Induced Local Translation of a Polarity Complex Protein." *Nature Cell Biology* 11(8):1024–30.

Hertel, Jana et al. 2006. "The Expansion of the Metazoan MicroRNA Repertoire." *BMC Genomics* 7.

Hu, Hai Yang et al. 2012. "Evolution of the Human-Specific MicroRNA MiR-941." *Nature Communications* 3.

Huang, Tianwen, Yueguang Liu, Menggui Huang, Xiaolin Zhao, and Leping Cheng. 2010. "Wnt1-Cre-Mediated Conditional Loss of Dicer Results in Malformation of the Midbrain and Cerebellum and Failure of Neural Crest and Dopaminergic Differentiation in Mice." *Journal of Molecular Cell Biology* 2:152–63.

Hur, Eun-Mi and Feng-Quan Zhou. 2010. "GSK3 Signalling in Neural Development." *Nature Reviews. Neuroscience* 11(8):539–51.

Irie, F., H. Badie-Mahdavi, and Y. Yamaguchi. 2012. "Autism-like Socio-Communicative Deficits and Stereotypies in Mice Lacking Heparan Sulfate." *Proceedings of the National Academy of Sciences* 109(13):5052–56.

Ito, Shinya et al. 2014. "Large-Scale, High-Resolution Multielectrode-Array Recording Depicts Functional Network Differences of Cortical and Hippocampal Cultures." *PloS One* 9(8):e105324.

Iwama, Hisakazu, Kiyohito Kato, Hitomi Imachi, Koji Murao, and Tsutomu Masaki. 2013. "Human MicroRNAs Originated from Two Periods at Accelerated Rates in Mammalian Evolution." *Molecular Biology and Evolution* 30(3):613–26.

Iyer, Archana N., AnaÃ¯s Bellon, and Marie-Laure Baudet. 2014. "MicroRNAs in Axon Guidance." *Frontiers in Cellular Neuroscience* 8:78.

Iyer, Archana N., Anaïs Bellon, and Marie-Laure Baudet. 2014. "MicroRNAs in Axon Guidance." *Frontiers in Cellular Neuroscience* 8:78.

Jansson, Martin D. and Anders H. Lund. 2012. "MicroRNA and Cancer." *Molecular Oncology* 6(6):590–610.

Jaworski, Jacek and Morgan Sheng. 2006. "The Growing Role of MTOR in Neuronal Development and Plasticity." *Molecular Neurobiology* 34(3):205–19.

Jiang, Haiyang et al. 2014. "MiR-99a Promotes Proliferation Targeting FGFR3 in Human Epithelial Ovarian Cancer Cells." *Biomedicine & Pharmacotherapy* 68(2):163–69.

Jiang, J. J. et al. 2015. "MicroRNA-26a Supports Mammalian Axon Regeneration in Vivo by Suppressing GSK3β Expression." *Cell Death and Disease* 6(8):e1865.

Jimbo, Y. 2007. "MEA-Based Recording of Neuronal Activity in Vitro." *Archives Italiennes de Biologie* 145(3–4):289–97.

Jimbo, Y., H. P. C. Robinson, and A. Kawana. 1993. "Simultaneous Measurement of Intracellular Calcium and Electrical Activity from Patterned Neural Networks in Culture." *IEEE Transactions on Biomedical Engineering* 40(8):804–10.

Jin, Hyun Yong et al. 2015. "Transfection of MicroRNA Mimics Should Be Used with Caution." *Frontiers in Genetics* 6:340.

Jung, Hosung, Byung C. Yoon, and Christine E. Holt. 2012. "Axonal MRNA Localization and Local Protein Synthesis in Nervous System Assembly, Maintenance and Repair." *Nature Reviews Neuroscience* 13:514–514.

Kalkkila, Juha-Pekka et al. 2004. "Cloning and Expression of Short Interspersed Elements B1 and B2 in Ischemic Brain." *European Journal of Neuroscience* 19(5):1199–1206.

Kamimura, Keisuke et al. 2004. "Regulation of Notch Signaling by Drosophila Heparan Sulfate 3-O Sulfotransferase." *The Journal of Cell Biology* 166(7):1069–79.

Kamioka, Hiroyuki, Eisaku Maeda, Yasuhiko Jimbo, Hugh P. C. Robinson, and Akio Kawana. 1996. "Spontaneous Periodic Synchronized Bursting during Formation of Mature Patterns of Connections in Cortical Cultures." *Neuroscience Letters* 206(2–3):109–12.

Kaneko, Hiroki et al. 2011. "DICER1 Deficit Induces Alu RNA Toxicity in Age-Related Macular Degeneration." *Nature* 471(7338):325–30.

Kaplan, Barry B., Amar N. Kar, Anthony E. Gioio, and Armaz Aschrafi. 2013. "MicroRNAs in the Axon and Presynaptic Nerve Terminal." *Frontiers in Cellular Neuroscience* 7(August):126.

Kar, Amar N., Margaret a MacGibeny, Noreen M. Gervasi, Anthony E. Gioio, and Barry B. Kaplan. 2013. "Intra-Axonal Synthesis of Eukaryotic Translation

Initiation Factors Regulates Local Protein Synthesis and Axon Growth in Rat Sympathetic Neurons." *The Journal of Neuroscience : The Official Journal of the Society for Neuroscience* 33:7165–74.

Karbiener, Michael, Christina Glantschnig, and Marcel Scheideler. 2014. "Hunting the Needle in the Haystack: A Guide to Obtain Biologically Meaningful MicroRNA Targets." *International Journal of Molecular Sciences* 15(11):20266–89.

Kass, D. H., M. E. Raynor, and T. M. Williams. 2000. "Evolutionary History of B1 Retroposons in the Genus Mus." *Journal of Molecular Evolution* 51(3):256–64.

Kaur, Harleen, Amit Arora, Jesper Wengel, and Souvik Maiti. 2006. "Thermodynamic, Counterion, and Hydration Effects for the Incorporation of Locked Nucleic Acid Nucleotides into DNA Duplexes †." *Biochemistry* 45(23):7347–55.

Kelleher, Raymond J., Arvind Govindarajan, and Susumu Tonegawa. 2004. "Translational Regulatory Mechanisms in Persistent Forms of Synaptic Plasticity." *Neuron* 44(1):59–73.

Kent, W. J. et al. 2002. "The Human Genome Browser at UCSC." *Genome Research* 12(6):996–1006.

Khanam, Tasneem et al. 2007. "Two Primate-Specific Small Non-Protein-Coding RNAs in Transgenic Mice: Neuronal Expression, Subcellular Localization and Binding Partners." *Nucleic Acids Research* 35(2):529–39.

Kiezun, Adam et al. 2012. "MiRviewer: A Multispecies MicroRNA Homologous Viewer." *BMC Research Notes* 5.

Kim, Eunjin and Hosung Jung. 2015. "Local Protein Synthesis in Neuronal Axons: Why and How We Study." *BMB Rep* 48(3):139–46.

Kim, V. Narry. 2005. "MicroRNA Biogenesis: Coordinated Cropping and Dicing." *Nature Reviews. Molecular Cell Biology* 6(May):376–85.

Kirkby, Lowry A., Georgeann S. Sack, Alana Firl, and Marla B. Feller. 2013. "A Role for Correlated Spontaneous Activity in the Assembly of Neural Circuits." *Neuron* 80(5):1129–44.

Koenig, E. 1967. "Synthetic Mechanisms in the Axon. IV. In Vitro Incorporation of [3H]Precursors into Axonal Protein and RNA." *Journal of Neurochemistry* 14(4):437–46.

de Koning, A. P. Jason, Wanjun Gu, Todd A. Castoe, Mark A. Batzer, and David D. Pollock. 2011. "Repetitive Elements May Comprise Over Two-Thirds of the Human Genome" edited by G. P. Copenhaver. *PLoS Genetics* 7(12):e1002384.

Korecka, J. A., S. Levy, and O. Isacson. 2016. "In Vivo Modeling of Neuronal Function, Axonal Impairment and Connectivity in Neurodegenerative and Neuropsychiatric Disorders Using Induced Pluripotent Stem Cells." *Molecular and Cellular Neuroscience* 73:3–12.

Kozomara, Ana and Sam Griffiths-Jones. 2014. "MiRBase: Annotating High Confidence MicroRNAs Using Deep Sequencing Data." *Nucleic Acids*

Research 42(Database issue):D68-73.

Krämer, Andreas, Jeff Green, Jack Pollard, and Stuart Tugendreich. 2014. "Causal Analysis Approaches in Ingenuity Pathway Analysis." *Bioinformatics* 30(4):523–30.

Kramerov, D. A. and N. S. Vassetzky. 2011. "Origin and Evolution of SINEs in Eukaryotic Genomes." *Heredity* 107(6):487–95.

KRAMEROV, D. and N. VASSETZKY. 2005. "Short Retroposons in Eukaryotic Genomes." *International Review of Cytology* 247:165–221.

Kramerov, Dmitri A. and Nikita S. Vassetzky. 2011. "SINEs." *Wiley Interdisciplinary Reviews: RNA* 2(6):772–86.

Krayev, A. S. et al. 1980. "The Nucleotide Sequence of the Ubiquitous Repetitive DNA Sequence B1 Complementary to the Most Abundant Class of Mouse Fold-Back RNA." *Nucleic Acids Research* 8(6):1201–15.

Kuwabara, Tomoko et al. 2009. "Wnt-Mediated Activation of NeuroD1 and Retro-Elements during Adult Neurogenesis." *Nature Neuroscience* 12(9):1097–1105.

Kye, Min-Jeong et al. 2007. "Somatodendritic MicroRNAs Identified by Laser Capture and Multiplex RT-PCR." *RNA (New York, N.Y.)* 13:1224–34.

Lagos-Quintana, Mariana et al. 2002. "Identification of Tissue-Specific MicroRNAs from Mouse." *Current Biology* 12:735–39.

Lander, Eric S. et al. 2001. "Initial Sequencing and Analysis of the Human Genome." *Nature* 409(6822):860–921.

Larsen, Peter A., Kelsie E. Hunnicutt, Roxanne J. Larsen, Anne D. Yoder, and Ann M. Saunders. 2018. "Warning SINEs: Alu Elements, Evolution of the Human Brain, and the Spectrum of Neurological Disease." *Chromosome Research* 26(1–2):93–111.

Lawrence, Roger, Tomio Yabe, Sassan Hajmohammadi, et al. 2007. "The Principal Neuronal GD-Type 3-O-Sulfotransferases and Their Products in Central and Peripheral Nervous System Tissues." *Matrix Biology : Journal of the International Society for Matrix Biology* 26(6):442–55.

Lawrence, Roger, Tomio Yabe, Sassan HajMohammadi, et al. 2007. "The Principal Neuronal GD-Type 3-O-Sulfotransferases and Their Products in Central and Peripheral Nervous System Tissues." *Matrix Biology* 26(6):442–55.

Lázaro-Peña, María I., Carlos A. Díaz-Balzac, Hannes E. Bülow, and Scott W. Emmons. 2018. "Synaptogenesis Is Modulated by Heparan Sulfate in Caenorhabditis Elegans." *Genetics* 209(1):195–208.

Lee, Jeong-Soo and Chi-Bin Chien. 2004. "When Sugars Guide Axons: Insights from Heparan Sulphate Proteoglycan Mutants." *Nature Reviews Genetics* 5(12):923–35.

Lehnert, Stefan et al. 2009. "Evidence for Co-Evolution between Human MicroRNAs and Alu-Repeats" edited by A. Christoffels. *PLoS ONE* 4(2):e4456.

Leucht, Christoph et al. 2008. "MicroRNA-9 Directs Late Organizer Activity of the Midbrain-Hindbrain Boundary." *Nature Neuroscience* 11(6):641–48.

Lewis, Tommy L., Julien Courchet, and Franck Polleux. 2013. "Cell Biology in Neuroscience: Cellular and Molecular Mechanisms Underlying Axon Formation, Growth, and Branching." *The Journal of Cell Biology* 202(6):837–48.

Li, Huinan, Cheng Wu, Rodolfo Aramayo, Matthew S. Sachs, and Mark L. Harlow. 2015. "Synaptic Vesicles Contain Small Ribonucleic Acids (SRNAs) Including Transfer RNA Fragments (TrfRNA) and MicroRNAs (MiRNA)." *Scientific Reports* 5:14918.

Li, T., J. Spearow, C. M. Rubin, and C. W. Schmid. 1999. "Physiological Stresses Increase Mouse Short Interspersed Element (SINE) RNA Expression in Vivo." *Gene* 239(2):367–72.

Li, Wen-Chang et al. 2007. "Axon and Dendrite Geography Predict the Specificity of Synaptic Connections in a Functioning Spinal Cord Network." *Neural Development* 2(1):17.

Linker, Sara B., Maria C. Marchetto, Iñigo Narvaiza, Ahmet M. Denli, and Fred H. Gage. 2017. "Examining Non-LTR Retrotransposons in the Context of the Evolving Primate Brain." *BMC Biology* 15(1):68.

Lippi, Giordano et al. 2016. "MicroRNA-101 Regulates Multiple Developmental Programs to Constrain Excitation in Adult Neural Networks." *Neuron* 92(6):1337–51.

Liu, W. M., W. M. Chu, P. V Choudary, and C. W. Schmid. 1995. "Cell Stress and Translational Inhibitors Transiently Increase the Abundance of Mammalian SINE Transcripts." *Nucleic Acids Research* 23(10):1758–65.

Livak, Kenneth J. and Thomas D. Schmittgen. 2001. "Analysis of Relative Gene Expression Data Using Real-Time Quantitative PCR and the 2−ΔΔCT Method." *Methods* 25(4):402–8.

Lu, Jian et al. 2008. "The Birth and Death of MicroRNA Genes in Drosophila." *Nature Genetics* 40(3):351–55.

Lu, Lu et al. 2017. "Tracking the Genome-Wide Outcomes of a Transposable Element Burst over Decades of Amplification." *Proceedings of the National Academy of Sciences of the United States of America* 114(49):E10550–59.

Lugli, Giovanni, John Larson, Maryann E. Martone, Ying Jones, and Neil R. Smalheiser. 2005. "Dicer and EIF2c Are Enriched at Postsynaptic Densities in Adult Mouse Brain and Are Modified by Neuronal Activity in a Calpain-Dependent Manner." *Journal of Neurochemistry* 94:896–905.

Lugli, Giovanni, Vetle I. Torvik, John Larson, and Neil R. Smalheiser. 2008a. "Expression of MicroRNAs and Their Precursors in Synaptic Fractions of Adult Mouse Forebrain." *Journal of Neurochemistry* 106(2):650–61.

Lugli, Giovanni, Vetle I. Torvik, John Larson, and Neil R. Smalheiser. 2008b. "Expression of MicroRNAs and Their Precursors in Synaptic Fractions of Adult Mouse Forebrain." *Journal of Neurochemistry* 106(2):650–61.

Luhmann, Heiko J. et al. 2016. "Spontaneous Neuronal Activity in Developing

Neocortical Networks: From Single Cells to Large-Scale Interactions." *Frontiers in Neural Circuits* 10:40.

Maag, Jesper L. V et al. 2015. "Dynamic Expression of Long Noncoding RNAs and Repeat Elements in Synaptic Plasticity." *Frontiers in Neuroscience* 9:351.

Maeda, Eisaku, HP P. Robinson, and A. Kawana. 1995. "The Mechanisms of Generation and Propagation of Synchronized Bursting in Developing Networks of Cortical Neurons." *The Journal of Neuroscience : The Official Journal of the Society for Neuroscience* 15(10):6834–45.

Makeyev, Eugene V., Jiangwen Zhang, Monica A. Carrasco, and Tom Maniatis. 2007. "The MicroRNA MiR-124 Promotes Neuronal Differentiation by Triggering Brain-Specific Alternative Pre-MRNA Splicing." *Molecular Cell* 27:435–48.

Manakov, Sergei A., Seth G. N. Grant, and Anton J. Enright. 2009. "Reciprocal Regulation of MicroRNA and MRNA Profiles in Neuronal Development and Synapse Formation." *BMC Genomics* 10:419.

Maraia, R. J. 1991. "The Subset of Mouse B1 (Alu-Equivalent) Sequences Expressed as Small Processed Cytoplasmic Transcripts." *Nucleic Acids Research* 19(20):5695–5702.

Marler, Katharine J. et al. 2014. "BDNF Promotes Axon Branching of Retinal Ganglion Cells via MiRNA-132 and P250GAP." *The Journal of Neuroscience : The Official Journal of the Society for Neuroscience* 34(3):969–79.

McCLINTOCK, B. 1951. "Chromosome Organization and Genic Expression." *Cold Spring Harbor Symposia on Quantitative Biology* 16:13–47.

McCreight, Jennifer C., Sean E. Schneider, Damien B. Wilburn, and Willie J. Swanson. 2017. "Evolution of MicroRNA in Primates" edited by Y. Zheng. *PLOS ONE* 12(6):e0176596.

McFadden, Kathryn and Nancy J. Minshew. 2013. "Evidence for Dysregulation of Axonal Growth and Guidance in the Etiology of ASD." *Frontiers in Human Neuroscience* 7:671.

McNeill, Elizabeth and David Van Vactor. 2012. "MicroRNAs Shape the Neuronal Landscape." *Neuron* 75:363–79.

McSweeney, K. Melodi et al. 2016. "Inhibition of MicroRNA 128 Promotes Excitability of Cultured Cortical Neuronal Networks." *Genome Research* 26(10):1411–16.

Mestdagh, Pieter et al. 2009. "A Novel and Universal Method for MicroRNA RT-QPCR Data Normalization." *Genome Biology* 10(6):R64.

Meunier, Julien et al. 2013. "Birth and Expression Evolution of Mammalian MicroRNA Genes." *Genome Research* 23(1):34–45.

Mi, Huaiyu et al. 2017. "PANTHER Version 11: Expanded Annotation Data from Gene Ontology and Reactome Pathways, and Data Analysis Tool Enhancements." *Nucleic Acids Research* 45(D1):D183–89.

Mi, Huaiyu, Anushya Muruganujan, John T. Casagrande, and Paul D. Thomas. 2013. "Large-Scale Gene Function Analysis with the Panther Classification

System." *Nature Protocols* 8(8):1551–66.

Mi, Huaiyu and Paul Thomas. 2009. *Protein Networks and Pathway Analysis*. Vol. 563.

Minge, Daniel et al. 2017. "Heparan Sulfates Support Pyramidal Cell Excitability, Synaptic Plasticity, and Context Discrimination." *Cerebral Cortex (New York, N.Y. : 1991)* 27(2):903–18.

Mita, Paolo and Jef D. Boeke. 2016. "How Retrotransposons Shape Genome Regulation." *Current Opinion in Genetics & Development* 37:90–100.

Mody, M. et al. 2001. "Genome-Wide Gene Expression Profiles of the Developing Mouse Hippocampus." *Proceedings of the National Academy of Sciences* 98(15):8862–67.

Morales-Hernández, Antonio et al. 2016. "*Alu* Retrotransposons Promote Differentiation of Human Carcinoma Cells through the Aryl Hydrocarbon Receptor." *Nucleic Acids Research* 44(10):4665–83.

Mukai, Jun et al. 2015. "Molecular Substrates of Altered Axonal Growth and Brain Connectivity in a Mouse Model of Schizophrenia." *Neuron* 86(3):680–96.

Muotri, A. R., M. C. N. Marchetto, N. G. Coufal, and F. H. Gage. 2007. "The Necessary Junk: New Functions for Transposable Elements." *Human Molecular Genetics* 16(R2):R159–67.

Muotri, Alysson R. et al. 2005. "Somatic Mosaicism in Neuronal Precursor Cells Mediated by L1 Retrotransposition." *Nature* 435(7044):903–10.

Muramoto, Kazuyo, Masumi Ichikawa, Masahiro Kawahara, Kazuo Kobayash, and Yoichiro Kuroda. 1993. "Frequency of Synchronous Oscillations of Neuronal Activity Increases during Development and Is Correlated to the Number of Synapses in Cultured Cortical Neuron Networks." *Neuroscience Letters* 163(163).

Muramoto, Kazuyo, Masumi Ichikawa, Masahiro Kawahara, Kazuo Kobayashi, and Yoichiro Kuroda. 1993. "Frequency of Synchronous Oscillations of Neuronal Activity Increases during Development and Is Correlated to the Number of Synapses in Cultured Cortical Neuron Networks." *Neuroscience Letters* 163(2):163–65.

Myers, Jonathan P., Miguel Santiago-Medina, and Timothy M. Gomez. 2011. "Regulation of Axonal Outgrowth and Pathfinding by Integrin-Ecm Interactions." *Developmental Neurobiology* 71(11):901–23.

Naguibneva, I. et al. 2006. "An LNA-Based Loss-of-Function Assay for Micro-RNAs." *Biomedicine & Pharmacotherapy* 60(9):633–38.

Natera-Naranjo, Orlangie, Armaz Aschrafi, Anthony E. Gioio, and Barry B. Kaplan. 2010. "Identification and Quantitative Analyses of MicroRNAs Located in the Distal Axons of Sympathetic Neurons." *RNA (New York, N.Y.)* 16(8):1516–29.

Nielsen, Joseph A., Pierre Lau, Dragan Maric, Jeffery L. Barker, and Lynn D. Hudson. 2009a. "Integrating MicroRNA and MRNA Expression Profiles of Neuronal Progenitors to Identify Regulatory Networks Underlying the Onset

of Cortical Neurogenesis." *BMC Neuroscience* 10(1):98.

Nielsen, Joseph A., Pierre Lau, Dragan Maric, Jeffery L. Barker, and Lynn D. Hudson. 2009b. "Integrating MicroRNA and MRNA Expression Profiles of Neuronal Progenitors to Identify Regulatory Networks Underlying the Onset of Cortical Neurogenesis." *BMC Neuroscience* 10(1):98.

Obien, Marie Engelene J., Kosmas Deligkaris, Torsten Bullmann, Douglas J. Bakkum, and Urs Frey. 2014. "Revealing Neuronal Function through Microelectrode Array Recordings." *Frontiers in Neuroscience* 8:423.

Ohnishi, Yusuke et al. 2012. "Active Role of Small Non-Coding RNAs Derived from SINE/B1 Retrotransposon during Early Mouse Development." *Molecular Biology Reports* 39(2):903–9.

Opitz, T. 2002. "Spontaneous Development of Synchronous Oscillatory Activity During Maturation of Cortical Networks In Vitro." *Journal of Neurophysiology*.

Paraskevopoulou, Maria D. et al. 2013. "DIANA-MicroT Web Server v5.0: Service Integration into MiRNA Functional Analysis Workflows." *Nucleic Acids Research* 41(Web Server issue).

Park, Jeong Won, Behrad Vahidi, Anne M. Taylor, Seog Woo Rhee, and Noo Li Jeon. 2006. "Microfluidic Culture Platform for Neuroscience Research." *Nature Protocols* 1(4):2128–36.

Patel, Tapan P., Karen Man, Bonnie L. Firestein, and David F. Meaney. 2015. "Automated Quantification of Neuronal Networks and Single-Cell Calcium Dynamics Using Calcium Imaging." *Journal of Neuroscience Methods* 243:26–38.

Peltier, H. J. and G. J. Latham. 2008. "Normalization of MicroRNA Expression Levels in Quantitative RT-PCR Assays: Identification of Suitable Reference RNA Targets in Normal and Cancerous Human Solid Tissues." *RNA* 14(5):844–52.

Peng, C. et al. 2012. "A Unilateral Negative Feedback Loop Between MiR-200 MicroRNAs and Sox2/E2F3 Controls Neural Progenitor Cell-Cycle Exit and Differentiation." *Journal of Neuroscience* 32(38):13292–308.

Perrat, Paola N. et al. 2013. "Transposition-Driven Genomic Heterogeneity in the Drosophila Brain." *Science (New York, N.Y.)* 340(6128):91–95.

Peterson, Sarah M. et al. 2014. "Common Features of MicroRNA Target Prediction Tools." *Frontiers in Genetics* 5:23.

Pichardo-Casas, Israel et al. 2012. "Expression Profiling of Synaptic MicroRNAs from the Adult Rat Brain Identifies Regional Differences and Seizure-Induced Dynamic Modulation." *Brain Research* 1436:20–33.

Pickering, Mark, Brian W. Pickering, Keith J. Murphy, and John J. O'Connor. 2008. "Discrimination of Cell Types in Mixed Cortical Culture Using Calcium Imaging: A Comparison to Immunocytochemical Labeling." *Journal of Neuroscience Methods* 173(1):27–33.

De Pietri Tonelli, Davide et al. 2008. "MiRNAs Are Essential for Survival and Differentiation of Newborn Neurons but Not for Expansion of Neural

Progenitors during Early Neurogenesis in the Mouse Embryonic Neocortex." *Development (Cambridge, England)* 135:3911–21.

Piriyapongsa, J., L. Marino-Ramirez, and I. K. Jordan. 2007. "Origin and Evolution of Human MicroRNAs from Transposable Elements." *Genetics* 176(0016–6731 (Print)):1323–37.

Piriyapongsa, Jittima and I. King Jordan. 2007. "A Family of Human MicroRNA Genes from Miniature Inverted-Repeat Transposable Elements." *PLoS ONE* 2(2).

Piriyapongsa, Jittima, Leonardo Mariño-Ramírez, and I. King Jordan. 2007. "Origin and Evolution of Human MicroRNAs from Transposable Elements." *Genetics* 176(2):1323–37.

Polak, Paz and Eytan Domany. 2006. "Alu Elements Contain Many Binding Sites for Transcription Factors and May Play a Role in Regulation of Developmental Processes." *BMC Genomics* 7:133.

Polleux, F. and William Snider. 2010. "Initiating and Growing an Axon." *Cold Spring Harbor Perspectives in Biology* 2.

Ponicsan, Steven L., Jennifer F. Kugel, and James A. Goodrich. 2010. "Genomic Gems: SINE RNAs Regulate MRNA Production." *Current Opinion in Genetics & Development* 20(2):149–55.

Poulain, Fabienne E. 2015. "Analyzing the Role of Heparan Sulfate Proteoglycans in Axon Guidance in Vivo in Zebrafish." *Methods in Molecular Biology (Clifton, N.J.)* 1229:469–82.

Poulain, Fabienne E. and H. Joseph Yost. 2015. "Heparan Sulfate Proteoglycans: A Sugar Code for Vertebrate Development?" *Development* 142(20):3456–67.

Qin, Sheng, Ping Jin, Xue Zhou, Liming Chen, and Fei Ma. 2015. "The Role of Transposable Elements in the Origin and Evolution of MicroRNAs in Human." *PloS One* 10(6):e0131365.

Quentin, Y. 1989. "Successive Waves of Fixation of B1 Variants in Rodent Lineage History." *Journal of Molecular Evolution* 28(4):299–305.

Rajman, Marek and Gerhard Schratt. 2017. "MicroRNAs in Neural Development: From Master Regulators to Fine-Tuners." *Development (Cambridge, England)* 144(13):2310–22.

Reilly, Matthew T., Geoffrey J. Faulkner, Joshua Dubnau, Igor Ponomarev, and Fred H. Gage. 2013. "The Role of Transposable Elements in Health and Diseases of the Central Nervous System." *The Journal of Neuroscience : The Official Journal of the Society for Neuroscience* 33(45):17577–86.

Riffo-Campos, Ángela L., Ismael Riquelme, and Priscilla Brebi-Mieville. 2016. "Tools for Sequence-Based MiRNA Target Prediction: What to Choose?" *International Journal of Molecular Sciences* 17(12).

Roberts, Justin T., Sara E. Cardin, and Glen M. Borchert. 2014. "Burgeoning Evidence Indicates That MicroRNAs Were Initially Formed from Transposable Element Sequences." *Mobile Genetic Elements* 4:e29255.

Robinson, H. P. et al. 1993. "Periodic Synchronized Bursting and Intracellular Calcium Transients Elicited by Low Magnesium in Cultured Cortical Neurons." *Journal of Neurophysiology* 70(4):1606–16.

Rodriguez, Antony, Sam Griffiths-Jones, Jennifer L. Ashurst, and Allan Bradley. 2004. "Identification of Mammalian MicroRNA Host Genes and Transcription Units." *Genome Research* 14(10 A):1902–10.

Rudin, C. M. and C. B. Thompson. 2001. "Transcriptional Activation of Short Interspersed Elements by DNA-Damaging Agents." *Genes, Chromosomes & Cancer* 30(1):64–71.

Ryan, Brigid, Greig Joilin, and Joanna M. Williams. 2015. "Plasticity-Related MicroRNA and Their Potential Contribution to the Maintenance of Long-Term Potentiation." *Frontiers in Molecular Neuroscience* 8.

SALISBURY, E. 1946. "The Variation in Reproductive Capacity of Plants" edited by D. Penny. *Science Progress* 34(12):466–76.

Santangelo, Andrea M. et al. 2007. "Ancient Exaptation of a CORE-SINE Retroposon into a Highly Conserved Mammalian Neuronal Enhancer of the Proopiomelanocortin Gene." *PLoS Genetics* 3(10):1813–26.

Santpere, Gabriel, Maria Lopez-Valenzuela, Natalia Petit-Marty, Arcadi Navarro, and Yolanda Espinosa-Parrilla. 2016. "Differences in Molecular Evolutionary Rates among MicroRNAs in the Human and Chimpanzee Genomes." *BMC Genomics* 17:528.

Sasaki, T. et al. 2008. "Possible Involvement of SINEs in Mammalian-Specific Brain Formation." *Proceedings of the National Academy of Sciences* 105(11):4220–25.

Sasaki, Yukio, Christina Gross, Lei Xing, Yoshio Goshima, and Gary J. Bassell. 2014. "Identification of Axon-Enriched MicroRNAs Localized to Growth Cones of Cortical Neurons." *Developmental Neurobiology* 74(July):397–406.

Sayed, D. and M. Abdellatif. 2011. "MicroRNAs in Development and Disease." *Physiological Reviews* 91:827–87.

Scarfò, Irene, Elisa Pellegrino, Elisabetta Mereu, Giorgio Inghirami, and Roberto Piva. 2016. "Transposable Elements: The Enemies Within." *Experimental Hematology* 44(10):913–16.

Schindelin, Johannes et al. 2012. "Fiji: An Open Source Platform for Biological Image Analysis." *Nature Methods* 9(7):676–82.

Schmittgen, Thomas D. et al. 2008. "Real-Time PCR Quantification of Precursor and Mature MicroRNA." *Methods (San Diego, Calif.)* 44(1):31–38.

Schratt, Gerhard. 2009a. "Fine-Tuning Neural Gene Expression with MicroRNAs." *Current Opinion in Neurobiology* 19:213–19.

Schratt, Gerhard. 2009b. "MicroRNAs at the Synapse." *Nature Reviews. Neuroscience* 10(November 2009):842–49.

Schratt, Gerhard M. et al. 2006. "A Brain-Specific MicroRNA Regulates Dendritic Spine Development." *Nature* 439:283–89.

Schroeder, Andreas et al. 2006. "The RIN: An RNA Integrity Number for

Assigning Integrity Values to RNA Measurements." *BMC Molecular Biology* 7:3.

Schwarzenbach, Heidi, Andreia Machado da Silva, George Calin, and Klaus Pantel. 2015. "Data Normalization Strategies for MicroRNA Quantification." *Clinical Chemistry* 61(11):1333–42.

Semeralul, Mawahib O. et al. 2006. "Microarray Analysis of the Developing Cortex." *Journal of Neurobiology* 66(14):1646–58.

Sepulveda-Diaz, Julia Elisa et al. 2015. "HS3ST2 Expression Is Critical for the Abnormal Phosphorylation of Tau in Alzheimer's Disease-Related Tau Pathology." *Brain* 138(5):1339–54.

Sethupathy, Praveen, Molly Megraw, and Artemis G. Hatzigeorgiou. 2006. "A Guide through Present Computational Approaches for the Identification of Mammalian MicroRNA Targets." *Nature Methods* 3(11):881–86.

Shabalina, Svetlana A. and Eugene V. Koonin. 2008. "Origins and Evolution of Eukaryotic RNA Interference." *Trends in Ecology and Evolution* 23(10):578–87.

Sharma, Pranav, Lucio Schiapparelli, and Hollis T. Cline. 2013. "Exosomes Function in Cell-Cell Communication during Brain Circuit Development." *Current Opinion in Neurobiology* 23(6):997–1004.

Shelly, Maya et al. 2011. "Semaphorin3A Regulates Neuronal Polarization by Suppressing Axon Formation and Promoting Dendrite Growth." *Neuron* 71:433–46.

Shelly, Maya, Laura Cancedda, Sarah Heilshorn, Germán Sumbre, and Mu ming Poo. 2007. "LKB1/STRAD Promotes Axon Initiation During Neuronal Polarization." *Cell* 129:565–77.

Shibata, Mikihito, Hiromi Nakao, Hiroshi Kiyonari, Takaya Abe, and Shinichi Aizawa. 2011. "MicroRNA-9 Regulates Neurogenesis in Mouse Telencephalon by Targeting Multiple Transcription Factors." *The Journal of Neuroscience : The Official Journal of the Society for Neuroscience* 31(9):3407–22.

Shigeoka, Toshiaki et al. 2016. "Dynamic Axonal Translation in Developing and Mature Visual Circuits." *Cell* 166(1):181–92.

Shin, Chanseok et al. 2010. "Expanding the MicroRNA Targeting Code: Functional Sites with Centered Pairing." *Molecular Cell* 38(6):789–802.

Shukla, D. et al. 1999. "A Novel Role for 3-O-Sulfated Heparan Sulfate in Herpes Simplex Virus 1 Entry." *Cell* 99(1):13–22.

Siegel, Gabriele et al. 2009. "A Functional Screen Implicates MicroRNA-138-Dependent Regulation of the Depalmitoylation Enzyme APT1 in Dendritic Spine Morphogenesis." *Nature Cell Biology* 11(6):705–16.

Siegert, Sandra et al. 2015. "The Schizophrenia Risk Gene Product MiR-137 Alters Presynaptic Plasticity." *Nature Neuroscience* 18(7):1008–16.

Siepel, Adam et al. 2005. "Evolutionarily Conserved Elements in Vertebrate, Insect, Worm, and Yeast Genomes." *Genome Research* 15(8):1034–50.

Silva, J. C., S. A. Shabalina, D. G. Harris, J. L. Spouge, and A. S. Kondrashov. 2003. "Conserved Fragments of Transposable Elements in Intergenic Regions: Evidence for Widespread Recruitment of MIR- and L2-Derived Sequences within the Mouse and Human Genomes." *Genetical Research* 82(1):1–18.

Smalheiser, Neil R. 2014. "The RNA-Centred View of the Synapse: Non-Coding RNAs and Synaptic Plasticity." *Philosophical Transactions of the Royal Society of London. Series B, Biological Sciences* 369(1652):20130504.

Smalheiser, Neil R. and Vetle I. Torvik. 2006. "Alu Elements within Human MRNAs Are Probable MicroRNA Targets." *Trends in Genetics* 22(10):532–36.

Smalheiser, Neil R. and Vetle I. Torvik. 2005. "Mammalian MicroRNAs Derived from Genomic Repeats." *Trends in Genetics : TIG* 21(6):322–26.

Smalla, Karl-Heinz, Patricia Klemmer, and Ursula Wyneken. 2013. "Isolation of the Postsynaptic Density: A Specialization of the Subsynaptic Cytoskeleton." Pp. 265–80 in. Humana Press, Totowa, NJ.

Smetters, Diana, Ania Majewska, and Rafael Yuste. 1999. "Detecting Action Potentials in Neuronal Populations with Calcium Imaging." *Methods* 18(2):215–21.

Smit, A. F. 1999. "Interspersed Repeats and Other Mementos of Transposable Elements in Mammalian Genomes." *Current Opinion in Genetics & Development* 9(6):657–63.

Smit, AFA, R. Hubley, and P. Green. 2013. "RepeatMasker Open-4.0. 2013-2015 ." *Http://Www.Repeatmasker.Org*.

Somel, Mehmet et al. 2011. "MicroRNA-Driven Developmental Remodeling in the Brain Distinguishes Humans from Other Primates." *PLoS Biology* 9(12).

Sood, Pranidhi, Azra Krek, Mihaela Zavolan, Giuseppe Macino, and Nikolaus Rajewsky. 2006. "Cell-Type-Specific Signatures of MicroRNAs on Target MRNA Expression." *Proceedings of the National Academy of Sciences of the United States of America* 103(8):2746–51.

Sotelo-Silveira, Jose R., Aldo Calliari, Alejandra Kun, Edward Koenig, and Jose R. Sotelo. 2006. "RNA Trafficking in Axons." *Traffic* 7(5):508–15.

Spengler, Ryan M., Clayton K. Oakley, and Beverly L. Davidson. 2014. "Functional MicroRNAs and Target Sites Are Created by Lineage-Specific Transposition." *Human Molecular Genetics* 23(7):1783–93.

Stappert, Laura, Beate Roese-Koerner, and Oliver Brüstle. 2015. "The Role of MicroRNAs in Human Neural Stem Cells, Neuronal Differentiation and Subtype Specification." *Cell and Tissue Research* 359(1):47–64.

Stark, Kimberly L. et al. 2008. "Altered Brain MicroRNA Biogenesis Contributes to Phenotypic Deficits in a 22q11-Deletion Mouse Model." *Nature Genetics* 40(6):751–60.

Sutton, Michael A. and Erin M. Schuman. 2006. "Dendritic Protein Synthesis, Synaptic Plasticity, and Memory." *Cell* 127(1):49–58.

Takayama, Y., H. Moriguchi, K. Kotani, and Y. Jimbo. 2009a. "Spontaneous

Calcium Transients in Cultured Cortical Networks During Development." *IEEE Transactions on Biomedical Engineering* 56(12):2949–56.

Takayama, Y., H. Moriguchi, K. Kotani, and Y. Jimbo. 2009b. "Spontaneous Calcium Transients in Cultured Cortical Networks During Development." *IEEE Transactions on Biomedical Engineering* 56(12):2949–56.

Tan, Chan Lek et al. 2013. "MicroRNA-128 Governs Neuronal Excitability and Motor Behavior in Mice." *Science (New York, N.Y.)* 342(6163):1254–58.

Tay, Yvonne M. S. et al. 2008. "MicroRNA-134 Modulates the Differentiation of Mouse Embryonic Stem Cells, Where It Causes Post-Transcriptional Attenuation of Nanog and LRH1." *Stem Cells* 26(1):17–29.

Taylor, Anne M. et al. 2005. "A Microfluidic Culture Platform for CNS Axonal Injury, Regeneration and Transport." *Nature Methods* 2:599–605.

Taylor, Anne M. et al. 2009. "Axonal MRNA in Uninjured and Regenerating Cortical Mammalian Axons." *The Journal of Neuroscience : The Official Journal of the Society for Neuroscience* 29(15):4697–4707.

Tehler, Disa, Nina Molin Høyland-Kroghsbo, and Anders H. Lund. 2011. "The MiR-10 MicroRNA Precursor Family." *RNA Biology* 8(5):728–34.

Thacker, Bryan E. et al. 2016. "Expanding the 3- *O* -Sulfate Proteome—Enhanced Binding of Neuropilin-1 to 3- *O* -Sulfated Heparan Sulfate Modulates Its Activity." *ACS Chemical Biology* 11(4):971–80.

Thacker, Bryan E., Ding Xu, Roger Lawrence, and Jeffrey D. Esko. 2014. "Heparan Sulfate 3-O-Sulfation: A Rare Modification in Search of a Function." *Matrix Biology : Journal of the International Society for Matrix Biology* 35:60–72.

Thomas, Kristen Therese et al. 2017. "Inhibition of the Schizophrenia-Associated MicroRNA MiR-137 Disrupts Nrg1α Neurodevelopmental Signal Transduction." *Cell Reports* 20(1):1–12.

Tiedge, H., W. Chen, and J. Brosius. 1993. "Primary Structure, Neural-Specific Expression, and Dendritic Location of Human BC200 RNA." *The Journal of Neuroscience : The Official Journal of the Society for Neuroscience* 13(6):2382–90.

Tiedge, H., R. T. Fremeau, P. H. Weinstock, O. Arancio, and J. Brosius. 1991. "Dendritic Location of Neural BC1 RNA." *Proceedings of the National Academy of Sciences of the United States of America* 88(6):2093–97.

Tsirigos, Aristotelis and Isidore Rigoutsos. 2009. "Alu and B1 Repeats Have Been Selectively Retained in the Upstream and Intronic Regions of Genes of Specific Functional Classes." *PLoS Computational Biology* 5(12):e1000610.

Uhlén, Mathias et al. 2015. "Proteomics. Tissue-Based Map of the Human Proteome." *Science (New York, N.Y.)* 347(6220):1260419.

Umylny, Boris, Gernot Presting, Jimmy T. Efird, Boris I. Klimovitsky, and W. Steven Ward. 2007. "Most Human Alu and Murine B1 Repeats Are Unique." *Journal of Cellular Biochemistry J. Cell. Biochem* 102(102):110–21.

Van Vactor, David, Dennis P. Wall, Karl G. Johnson, and Van Vactor. 2006.

"Heparan Sulfate Proteoglycans and the Emergence of Neuronal Connectivity." *Current Opinion in Neurobiology* 16:40–51.

Valadkhan, Saba and Lalith S. Gunawardane. 2013. "Role of Small Nuclear RNAs in Eukaryotic Gene Expression." *Essays In Biochemistry* 54:79–90.

Vandesompele, Jo et al. 2002. "Accurate Normalization of Real-Time Quantitative RT-PCR Data by Geometric Averaging of Multiple Internal Control Genes." *Genome Biology* 3(7):RESEARCH0034.

Veniaminova, Natalia A., Nikita S. Vassetzky, and Dmitri A. Kramerov. 2007. "B1 SINEs in Different Rodent Families." *Genomics* 89(6):678–86.

Verma, Pushpa, George J. Augustine, Mohamed-Raafet Ammar, Ayumu Tashiro, and Stephen M. Cohen. 2015. "A Neuroprotective Role for MicroRNA MiR-1000 Mediated by Limiting Glutamate Excitotoxicity." *Nature Neuroscience* (November 2014):1–9.

Verstraelen, Peter et al. 2014. "Pharmacological Characterization of Cultivated Neuronal Networks: Relevance to Synaptogenesis and Synaptic Connectivity." *Cellular and Molecular Neurobiology* 34(5):757–76.

Vijaya Kumar, Archana et al. 2014. "*HS3ST2* Modulates Breast Cancer Cell Invasiveness via MAP Kinase- and Tcf4 (Tcf7l2)-Dependent Regulation of Protease and Cadherin Expression." *International Journal of Cancer* 135(11):2579–92.

Volvert, M. L., F. Rogister, G. Moonen, B. Malgrange, and L. Nguyen. 2012. "MicroRNAs Tune Cerebral Cortical Neurogenesis." *Cell Death and Differentiation* 19(10):1573–81.

Wagenaar, Daniel A., Jerome Pine, and Steve M. Potter. 2006. "An Extremely Rich Repertoire of Bursting Patterns during the Development of Cortical Cultures." *BMC Neuroscience* 7:11.

Wagenaar, DanielA, Jerome Pine, and SteveM Potter. 2006. "An Extremely Rich Repertoire of Bursting Patterns during the Development of Cortical Cultures." *BMC Neuroscience* 7(1):11.

Wang, Bin and Lan Bao. 2017. "Axonal MicroRNAs: Localization, Function and Regulatory Mechanism during Axon Development." *Journal of Molecular Cell Biology* 9(2):82–90.

Wang, Wenyuan, Ester J. Kwon, and Li-Huei Tsai. 2012. "MicroRNAs in Learning, Memory, and Neurological Diseases." *Learning & Memory (Cold Spring Harbor, N.Y.)* 19(9):359–68.

Wayman, Gary A. et al. 2008. "An Activity-Regulated MicroRNA Controls Dendritic Plasticity by down-Regulating P250GAP." *Proceedings of the National Academy of Sciences of the United States of America* 105:9093–98.

Wheeler, Benjamin M. et al. 2009. "The Deep Evolution of Metazoan MicroRNAs." *Evolution & Development* 11(1):50–68.

Williams, Warren P., Lillian Tamburic, and Caroline R. Astell. 2004. "Increased Levels of B1 and B2 SINE Transcripts in Mouse Fibroblast Cells Due to Minute Virus of Mice Infection." *Virology* 327(2):233–41.

Wong, Hovy Ho-Wai et al. 2017. "RNA Docking and Local Translation Regulate Site-Specific Axon Remodeling In Vivo." *Neuron* 95(4):852–868.e8.

Xu, Bing et al. 2017. "Neurons Secrete MIR-132-Containing Exosomes to Regulate Brain Vascular Integrity." *Cell Research* 27(7):882–97.

Xu, Ding and Jeffrey D. Esko. 2014. "Demystifying Heparan Sulfate–Protein Interactions." *Annu. Rev. Biochem* 83:129–57.

Xu, Jie, Qun Chen, Ke Zen, Chenyu Zhang, and Qipeng Zhang. 2013. "Synaptosomes Secrete and Uptake Functionally Active MicroRNAs via Exocytosis and Endocytosis Pathways." *Journal of Neurochemistry* 124(1):15–25.

Yabe, Tomio, Toshihiro Hata, Jue He, and Nobuaki Maeda. 2005. "Developmental and Regional Expression of Heparan Sulfate Sulfotransferase Genes in the Mouse Brain." *Glycobiology* 15(10):982–93.

Yan, Dong, Li Guo, and Yizheng Wang. 2006. "Requirement of Dendritic Akt Degradation by the Ubiquitin-Proteasome System for Neuronal Polarity." *Journal of Cell Biology* 174:415–24.

Yang, Z., Y. Han, K. Cheng, G. Zhang, and X. Wang. 2014. "MiR-99a Directly Targets the MTOR Signalling Pathway in Breast Cancer Side Population Cells." *Cell Proliferation* 47(6):587–95.

Yao, Mao-Jin et al. 2012. "Transcriptome Analysis of MicroRNAs in Developing Cerebral Cortex of Rat." *BMC Genomics* 13(1):232.

Yi, Jason J., Anthony P. Barnes, Randal Hand, Franck Polleux, and Michael D. Ehlers. 2010. "TGF-β Signaling Specifies Axons during Brain Development." *Cell* 142:144–57.

Yoo, Andrew S., Brett T. Staahl, Lei Chen, and Gerald R. Crabtree. 2009. "MicroRNA-Mediated Switching of Chromatin-Remodelling Complexes in Neural Development." *Nature* 460(7255):642–46.

Yoon, Byung C., Krishna H. Zivraj, and Christine E. Holt. 2009. "Local Translation and MRNA Trafficking in Axon Pathfinding." *Results and Problems in Cell Differentiation* 48:269–88.

Yoshimura, Takeshi et al. 2005. "GSK-3β Regulates Phosphorylation of CRMP-2 and Neuronal Polarity." *Cell* 120:137–49.

Yuan, Zhidong et al. 2010. "Origin and Evolution of a Placental-Specific MicroRNA Family in the Human Genome." *BMC Evolutionary Biology* 10(1):346.

Yuan, Zhidong, Xiao Sun, Hongde Liu, and Jianming Xie. 2011. "MicroRNA Genes Derived from Repetitive Elements and Expanded by Segmental Duplication Events in Mammalian Genomes." *PloS One* 6(3):e17666.

Zhang, Haijun, Benjamin Shykind, and Tao Sun. 2012. "Approaches to Manipulating MicroRNAs in Neurogenesis." *Frontiers in Neuroscience* 6:196.

Zhang, Jian et al. 2015. "Exosome and Exosomal MicroRNA: Trafficking, Sorting, and Function." *Genomics, Proteomics and Bioinformatics* 13(1):17–24.

Zhang, Wenchi et al. 2015. "Structural Basis of Arc Binding to Synaptic Proteins:

Implications for Cognitive Disease." *Neuron* 86(2):490–500.

Zhang, Xiao hui and Mu-ming Poo. 2002. "Localized Synaptic Potentiation by BDNF Requires Local Protein Synthesis in the Developing Axon." *Neuron* 36(4):675–88.

Zhang, Yi et al. 2015. "MicroRNAs in the Axon Locally Mediate the Effects of Chondroitin Sulfate Proteoglycans and CGMP on Axonal Growth." *Developmental Neurobiology* 75(12):1402–19.

Zhang, Yi et al. 2013. "The MicroRNA-17-92 Cluster Enhances Axonal Outgrowth in Embryonic Cortical Neurons." *The Journal of Neuroscience : The Official Journal of the Society for Neuroscience* 33:6885–94.

Zhao, Chunnian, GuoQiang Sun, Shengxiu Li, and Yanhong Shi. 2009. "A Feedback Regulatory Loop Involving MicroRNA-9 and Nuclear Receptor TLX in Neural Stem Cell Fate Determination." *Nature Structural & Molecular Biology* 16(4):365–71.

Zhong, J. et al. 2009. "BC1 Regulation of Metabotropic Glutamate Receptor-Mediated Neuronal Excitability." *Journal of Neuroscience* 29(32):9977–86.

Zivraj, Krishna H. et al. 2010. "Subcellular Profiling Reveals Distinct and Developmentally Regulated Repertoire of Growth Cone MRNAs." *The Journal of Neuroscience : The Official Journal of the Society for Neuroscience* 30:15464–78.